Performance-Based Evaluation of Joint Sealants for Concrete Pavements

by
Ramzi E. Khuri

Thesis submitted to the Faculty of the
Virginia Polytechnic Institute and State University
in partial fulfillment of the requirements for the degree of

Master of Science
In
Civil and Environmental Engineering

APPROVED

____
Dr. Imad L. Al-Qadi, Chair
Professor of Civil and Environmental Engineering

____
Dr. Richard E. Weyers
Professor of Civil and Environmental Engineering

____
Dr. John G. Dillard
Professor of Chemistry

December 1998

Performance-Based Evaluation of Joint Sealants for Concrete Pavements

Ramzi E. Khuri

Chair: Dr. Imad L. Al-Qadi

The Via Department of Civil and Environmental Engineering

ABSTRACT

Pavement concrete joints are the weakest locations in concrete pavement systems. They are man-made cracks to accommodate concrete slab expansion and contraction due to temperature fluctuations. Sealant is usually used in pavement joints to prevent roadway debris, deicing chemicals, and moisture from entering the joint. When sealant fails, the pavement deteriorates rapidly; and when joint sealant performs adequately, the pavement preserves its intended performance. In the field, joint sealant undergoes two types of mechanical loading simultaneously. The sealant is experiencing tension or compression as slabs contract (low temperature) or expand (high temperature), respectively. Sealants also experience shear as heavy trucks travel over the joint and deflect the ends of the pavement slabs. In addition, sealants may also be exposed to a variety of environmental conditions, such as moisture, ultraviolet light, and jet fuel, which in some cases could be detrimental to their performance. In this study, the effects of vehicular and environmental loading on joint sealant performance were evaluated. To simulate the sealed joint performance, specimens were constructed by sandwiching a sealant between two 50.8 mm Portland cement concrete (PCC) cubes. Prior to mechanical loading, specimens were subjected to partial immersion in distilled water, partial immersion in jet fuel, and/or exposure to UV-A light. The specimens were then subjected to static horizontal tension, simulating slab contraction, and cyclic deflection-controlled shear, simulating heavy trucks travelling over the joint. The cycle consists of one 0.2 second period of sinusoidal loading (total 6.4 mm deflection) followed by a 0.4 second relaxation. The mechanical loading was applied using a special fixture developed at Virginia Tech, which is connected to a closed-loop servo-hydraulic loading machine. Two types of sealants (preformed neoprene and field-molded silicone with a primer) were tested using PCC mixes with two different aggregate types. In, addition, two different joint widths were evaluated for each sealant type. From the results of the cyclic testing and environmental conditioning, it was shown that the use of a primer greatly enhances the performance of the silicone sealant used with concrete containing limestone aggregate. In addition, severe swelling occurs when silicone sealant is exposed to jet fuel, and the failure of the field-molded silicone initiated at the bottom of the sealant and propagated upward. The preformed neoprene sealants proved very durable despite any combination of environmental conditioning, provided that the sealant remained in compression.

ACKNOWLEDGEMENT

The author expresses his sincere gratitude to his advisor, Dr. Imad L. Al-Qadi for guidance during the guidance necessary to undertake and complete such a research project. In addition, thanks are given to the committee members, Dr. Richard E. Weyers and Dr. John G. Dillard, for giving their time and expertise to help in the completion of this work.

The author extends his heartfelt appreciation to his family and friends for their unending support and understanding. Additionally, there is much gratitude to the author's colleagues, Amara, Salman, Stacey, Alex, Erin, Mostafa, James, Kiran, Brian, Walid, David, Agata, Jurek, and Mike from the Civil Engineering Materials Program and Monica from the Chemistry Department, for their great contribution of knowledge and camaraderie. The assistance of the Denson, Dennis, and Brett is also very appreciated.

The author also recognizes the Center for Adhesive and Sealant Science and the Adhesive and Sealant Council Education Foundation for their gracious support of this research. Dow Corning and the D. S. Brown Company are also recognized for providing testing materials and financial support.

TABLE OF CONTENTS

CHAPTER ONE

INTRODUCTION

1.1 GENERAL

The low tensile strength of concrete makes it necessary to provide joints for many concrete structures, including highway and airport rigid pavements. The function of a pavement joint is to provide space for the concrete pavement slabs to expand and contract during hot and cold temperatures, respectively. However, to keep incompressible materials from intruding between slabs, especially in the winter, a joint sealant may be used. With the increased truck traffic just before World War II, it was evident that pumping could also be a serious problem with unsealed jointed rigid pavements. In addition, deicing chemicals that enter joints would facilitate the corrosion of reinforcement bars and dowels (Reagan, 1992). Sealed joints were also needed to keep moisture from infiltrating the subgrade (Huang, 1993). Many materials have been used to seal rigid pavement joints, including wood, tar, asphalt, rubber, and inorganic-elastomers (Collins *et al.*, 1986).

Of the approximately 3.5 million km of paved roads in the US, almost 210,000 km are Portland cement concrete (PCC) pavements (Huang, 1993). It is an accepted fact that a high percentage of failures in highway and airport concrete pavements occur at or near the joints. The primary cause of the premature failure of jointed PCC pavements is improper joint sealing and joint maintenance (Jackson, 1988). Failure in a rigid pavement joint may occur due to joint creeping, joint seal loss, bond (adhesion) or cohesion loss in the sealant material, extrusion of the joint sealant, or impregnating the sealant with incompressible material (ACI, 1992). Not all problems in rigid pavements may occur at the joints; however, a failed joint can lead to more extensive damage. Although the failure of the sealant itself is not catastrophic, this failure can quickly lead to further damage, and thus, a drastic reduction of the surrounding pavement service life. Failures of rigid pavements that are associated with joint sealant include pumping, spalling, faulting, and blowups.

As could be expected, the performance of a rigid pavement joint is imperative to the life of the pavement. The proper design of joints and the use of proper sealants are keys to pavement performance. The premature deterioration of rigid pavement joint sealants can be avoided by a good initial design and regular maintenance. Knowledge of sealant performance is an important factor in the initial design, and in the repair, maintenance, and rehabilitation strategies. Thus, the performance and service life of joint sealants are crucial for developing any rigid pavement management system.

1.2 PROBLEM STATEMENT

With the current infrastructure quickly crumbling, engineers must use preventative techniques to preserve the integrity of structures and reduce the cost of repair, maintenance, and rehabilitation. In order to do this, engineers must have sufficient information about the performance of the materials that are being used. Millions of dollars are spent each year in the United States to repair deteriorated and failed joints in highway and airport rigid pavements. Joint sealants used usually pass related ASTM standards; however most existing specifications for evaluating and testing joint sealants consist of requirements pertaining to the sealant's physical properties, fabrication, shape, size, and configuration (Abo-Qudais, 1995). The relationship between these requirements and the performance of joint sealants has not been fully developed. Also, correlation between field performance of joint sealants and laboratory testing has not been established.

1.3 OBJECTIVES

The main objective of this study is to better understand rigid pavement joint sealant performance. Laboratory testing that simulates field conditions, which was developed at Virginia Tech, was used to evaluate joint sealant performance under cyclic loading and different environmental conditions. Different types of sealant were used with two different concrete mixes (containing two different types of aggregate). To simulate environmental field conditions, sealants were exposed to moisture, jet fuel, and ultraviolet light (UV).

1.4 RESEARCH SCOPE

While the concept of sealant application is certainly understood, its performance has not been able to be predicted. To address this lack of predictability, a mechanistic method to evaluate sealant in concrete pavements was developed at Virginia Tech (Abo-Qudais, 1995). Unlike most tests for sealants, which involve static loading, the Virginia Tech testing setup is designed to apply simultaneous cyclic shear and static normal deflections to a sealant. Shear deflection simulates the relative movement of heavy vehicles over jointed rigid pavement, while horizontal deflection resembles a slab shrinking or expanding due to temperature fluctuations (Abo-Qudais, 1995).

Specimens were fabricated by sandwiching a sealant between two 51 x 51 x 51 mm concrete cubes; there were two types of sealants -- field-molded silicone and preformed neoprene. Two aggregate types (limestone and granite) were used in the concrete mixes. Two different joint widths were used for each sealant/aggregate combination.

The environmental conditioning was performed prior to exposing the specimen to cyclic loading. This includes a combination of 1000 hours exposure to UV-A radiation, 120 hours of partial immersion in jet fuel (kerosene-type), and/or 120 hours of partial immersion in distilled water (at room temperature) for each specimen. Following the aforementioned environmental conditioning, specimens were evaluated using the Virginia Tech fixture that was attached to a servo-hydraulic system. Specified dynamic vertical deflection and static horizontal deflection were applied. The vertical and horizontal stresses were monitored and recorded throughout the test. The number of loading cycles to failure was observed to determine the sealant performance.

A fatigue regression line of stress versus the log number of cycles was developed. It was observed that as the sealant reached failure, the stress (vertical or horizontal) would asymptote to a finite value, where the slope becomes infinitesimal (≈ 0). This suggests that the sealant may not become any more compliant with additional loading, and thus may be considered to have failed.

In this thesis, chapter two presents an overview of the current state of knowledge. Chapter three describes the experimental program including specimen preparation and testing. Data analysis and discussion are presented in chapter four. Conclusions and recommendations are presented in chapters five and six, respectively.

CHAPTER TWO

LITERATURE REVIEW

2.1 BACKGROUND

Since the building of the first concrete road in Detroit, Michigan in 1908, pavement engineers have been striving to improve the quality of rigid pavements in this country (Huang, 1993). Rigid pavements were first used in airports in the 1930s; however, they were not used extensively until the advent of World War II in 1941 (Ray, 1986). During these years, joints were constructed crudely and were very wide, providing poor ride quality. Tar and asphalt were the sealants that were primarily used, and joint surface preparation was not exceptional. Joints were usually resealed without the removal of the old sealant, resulting in a bump at the end of each pavement slab. If the sealant was removed, debris was swept out of the joint with a broom prior to resealing. This type of resealing preparation was not very effective (Ray, 1986).

At the end of World War II, the quality of concrete pavements improved dramatically, as shorter slabs and thus smaller joints were being used. Sawing joints, rather than forming the joint in the plastic concrete, greatly improves the sealant adhesion to the pavement slab. The depth of the joints also increased to approximately ¼ of the pavement slab depth with the advent of the sawing technique. However, these narrow and deep joints greatly increased the sealant strains. This forced engineers to look into using better materials that would withstand these strains. In addition, the traditional tar and asphalt sealants had to be replaced on airport slabs because jet fuel spills dissolved them. Research into the use of elastomers as sealants and improving joint surface preparation was undertaken. The importance of the shape factor (sealant depth to width ratio) in field-molded sealants was also affirmed during this time (Ray, 1986).

Today the average life of joint sealants within concrete pavements is five years. Even with this great improvement from the World War II era, sealant life needs to be much greater. Agencies still remain divided when deciding what is best to preserve a long-lasting concrete pavement. The use of continuous reinforced concrete pavements (CRCP) and prestressed concrete pavements (PCP) have not always been a suitable replacement of jointed concrete pavement. Even with jointed concrete pavements, the need for a joint sealant is currently debatable; when sealants are to be used in joints, the choice is not clear as to which is the best one to apply.

2.2 JOINT DESIGN AND CONSTRUCTION

Within the classification of rigid pavements are four specific types: jointed plain concrete pavement (JPCP), jointed reinforced concrete pavements (JRCP), prestressed concrete pavement (PCP), and. continuous reinforced concrete pavement (CRCP). For JPCP, no steel reinforcement is used and joint spacing is usually between 4.6 and 9.1 meters, depending on the aggregate type and climate. Jointed reinforced concrete pavements contain wire mesh steel reinforcement, which allows the use of larger joint spacings (9.1 to 30 meters), but does not increase the structural capacity of the slab. The prestressed steel reinforcement in PCP allows the use of much larger joint spacings (91 to 232 meters). Continuous reinforced concrete pavements eliminate the need for joints altogether as steel reinforcement is uninterrupted throughout the pavement slab (Huang, 1993). Transverse (perpendicular to the flow of traffic) expansion joints are used to relieve compressive stresses, however are rarely used today because they are difficult to maintain and are susceptible to pumping. Longitudinal joints (parallel to the flow of traffic) are used in concrete pavements to relieve curling and warping stresses resulting from temperature or moisture gradients that occur in the slab. Contraction joints are transverse joints used to relieve tensile stresses in concrete that arise from thermal volumetric changes. In order to have a contraction joint that adequately relieves thermal stresses from a concrete slab, certain characteristics must be evident. Four elements that should be considered for a good joint system design are joint width, joint depth, backer rod selection, and sealant selection and placement (Jackson, 1988). In addition to allowing easy installation of sealant, the width of a joint has to accommodate the adjacent slabs to expansion during warm climates.

The equation used to calculate the thermal expansion of a concrete slab is as follows:

$$\Delta L = C*L*(\alpha_{concrete} *\Delta T + \varepsilon) \tag{1}$$

where,

ΔL = change in length of the concrete slab;

C = subbase/slab frictional factor (0.65 for stabilized material, 0.80 for granular material);

L = original length of the concrete slab;

$\alpha_{concrete}$ = coefficient of thermal expansion for concrete (≈6 x 10^{-6} 1/°F);

ΔT = maximum temperature range; and

ε = shrinkage coefficient of concrete.

According to Bodocsi *et al.* (1993), the above equation may be simplified to $\Delta L = L*\alpha_{concrete} *\Delta T$ for concrete pavements that are at least 20 years old. In addition to the concrete slab length, the type of aggregate used in the concrete greatly affects the thermal coefficient (McGhee, 1995). The joint reservoir depth is usually recommended to be one-fourth to one-fifth of the slab thickness and a minimum of 25 millimeters. A contraction joint spacing of 4.6 to 6.1 meters (15 to 20 feet) is usually used for plain rigid pavements, but good quality concrete has performed adequately when the joint spacing (in feet) does not exceed four times the slab thickness (in inches). Joint spacing has been randomized in some states to prevent possible resonance in automobile suspension systems at high speeds (Waddell and Dobrowolski, 1993).

The method for constructing a contraction joint also may vary. They may be formed manually with a jointer and an edger, placement of plastic strips, sawing after sufficient hardening, or mechanically inserting a steel T-bar to form a groove. When constructed using a jointer and an edger, care must be taken to ensure that the required joint depth is achieved. Joint construction using plastic strips is usually done in conjunction with the screeding. However, great care must be taken to assure that the joint is perfectly straight and vertical. Sawing the contraction joint should be done as soon as the concrete is hard enough to prevent raveling of the edges by the saw blade, but still prevent random cracking (Waddell and Dobrowolski, 1993). After the sawing is completed, the joint should be cleaned of any shavings before the backer rod or sealant is installed. Most agencies employ sandblasting, water blasting, wire brushing or some combination thereof, followed by air blasting just prior to sealing (McGhee, 1995). Thorough cleaning methods provide a better adhesion surface for the sealant and would also help prevent future spalling due to slab thermal expansion. The joint should also be dry, as a wet joint generally has an adverse effect on adhesion. Grease and oil-type contaminants will also interfere with the formation of a sound bond (ACI, 1992). Joint formation with a steel T-bar is similar to using the plastic strips; the joint is formed in the freshly placed concrete.

Once the joint is constructed and cleaned, the backer rod material may be inserted. The backer rod is a compressible material, such as Styrofoam, which is inserted in the bottom of the joint and serves three purposes. The backer rod material prevents the sealant from bonding with the bottom surface of the joint. Three-sided adhesion places excessive stress upon the sealant and drastically reduces its extension capability (Jackson, 1988). The backer rod also helps control the thickness of the sealant as it is applied to the joint. Therefore, it is essential that the backer rod is placed at the proper depth within the joint. The backer rod also acts as a tooling aid when the sealant is being applied. A diagram of a pavement joint with a backer rod and sealant is shown in Figure 2.1. With the backer rod in place, the sealant may then be applied.

The joint seal may be one of two types: field-molded or preformed. When using a field molded joint sealant, a major parameter that must be considered is the shape factor of the sealant. The shape factor must be quantified such that cohesive strains are minimized while still providing a sufficient bond area to accommodate adhesive stresses at the sealant-joint interface (McGhee, 1995). Typical values for the shape factor range from 0.5 to 1.0.

Some guidelines that should be used to select a specific sealant material include sealant ductility at cold temperatures, rigidity at high temperatures, compatibility with the aggregate within the concrete slabs, and durability to weather, traffic, and chemical attack. Other details that should also be considered in sealant selection include life cycle cost, ease of installation, and ease of replacement (Klosowski, 1989). Field molded sealants may either be hot-poured or cold-poured. Slow heating of hot-poured sealants is absolutely necessary to avoid overheating. This tends to make the sealant lose some of its elasticity. Underheating, however, makes the sealant unworkable and hard to place in the joint. Cold-poured sealants, on the other hand, are fabricated by mixing two or more components on the job site just prior to sealing. It is very important that the correct material proportions are used and that the components are thoroughly mixed. This will insure the proper curing of the seal material.

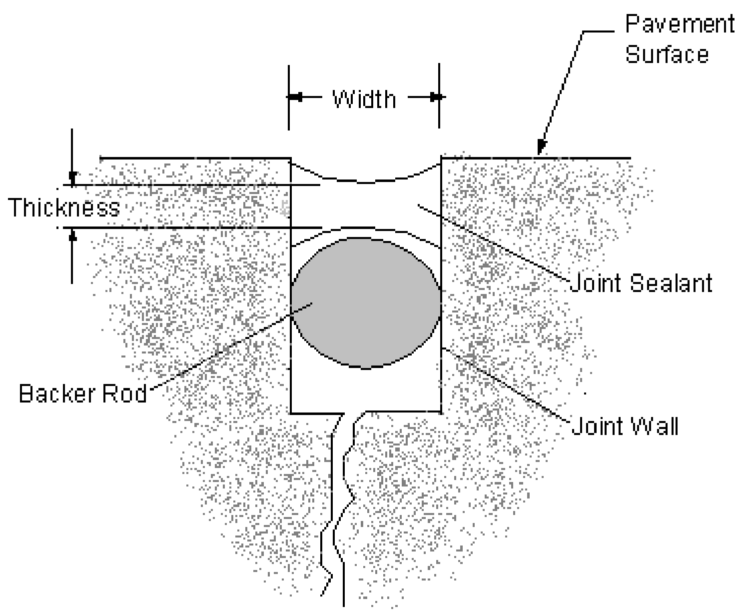

Figure 2.1 Typical concrete expansion joint using a field molded sealant

Preformed joint seals are molded prior to installation in the field and do not require the use of backer material during installation. The important characteristics of materials used for preformed seals include durability, resiliency, and compressibility, as well as the ability of the material to sustain a long-term compressible state without developing "compression set," a condition permitting the seal to either drop into the joint or come out under traffic (McGhee, 1995). One characteristic of most preformed seals that allows them to stay compressed during its entire service life is the webbed cross-section. The selected seal should have an uncompressed width of approximately twice the minimum expected width of the joint (McGhee, 1995).

2.3 VISCOELASTIC NATURE OF SEALANT MATERIAL

An elastic material is one in which all strain that is induced during loading is recoverable once the load is removed. A viscous material, in contrast, will not recover any strain once the loading is removed. A material that exhibits both viscous and elastic behavior at a certain temperature and under a certain loading rate is termed viscoelastic. Viscoelastic materials, however, exhibit different behaviors at different loading rates and temperatures, or time dependent properties. For example, a ball of Silly Putty bounces if it is dropped. However, it can also be shaped by the slow application of pressure (Stevens, 1990). In linear viscoelastic theory, the effects of temperature change and time are essentially the same, and thus allow the use of time-temperature superposition.

In order to have a better physical representation of material behavior, the mechanical analogues of a spring and a dashpot are used to represent elastic and viscous materials, respectively. A spring follows simple elastic theory; when a load is applied and then released, all strain is recovered instantly. A dashpot represents viscous materials (a piston moving through a highly viscous fluid). In this case, all strain is permanent. However, in order to model viscoelastic materials, the spring and dashpot must be combined in series and in parallel. These combinations of elements more or less faithfully reproduce the viscoelastic response of real systems (Aklonis and MacKnight, 1983). When combined in series, the spring and dashpot form the Maxwell model. The Kelvin (Voigt) is built up of a spring and a dashpot in parallel (Haddad, 1995). A diagram of the spring, dashpot, Maxwell, and Kelvin models are shown in Figure 2.2. The parameter E is the elastic modulus for the spring element, and the parameter η is the viscosity of the fluid in the dashpot; σ, ε, and t are stress, strain, and time, respectively. Arranging Maxwell elements in parallel or Kelvin elements in series may derive more complex models of viscoelastic materials.

2.4 POLYMER PROPERTIES

Three of the main polymer properties that decide whether a sealant is applicable under certain field conditions are the glass transition temperature (T_g), the melt transition temperature (T_m), and the modulus (E). The T_g, which is a second order thermodynamic transition, characterizes at what temperatures an amorphous polymer behaves rubbery or glass-like. This transition from glassy to rubbery properties is due to the increased rotation of polymer chains (Rosen, 1993). Several factors influence the T_g of a polymer:

free volume, attractive forces between molecules, internal mobility of the chains, chain stiffness, and crosslinking. An increase in free volume will allow more space for molecules to move around, and thus lower the glass transition temperature (Aklonis and MacKnight, 1983). Also, with weak intermolecular bonds, less energy is required to produce motion, and thus the T_g decreases. When the chains within a polymer network may rotate around the bonds, the T_g decreases.

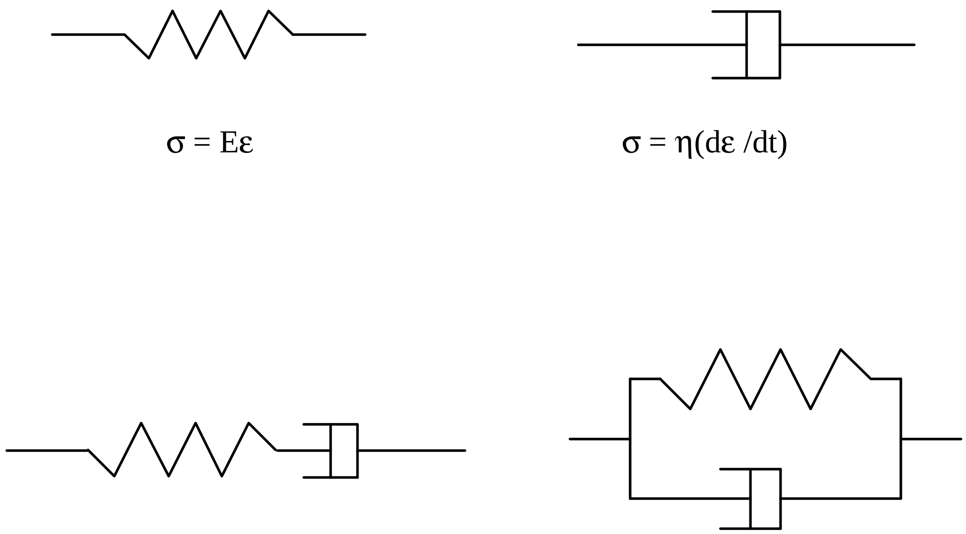

$\sigma = E\varepsilon$ $\qquad$ $\sigma = \eta(d\varepsilon/dt)$

$\sigma + \eta/E(d\sigma/dt) = \eta(d\varepsilon/dt)$ $\qquad$ $\sigma = E\varepsilon + \eta(d\varepsilon/dt)$

Figure 2.2 Mechanical analogs and governing differential equations for spring, dashpot, Maxwell, and Kelvin models

The stiffness of the polymer backbone also influences the glass transition temperature; lower chain stiffness constitutes a lower T_g. Finally, crosslinking, bulky substituents, and large groups of atoms hinder molecular movement and raise the glass transition temperature. It is ideal for a sealant to have rubbery qualities when used in the field; the service temperature should be higher than the glass transition temperature. Therefore, a low T_g will allow a greater temperature range in which the sealant will behave rubbery.

The melt transition temperature is also very important for determining how applicable a sealant will be in the field. The T_m of a polymer is a first order transition in which the crystalline part melts from an ordered crystal to a liquid state (Rosen, 1993; Aklonis and MacKnight, 1983). Entropy, which is the amount of disorder in a system, affects the melt transition temperature of a polymer; lower entropy results in a higher T_m. Since crystals are very ordered, condensed structures, highly crystalline polymers have higher melt transition temperatures. The melt transition temperature also increases with an increase in molecular weight; however, as is also the case with T_g, this is only true up to a molecular weight of 100,000 grams per mole (Callister, 1994).

The modulus of elasticity may be defined as "the ratio of force needed to elongate a sealant by a given a amount" (Klosowski, 1989). The modulus of a sealant generally increases with an increase in cure and crosslink density. Modulus is a polymer property that is termed "time dependant." Modulus is not only affected by the temperature at which it is measured, but also by the loading frequency.

2.5 PARAMETERS AFFECTING POLYMER PROPERTIES

Polymer chemical parameters include chemical composition, molecular weight, stereochemistry, morphology, and topology. These parameters define the behavior of polymer sealants. By understanding these parameters, better sealants may be synthesized to suit the needs of the engineer. Silicone and neoprene are rubber-like elastomers, meaning that they retract to their original shape once an applied load is removed and they have limited extensibility.

2.5.1 Silicone Sealants

Silicones are intermediate between organic and inorganic polymers. The basic repeat unit of a silicone is a hydroxyl-ended polydimethylsiloxane, as shown in Figure 2.3. Polydimethylsiloxane has an average molecular weight of about 200,000 grams per mole (Noll, 1968). The siloxane backbone has a low barrier of rotation and the bonds have a significant polar component, allowing the molecule to orient itself so that the side groups are pointed outward (Klosowski, 1989; Noll, 1968). The outer groups protect the siloxane bonds. The hydroxyl groups of the siloxane bond to hydroxyl groups on the substrate, forming hydrogen or van der Waals' bonds. The methyl groups are then pushed away from the backbone of the polymer, allowing some free rotation about the Si-O and Si-C bonds. The free rotation contributes to a relatively low modulus, low glass transition temperature, and high permeability (Kerr and Linn, 1994).

Hydrogen bonding or dipole interactions increase the crystallinity of a polymer, thus raising its melting point and increasing its modulus (Rosen, 1993). However, an increase in crystallinity decreases the solubility of a polymer, as does crosslinking; polymers with crosslinks tend to swell rather than dissolve (Rosen, 1993). Silicone sealants are most commonly crosslinked using trifunctional monomers. The crosslink density within the silicone depends on the functionality and concentration of the crosslinker, the polymer chain length, and the concentration of the crosslinkable filler (Klosowski, 1989). Fillers are usually used to improve the tensile and compressive strengths of a polymer, the abrasion resistance, toughness, and thermal stability. Fumed silica is the most common filler for silicone sealants. Silicone sealants generally have a good combination of physical strength, cure rate, temperature resilience, adhesion, and weatherabilty. Silicones retain both their ductility in cold temperatures and their elasticity in hot climates (Klosowski and Gant, 1979).

A disadvantage of silicone sealants is that they are relatively expensive. Also, they tend to become impregnated with debris easily and tear. Silicones are incompatible with some substrates, thus limiting their use; silicones are unsuitable for use with concrete containing limestone unless a primer is used (Abo-Qudais, 1995). The Si-O-Si structure is transparent to UV radiation; however, UV light does break some of the covalent bonds along the molecular chain (Callister, 1994).

Figure 2.3 Basic structure of the silicone repeat unit

2.5.2 Neoprene Sealants

Neoprene sealants are a type of butyl sealant, such as polyisobutylene, isobutylene, and isoprene. They usually have good oil, chemical, ozone, oxidation, and heat resistance (Kumar *et al.*, 1993). The hydrocarbon backbone of neoprene contains both single and double bonds. Hydrocarbons have strong covalent bonds in addition to van der Waals' bonds between molecules, resulting in relatively low glass and melt transition temperatures. Neoprene usually consists of a long chain with a high molecular weight; the melt transition temperature increases as the molecular weight increases. The repeat unit for neoprene is shown in Figure 2.4.

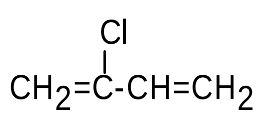

Figure 2.4 Chloroprene, the repeat unit for neoprene (after Callister, 1994)

Butyl rubbers usually do not need any reinforcing filler to achieve high mechanical strengths. This is because natural crystallization occurs, thus acting as reinforcement, when strain is applied (Rosen, 1993). However, the double bonds in neoprene cause kinks and bends, preventing a tight crystalline structure from forming (Bruice, 1995). Neoprene, however, is very rigid due to its normally high crosslink density.

2.6 FAILURE OF JOINT SEALANT SYSTEMS

The major joint sealant failure types are adhesive, cohesive, intrusion and extrusion, and intrusion of incompressible material into the sealant. Adhesive failure occurs due to tensile forces in the joint when the sealant detaches from the joint wall. Cohesive failure occurs when the material is stressed beyond its tensile limit, causing tears in the sealant body. Intrusion failure occurs when a sealant has relaxed during extension, and it does not possess adequate resilience to return to its original shape as the joint closes. Extrusion failure occurs when a joint has been sealed to its full height and when the joint is open. As the joint closes at high temperatures, the material is placed in compression, and the sealant either plugs or flows out of the joint. Once the sealant is higher than the pavement surface, it will be either flattened out onto the pavement or pulled out of the joint by vehicle tires. When the joint expands again, not enough sealant is left to properly seal the joint (Collins *et al.*, 1986).

Incompressible intrusion failure occurs when extremely high compressive stress develops in concrete pavement due to the presence of incompressible materials collected in the joints which prevent the joint from closing. System failure will then occur when either compressive or buckling strength is exceeded. At high temperatures, the slabs expand

and the joints contract; therefore, dirt may become trapped within the sealant. The sealant then may fail during the following slab extension (Bugler, 1983).

The failure of a joint sealant can be traced to several causes. The sealant could possibly fail if the geometrics of the joint are incompatible with the sealant material selected. This could be a result of the joint being too narrow for the expected movement, the shape factor being incorrect, or the material not having the proper extensibility to accommodate the movement (McGhee, 1995). The sealant may also fail once it has aged considerably and no longer has adequate extensibility. However, the most critical factor that causes sealant failure is poor surface preparation of the joint before sealing. If debris, moisture, and chemicals are not adequately removed from the joint just before sealing, a good bond between the concrete and the seal cannot develop. Also, a primer might be needed for some sealants to adhere to the joint wall.

The failure of the sealant itself is not catastrophic; however, this can lead to the reduction of service life for the surrounding pavement section. Pavement deteriorations that are associated with joint sealant failure are pumping, faulting, spalling, and blowups. Pumping is the ejection of water and fine particles from a rigid pavement joint, which occurs under the pressure of heavy vehicles. However, for pumping to occur, moisture must be able to infiltrate the joint, and the material beneath the pavement slab must be erodible. Once pumping incurs, the support beneath the edge of the slab decreases and faulting may develop. Faulting is when adjacent pavement slabs are at different elevations. When faulting occurs, the effectiveness of load transfer devices is greatly compromised. A joint spall is a shallow crack or a chip that occurs near the edge of a joint. Spalling usually results from excessive stresses at the joint caused by the infiltration of incompressible materials and subsequent expansion or traffic loading (Huang, 1993). Blowups also occur where joints are infiltrated by incompressible material, but are generally more severe than spalls. A blowup results in cracking through the full depth of the pavement slabs on both sides of the joint.

2.7 FIELD EVALUATIONS OF JOINT SEALANTS

Many field studies have been conducted to better evaluate joint sealants under harsh conditions. An innovative, non-destructive, broad coverage joint seal tester that yields quick results has been designed and developed by Steffes (1993). This test method, which was developed by the Iowa Department of Transportation, uses a foaming shampoo-water solution and a vacuum. The foaming solution is administered to the sealant area and then the vacuum is applied. Any leak in the seal quickly becomes evident by the presence of bubbles. This allows the identification of sealant cracks that might be unnoticeable by ordinary inspection.

Joint cleaning, shape factor, and good sealant installation practice are very important in the service life of sealants (Zimmer, *et al.,* 1984). Kinchen *et al.* (1977) suggested that the service life of sealants varied from zero to six years with most observed failures being adhesive; whereas Oehler and Bashore (1973) reported sealant failure between 10 and 15 years of service, with spalling and blowups as the result of failed joint sealants.

The New Jersey Department of Transportation concentrated on testing and improving the suggested methods of design and construction of joint systems in the 1960s and 1970s (Kozlov and Cosaboom, 1977). Two simple-span, composite design bridges were monitored from 1965 until 1974. The study concluded that the combined use of a preformed, elastomeric joint sealant, and an armored joint design would adequately prevent the intrusion of moisture and debris into the bridge deck. In addition, formed and sawed methods of joint construction were unsuccessful because of the unattainable workmanship needed from the contractor.

The effects of base material, joint spacing, and dowel type on the horizontal movements of concrete pavement joints were examined through the use of a pavement test section in Chillicothe, Ohio (Bodocsi *et al.*, 1993). The pavement sections were prepared using a 6.4 or 12.2-meter joint spacing, a stabilized or granular base, and a standard or a plastic coated dowel. Horizontal expansion measurements were taken continuously in order to be compared with the theoretical slab expansion. The study, which began in 1972 and concluded in 1992, revealed that the type of base material, type of base stabilization, joint spacing, and type of dowel bars have an insignificant effect on the horizontal joint movements 20 years after their construction.

Another field study performed in Ohio rated about 360 joint seals in eight rating categories based on visual inspection (Weisgerber *et al.*, 1987). The goal of the study was to rate the effectiveness of seals in categories such as general appearance, condition of anchorage, debris accumulation, water tightness, surface damage, noise under traffic, ease of cleaning, ease of replacement, and age. Twenty-four sealant types were evaluated with ages ranging from one month to 15 years. For all cases, poor workmanship during seal installation was found to be the most significant cause of poor sealant performance.
In another study by Noble (1987), three joint sealants in Charlottesville, Virginia were evaluated. The investigation ascertained that compartmented and closed cellular preformed neoprene sealants perform better than two-component cold-mixed polysulfide sealants. The polysulfide sealants failed prematurely due to compression set. Any incompressible material that infiltrated the joints caused damage to the load transfer devices, but did not cause considerable spalling.

Collins *et al.* (1986) conducted field studies on twelve joints sealed with silicone and monitored them for eight years after sealing. Although results indicated excellent bonding, a total failure of nine percent in the first nine months was observed. Some sealants, like rubberized asphalt, experienced failure within two years and showed, in general, poor performance.

Wolters (1974) evaluated liquid and preformed sealants used in transverse joints. Periodic observations were made through the service life of each sealant. Liquid sealants performed sufficiently in the first three years, while preformed sealants showed failure up to 56 percent of the joint. In another study, sealants failed within two years in sawed joints, and performed satisfactorily when used as a rehabilitation technique to repair joints (Jones *et al.*, 1973).

One field study investigated whether there was a need to seal joints at all. In the 1950s and 1960s, the contraction joints in portions of several Wisconsin roadways were purposely left unsealed to determine the effect on the surrounding pavement performance (Shober, 1986). After subsequent observations, it seemed that the joint and pavement performance were, in fact, enhanced by the absence of joint seals. In 1974, a controlled experiment was designed by the Wisconsin Department of Transportation to verify those findings. The study investigated the effects of various joint spacings (6.1, 12.2, 18.3, and 24.4 meters) and sealant types (rubberized asphalt, coal tar-based PVC, two-component cold-poured polysulfide, preformed neoprene, and standard sealant), as well as the effect of leaving contraction joints unsealed in certain pavement sections. During 10 years of monitoring the pavement sections, no faulting or blowups were observed in the sections with unsealed joints. However, joint spalling was observed quite frequently. Following a cost effectiveness analysis of joint sealant maintenance, the Wisconsin Department of Transportation concluded that joint sealing might not be justified in some situations.

2.8 LABORATORY EVALUATIONS OF JOINT SEALANTS

Several laboratory studies attempted to find ways of accurately simulating field loading and/or environmental conditions. A series of tests have been performed on five types of sealants: two-part polysulfide, silicone, hot-poured rubberized asphalt, polyurethane, and preformed sealant (Collins *et al.*, 1986). The effect of load on elongation was evaluated; silicone performed the best at -7°C with an elongation of 760 percent at approximately 220 N tension, while rubberized asphalt performed the worst with only 12.8 percent elongation. It has also been noticed that loads were almost constant throughout the elongation of silicone sealant. Bond tests showed that no bonding was evident for any of the five tested materials after five extensions (6.5 mm) of the cold-applied sealant or three extensions of the hot-poured sealant after being maintained for four hours at -10°C. Other tests such as flow, stress relaxation, shear fatigue, penetration, and aging were conducted. However, this "almost" comprehensive investigation did not address the effect of simultaneous dynamic shear and horizontal deflections, but rather concentrated on material property-related tests.

Shisler and Klosowski (1990) determined modulus characteristics of several sealants in tension, longitudinal shear, and transverse shear. The validity of the Pythagorean Theorem for calculating shear movement with a known tension modulus was also assessed. The silicone sealants that were evaluated showed a greater elongation in shear than in tension. The use of the Pythagorean Theorem to calculate shear movement in silicone sealants actually incorporates an inherent safety factor because of the silicones' superior performance in shear. The polyurethane seals, however, exhibited approximately the same elongation when loaded in shear and tension. The Pythagorean Theorem may be used to calculate horizontal movement in the polyurethane seals, but there is no inherent safety factor as with silicones.

Wang and Weisgerber (1993) recently investigated the effect of the sealant geometry on the stresses that are developed within the seals. Seven different seal shapes were used in the study. Case 1, which was loaded in tension, had a shape factor of one and was only adhered to the sides of the joint. Cases 2 and 3 were similar to case 1 except that the shape factors were two and four, respectively. Case 4 was similar to case 1 except that the sealant was also bonded to the bottom face of the joint reservoir. Case 5 was also similar to case 1 except that shear loading was used instead of tensile loading. Case 6 employed a trapezoidal seal loaded in tension with two-sided adhesion. Case 7 used a concave seal, loaded in tension, with a shape factor of one and two-sided adhesion. The experimentation found that seals with concave upper and lower surfaces were superior to rectangular and trapezoidal-shaped seals. The rectangular seals with low shape factors performed better than those with high shape factors. Also, three-sided adhesion did not seem to affect the adhesion on the joint walls; however, it may lead to early cohesive failure.

A study performed at Virginia Tech incorporated simultaneous tensile and shear loading for evaluating sealant performance. A fixture was developed to test a sealant sandwiched between two concrete cubes (Abo-Qudais, 1995). Two sealant types were evaluated (silicone and polyurethane), and two aggregate types were used in the concrete cubes (limestone and granite). Various joint widths and horizontal deflections were also considered. Cyclic shear deflections simulate the heavy overpassing traffic, while static tensile deflections simulate slab contraction at cold temperatures. In addition, some sealant specimens were exposed to freeze/thaw cycles prior to mechanical loading. It was concluded that silicone is very reactive with the limestone in the concrete, thus causing poor adhesion to the substrate and premature failure at large horizontal deflections and joint widths. The best sealant/aggregate combination proved to be the silicone/granite. Polyurethane, on the other hand, performed moderately with either aggregate. It was also found that exposure to freeze/thaw cycles had an insignificant effect on sealant performance.

Jones et al. (1973) reported a correlation between heat aging and strength reduction in joint sealants. Strengths of sealant specimens were evaluated before and after exposure to thermal cycles. Low temperature aging was investigated by the Portland Cement Association (Kuenning, 1962); Kuenning designed a special machine to test sawed joints at 23°C and -18°C; the effect of joint width on the sealant performance was also investigated. Thornton (1978) used a weather-ometer to evaluate the effect of weathering on sealants, and to evaluate the bond of sealants when debris was incorporated into incurred material. No visible deterioration was noticeable in the silicone sealants evaluated in the weather-ometer. However, insufficiently cured specimens usually failed cohesively in bond testing, while cured specimens failed adhesively. Gurjar *et al.* (1996) conducted similar research, performing tensile relaxation tests on weathered and unweathered silicone sealant specimens. One-part, self-leveling silicone specimens were aged for 0, 500, 1000, 1500, and 2000 hours in a Ci65A Weather-ometer. A master curve for the sealant relaxation modulus was produced using the data.

Tock (1990) investigated the effects of moisture and temperature on silicone sealant performance. After submersion in water, sealant specimens were loaded in tension at a temperature range of 0°C to 30°C. The pH of the water ranged from 5 to 12. The study found that exposure to moisture had little effect on the measured tensile properties. Also, for a temperature range of 0°C to 30°C, the tensile properties were unaffected. However, strong acid solutions (pH < 2.0) seriously affected the performance of the sealant.

Problems with joint sealant performance are also a result of poor workmanship during installation and inadequate surface preparation of the concrete substrate. Evans (1987) attributes the harshness of concrete as a substrate for adhesives to its extreme alkalinity, the weak, powdery surface layer, and its tendency to crack soon after it is formed. His testing revealed that the nature of concrete substrate must be studied further in order to improve seal adhesion.

From the citations presented, it is clear that many studies have been conducted to investigate the properties of joint sealants as well as their performance in the field. However, those investigations resulted, in many cases, in presenting “conflicting” conclusions as to the way in which sealants have performed over the past thirty years. Thus, it is critical that sealants be evaluated under performance-related testing.

CHAPTER THREE

EXPERIMENTAL PROGRAM

A research program was developed to evaluate silicone and neoprene sealants under cyclic shear and static horizontal loading. Two types of aggregate were used in the concrete substrate. Different joint widths and environmental conditioning were also considered. This chapter details the experimental program.

3.1 TESTING FIXTURE

The fixture developed at Virginia Tech (Figure 3.1a and 3.1b) was used in this research program. The fixture is capable of transferring dynamic shear deflection and static horizontal deflection to the joint sealant. Testing using this fixture can be performed as stress- or deflection-controlled; a deflection-controlled test was adopted to simulate field conditions.

The fixture consists of two chambers for housing concrete specimens. Each chamber has four (inside) adjustable plates to prevent any rotation of the specimen during testing. One chamber connects to a loading shaft and a load cell that measures the applied vertical loading. The second chamber connects to a built-in control device and a load cell. The control device adjusts the horizontal deflection to a desired extension or contraction of the sealant to simulate concrete slab contraction/expansion and measures the applied horizontal load. This chamber is connected to the lower part of the loading system. The two parts of the fixture are completely isolated; however, for stability purposes, a sleeve with linear bearings connects the two parts and allows free vertical movement.

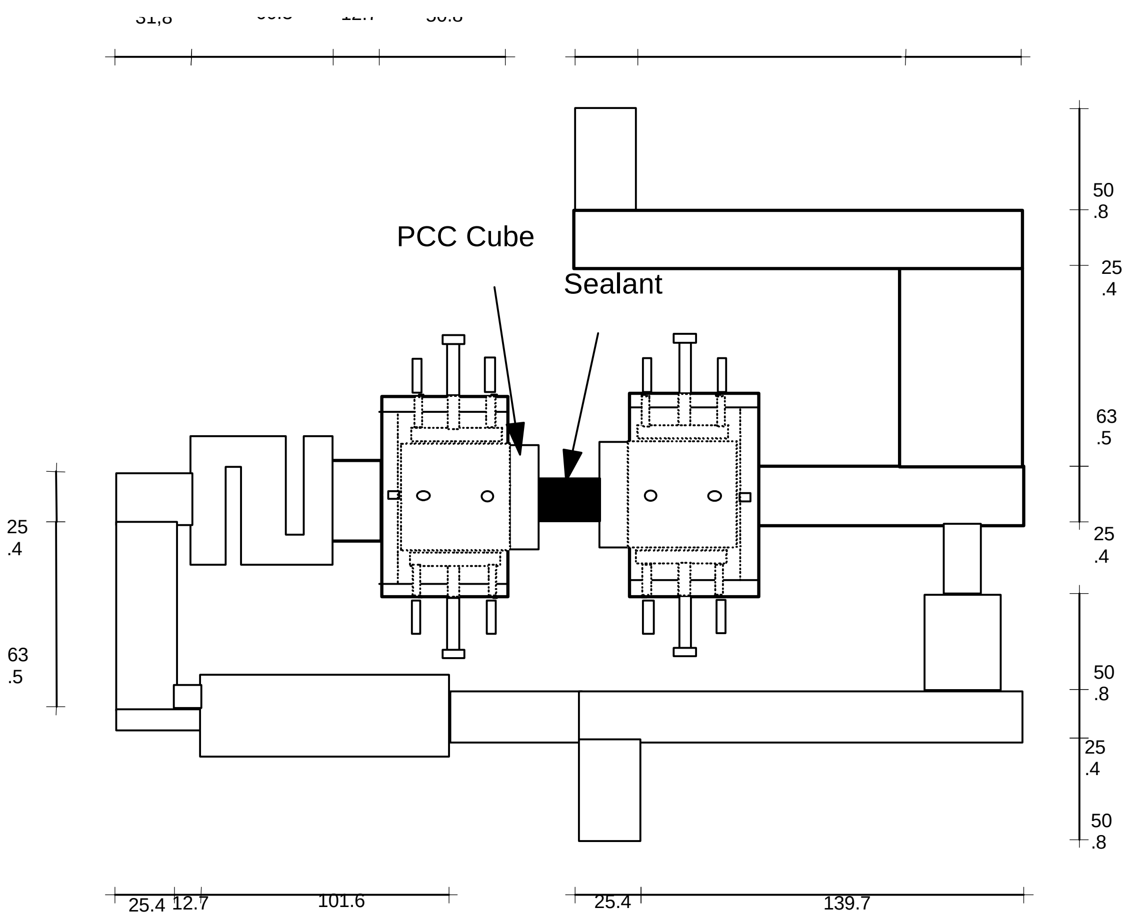

* All dimensions in mm, + Not to scale.

Figure 3.1a A schematic of the fixture developed at Virginia Tech

The loading shaft connects to a servo-hydraulic system that controls the vertical deflection. The servo-hydraulic system used is an MTS model 810 (controlled by an ATS data acquisition system) which controls the dynamic vertical loading characteristics. A built-in load cell and extensometers continuously measure the applied vertical stress and deflection during testing. An environmental chamber houses the fixture, which allows testing at different temperatures.

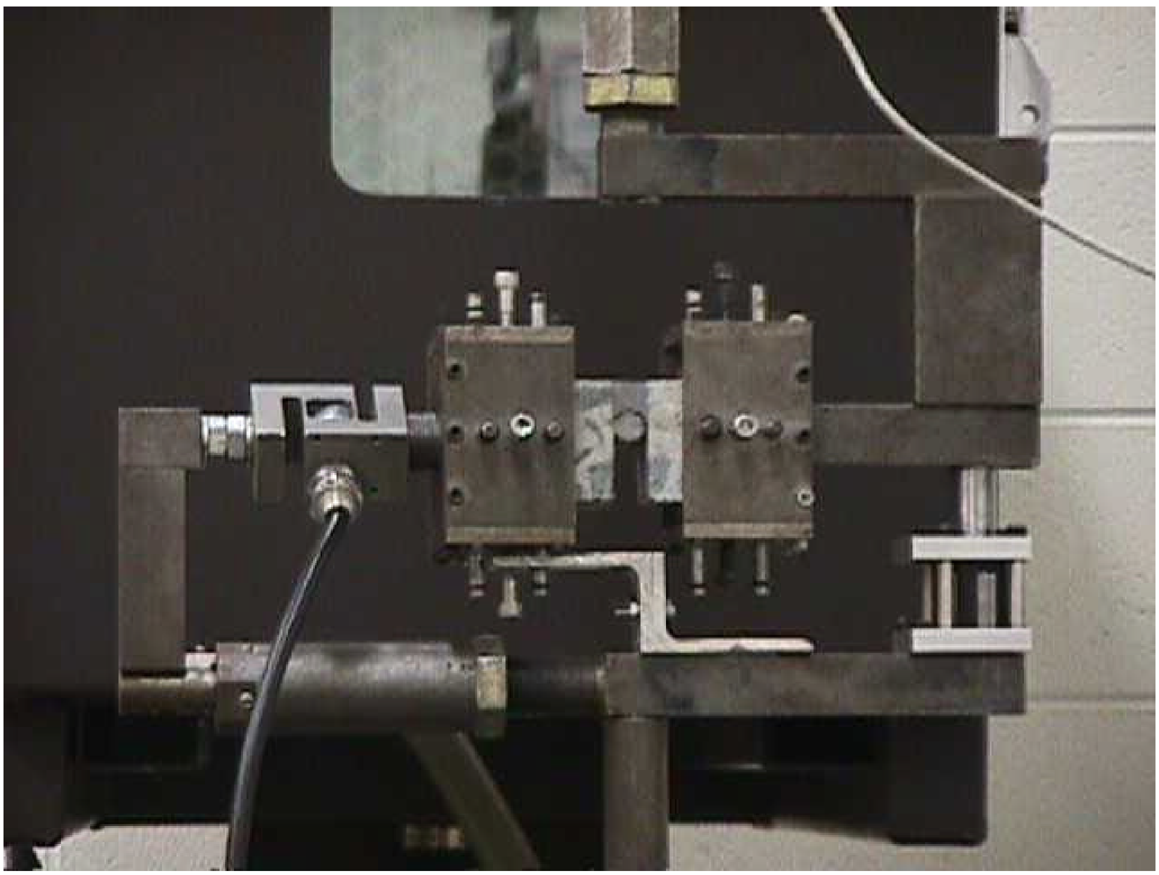

Figure 3.1b A picture of the fixture developed at Virginia Tech

3.2 SPECIMEN PREPARATION

Tested specimens consist of a sealant sandwiched between two concrete cubes (51 x 51 x

51 mm). The concrete cubes were prepared in accordance with the Virginia Department of Transportation (VDOT) specifications for A4 rigid pavements. Portland cement type I and two types of aggregate (granite and limestone) were used. The limestone coarse aggregate was AASHTO 57 and was obtained from Rockydale Quarry in Roanoke, Virginia; the granite coarse aggregate was AASHTO 57 and was obtained from Jack's Mountain Quarry in Franklin County, Virginia. The limestone fine aggregate was manufactured sand and was obtained from Rockydale Quarry in Roanoke, Virginia; the granite fine aggregate was a natural sand and was obtained from Concrete-Ready Mix in Roanoke, Virginia. The physical and chemical properties of the two aggregate types are presented in Tables A.1 through A.4 (Appendix A). The concrete, which had a water to cement (w/c) ratio of 0.42, was cast into 76 x 102 x 406 mm molds and then cut into the required size after 28 days of moist curing. The concrete mix proportions are presented in Tables A.5 and A.6 (Appendix A). Cutting specimens to desired sizes allows the aggregate to be exposed, which simulates saw cutting in the field.

Two types of sealant were used: a field-molded, two-part, cold-formed silicone (Dow Corning 902 Rapid Cure Silicone) and a preformed neoprene compression sealant (D.S. Brown E-686 and E-1006). Silicone sealants are commonly based on a polydimethylsiloxane fluid, which is composed of long-chain siloxane molecules with alternating Si-O bonds (Klosowski and Gant, 1979). Various types of silicones with different properties are available; tensile strengths may vary from 100 to 1000 psi. Neoprene is a synthetic rubber made by polymerizing chloroprene using a Ziegler-Natta catalyst. This catalyst causes the double bonds in neoprene to have a trans configuration (Bruice, 1995).

Two joint widths were considered for each sealant: 6.35 and 12.7 mm for silicone, and 8.7 and 12.7 mm for neoprene. A wooden dowel was placed in between the concrete cubes to achieve the desired joint width for the silicone sealant. Quick-clamps were used to hold the concrete cubes in place around the dowel, and then the backer rod was installed at the prescribed depth within the joint. A two-part primer (Dow Corning Construction Barrier Primer 84) was then applied to the concrete substrate. Duct tape was used to stabilize the backer rod and provide confinement once the sealant was injected. A caulking gun that mixes the two components of the sealant was used to inject sealant into the joint. The sealant was allowed to cure for 21 days at room temperature. Illustrations of the specimen preparation are included in Appendix A.

For the preformed sealant, no dowel was needed between the concrete cubes since preformed sealants are actually compressed to fit within a joint. A quick-clamp was used to hold two concrete cubes after the lubricant/adhesive was applied to the substrate. Then the preformed sealant was compressed and inserted in the joint. The amount of compression applied to the sealant depends on the shape factor of the sealant. The lubricant/adhesive was allowed to cure for 48 hours at room temperature. All substrate preparation and sealant installation was performed according to the manufacturer's specifications. Each specimen was visually inspected for flaws prior to environmental conditioning; specimens with flaws were not included in the study.

The depth and width of the silicone (field-molded) sealants were measured, and the shape factor (depth-to-width-ratio) could be calculated subsequently; a shape factor of 1.0 was desired. However, the shape factor was affected by the additional tooling required for a concave shape at the top of the silicone sealant. This concave shape is to insure that, in the field, the sealant will not bulge from the joint when the concrete slabs expand, resulting in extrusion by overpassing vehicles. Also, the concave shape minimizes the stresses that arise within the sealant due to mechanical loading (Wang and Weisgerber, 1993). It appeared that caulking gun provided to apply the silicone sealant did not mix the sealant components adequately.

The preformed sealants were also inspected. It is necessary that the preformed sealant is installed to the prescribed depth within the joint, and that it has the proper orientation within the joint. The lubricant/adhesive layer was also inspected for flaws. The specimen preparation was much easier for the preformed neoprene, resulting in more reproducible specimens.

3.3 TESTING PROGRAM

Because of the relative movement of one slab with respect to the adjacent slab across the joint during vehicular passing, the departure slab undergoes vertical loading in one direction, and when the vehicle applies load to the approach slab, the departure slab undergoes a rebound in the opposite direction. Thus, the traffic loading can be simulated by a sinusoidal wave pattern. Considering the field loading period, distance between axles, and highway speed, a loading wave at a frequency of 5 Hz, followed by a relaxation of 0.4 seconds, is considered a reasonable approximation of field-loading pattern (Figure 3.2). The total “relative” dynamic vertical deflection was 6.4 mm, a threshold value for joints is usually considered for maintenance.

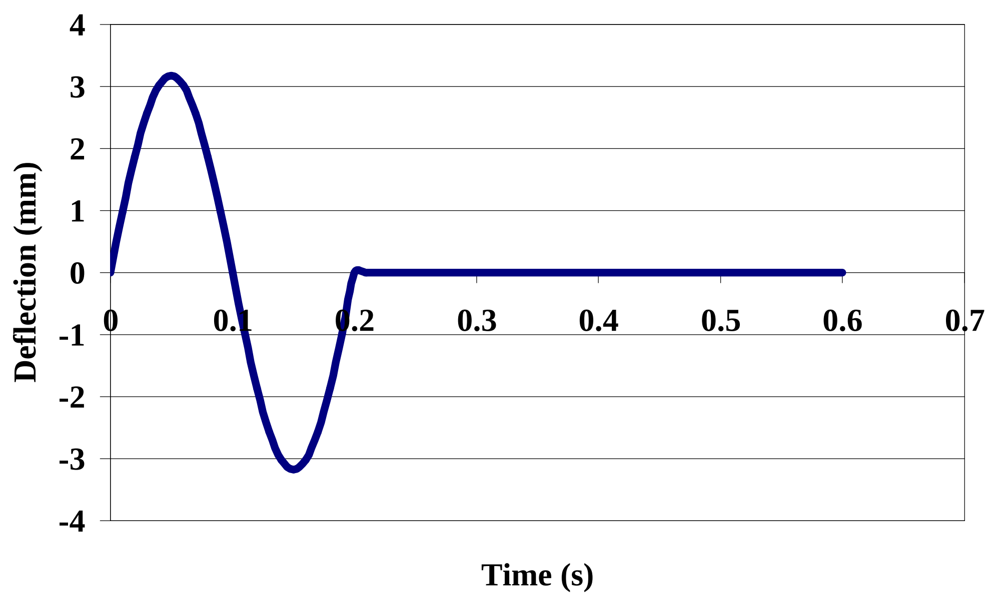

Figure 3.2 Vertical deflection cycle used for testing

Static tension on the joint sealant (which is a critical cause of failure as indicated earlier) was also applied during testing, which simulates slab contraction at low temperatures.

One horizontal deflection was used in the testing (25% of the joint width).

Environmental conditioning was applied (at room temperature) prior to testing. The environmental conditioning includes partial submersion in distilled water (DW), partial submersion in a jet fuel (JF), and exposure to ultraviolet light (UV). Sealants were exposed to jet fuel and distilled water by inverting the specimens and then submerging them in a 12.7 mm deep pool, resulting in only part of the specimen coming in contact with fluid. All specimens were subjected to partial submersion in distilled water for 120 hours. A relative humidity of 100% has the same effect on a sealant as total water immersion (Klosowski, 1989). Lubricating oil and hydraulic fluid were found to cause spalling in concrete airport runways when coupled with heat cycles (McVay *et. al.*, 1993). Therefore, specimens were partially submerged in Jet Fuel A for 1000 hrs to simulate constant exposure over the entire life cycle of the sealant. However, specimens with silicone sealant started swelling after being exposed to jet fuel for a few hours. A decision was made to stop exposing those specimens to jet fuel after two days. Specimens were tested before and after 1000 hrs of UV exposure using UV-A spectrum lamps, which closely replicate sunlight wavelengths (Fedor, 1992). The UV-A light spectrum lies between wavelengths of 320 to 400 nm. In addition, some specimens were exposed to both UV and jet fuel in order to examine the synergistic effects of the exposure conditions. The testing matrix is presented in Table 3.1.

The nomenclature used to name the specimens is fairly simple. An example is as follows: SG12_25JF1. The first letter signifies whether the sealant is silicone (S) or neoprene (N). The second letter indicates the aggregate type used in the concrete: limestone (L) and granite (G). The next number or letter indicates the sealant size. For the silicone sealant, a 6 signifies a 6.35 mm joint width and a 12 signifies a 12.7 mm joint width. For the neoprene, a number is not used to define the joint width; a B signifies the bigger sealant size (12.7 mm joint width), and an S signifies the smaller sealant size (8.7 mm joint width). The next number reports the horizontal tension applied to the sealant as a percentage of the joint width. The exposure conditions are: JF for jet fuel and UV for ultraviolet radiation. Finally, the duplicate identification is given: one (1) or two (2).

Table 3.1 Testing parameter matrix

	Sealant Type			
	Silicone		**Neoprene**	
Limestone Aggregate	**6.35 mm Joint Width**	**DW**	**8.7 mm Joint Width**	
		JF+DW		
		UV+DW		**UV+DW**
	12.7 mm Joint Width	**DW**	**12.7 mm Joint Width**	
		JF+DW		
		UV+DW		
Granite Aggregate	**6.35 mm Joint Width**		**8.7 mm Joint Width**	**DW**
		JF+DW		
		UV+DW		**UV+DW**
		UV+JF+DW		**UV+JF+DW**
	12.7 mm Joint Width	**DW**	**12.7 mm Joint Width**	
				JF+DW
				UV+DW

***Horizontal Deflection = 25%**

In summary, the experimental design includes the testing of the following inter-related parameters: two sealants, two aggregate types, two joint widths per sealant type, one horizontal deflection, and environmental conditioning.

CHAPTER FOUR

MEASUREMENTS AND DATA ANALYSIS

4.1 OBSERVATIONS

Measurements obtained were both qualitative and quantitative. Qualitative measurements mostly involved inspection of the specimens prior to environmental conditioning, inspection following the environmental conditioning and inspection as the mechanical load was being applied. Also, notes were taken during specimen preparation; therefore, addressing any application problems with either the field-molded or preformed sealants.

Specimens were loaded to failure or for two weeks of loading, whichever occurred first. The failure was considered when 20% of the sealant area had failed either adhesively or cohesively, which corresponded to a constant value of horizontal stress. The failure criterion corresponds to the situation where the change between two consecutive horizontal stress values varies less than 0.00003%. The collected data were analyzed for the type of sealant failure, the effect of aggregate, horizontal deflection, joint width, and environmental conditioning. Specimens were loaded and examined visually after approximately every 130,000 loading cycles.

The collected data (horizontal and vertical stresses, horizontal and vertical deflections, and number of cycles) were statistically analyzed following the conclusion of the testing.

The environmental conditioning seemed to have more effect on the field-molded silicone than on the preformed neoprene sealant. Silicone specimens that were exposed to 1000 hours of UV-A radiation appeared to become slightly stiffer; however, no adhesive or cohesive damage was visually evident. The sealant color also became duller with UV exposure. The effect of jet fuel immersion was pronounced on the silicone specimens. Originally, all specimens were to be immersed in a 12.7-mm-deep layer of jet fuel for 1000 hours. The silicone sealant specimens showed severe swelling after 48 hours, and thus were removed from the jet fuel. The swelling subsided somewhat as the jet fuel evaporated from the silicone. The specimens that were exposed to UV-A followed by jet fuel exhibited extensive adhesive failure. Immersion in distilled water, on the other hand, had no visible effect on the silicone sealant.

The preformed neoprene sealant was not considerably affected by the environmental conditioning. The UV-A exposure dulled the color of the sealant, but it did not affect the integrity of the seal or the lubricant/adhesive layer. The neoprene specimens endured 1000 hours of jet fuel exposure without significant deterioration; some of the lubricant/adhesive layer dissolved in the jet fuel, but the neoprene still remained bonded (observed visually) to the concrete cubes in some areas. The neoprene showed no swelling or dissolution in the jet fuel. Moisture had no visual effect on the neoprene or the lubricant/adhesive layer. Environmentally conditioned specimens are shown in Appendix B.

The failure mechanisms for the two types of sealants were completely different during mechanical testing. For the silicone specimens, failure would usually initiate at the sealant/concrete interface just above the backer rod, generally on the approach slab side. The crack would then propagate to the surface of the sealant with continued loading; however, it is not certain that the failure mode is entirely adhesive without a surface analysis of the failed specimens.

The neoprene specimens would always withstand the allotted two weeks of mechanical loading, provided that the sealant was in compression. As a preliminary test, two neoprene specimens were evaluated using the same mechanical vertical loading, but they had no compression or tension in the horizontal direction. Failure, which occurred quite quickly, was completely within the lubricant/adhesive layer; therefore, horizontal compression is essential for these sealants to function properly.

4.2 CYCLIC-LOADING RESULTS FOR SILICONE

The silicone sealant's ability to withstand the applied loading cycles depended on the effect of environmental conditioning, the type of aggregate used in the PCC, and the joint width. The horizontal stress data collected during the testing was fit to a typical fatigue regression line according to the following equation: **Stress = A(Number of Cycles)^{B} + C**.

4.2.1 Effect of Environmental Conditioning

The environmental conditioning, except for moisture, appeared to have an adverse effect on the silicone sealant performance. Jet fuel exposure resulted in severe swelling, but did not always cause early failure. The silicone would swell approximately 100% and become very soft when in contact with the jet fuel; however, the swelling would subside substantially a few days after ceasing the jet fuel exposure. Nevertheless, the sealant would still be notably softer than one that had not been exposed to jet fuel. This increased the sealant compliance, as is evident by the lower measured stresses when compared to control specimens. Silicone exposed to jet fuel usually was able to withstand a greater number of loading cycles compared to the control, given that no cracks were initiated during the swelling period. However, in the field, the presence of gravel and debris on the pavement surface, in addition to vehicles passing, will certainly cause a soft sealant to be torn from the joint. Figures 4.1, and C.1 and C.2 (Appendix C) show the cyclic loading curves for SG6_25JF1, SL12_25JF1, and SL6_25JF2, respectively, while Figures 4.2, and C.3 and C.4 present the cyclic loading curves for control specimens. Specimen SG6_25JF1 achieved failure within the first week of cyclic loading; adhesive debonding began at the bottom of the sealant (on one side only) and propagated upward. However, debonding ultimately was evident on both sides of the sealant. For the SL12_25JF1 specimen, adhesive failure began only a couple of days after initiating cyclic loading; however, 20% adhesive loss could not be accurately inspected due to the depth of the debondment. The number of cycles to failure for this specimen is reported at approximately 60% adhesive loss. SL6_25JF2 had no adhesive or cohesive failure during one week of cyclic loading; the number of cycles to failure was extrapolated from the regression curve.

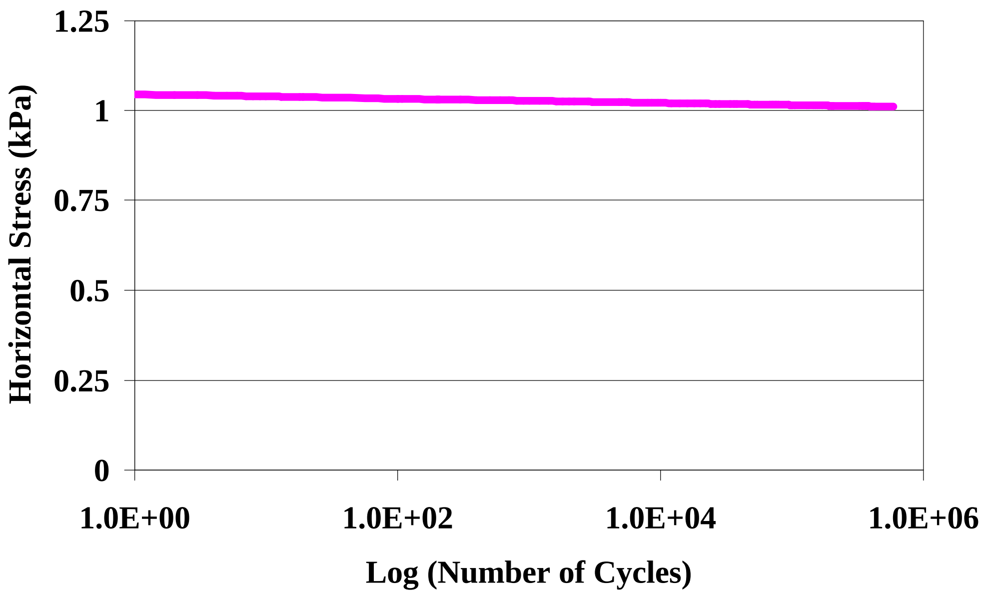

Figure 4.1 Horizontal stress versus number of cycles for silicone sealant used with concrete (with granite aggregate) at a 6.35 mm joint width, 25% static tension, and exposed to jet fuel and distilled water

The effect of UV is contrary to that of the jet fuel. When exposed to UV, there is no noticeable volumetric change in the silicone; however, the sealant does become stiffer.

Again, this is evident by the higher stress levels measured during testing. An increased modulus will make the sealant more tear-resistant to debris in the field, but hinders it during the fatigue testing. Figures 4.2, and C.3 and C.4 (Appendix C) present the fatigue curves for SG6_25UV2, SL12_25UV1, and SL6_25UV1, respectively. SG6_25UV2 failed quite dramatically, as almost 80% debonding occurred within the first 100,000 cycles. SL12_25UV1 developed 20% adhesive failure after one and a half weeks of cyclic loading; the failure, again, propogated from the bottom of the sealant upward. Quick failure was also evident with SL6_25UV1, although some uncured sealant is evident on the fracture surface.

The effect of moisture on the silicone sealant performance was minimal. Neither swelling nor sealant stiffening occurred during the 120 hours of exposure. Figures 4.3, and C.5 and C.6 (Appendix C) present the fatigue curves for SG12_25_2, SL6_25_1, and SL12_25_1, respectively. The SG12_25_2 specimen only developed 10% adhesive loss after two weeks of cyclic loading; the number of cycles to failure was extrapolated from the regression curve and is also shown in Figure 4.3. The SL6_25_1 surprisingly failed after only 18,000 cycles; lack of curing was noticed in the sealant fracture surface. SL12_25_1 reached failure after five days of cyclic loading; failure initiated under the sealant (on the side of the approach slab) and propagated upward.

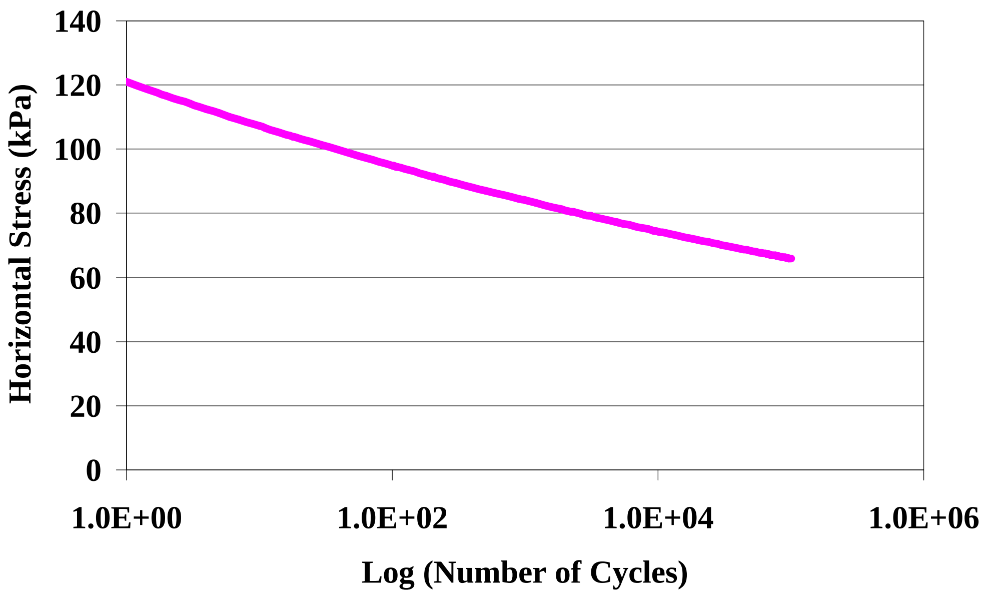

Figure 4.2 Horizontal stress versus number of cycles for silicone sealant used with concrete (with granite aggregate) at a 6.35 mm joint width, 25% static tension, and exposed to UV-A light and distilled water

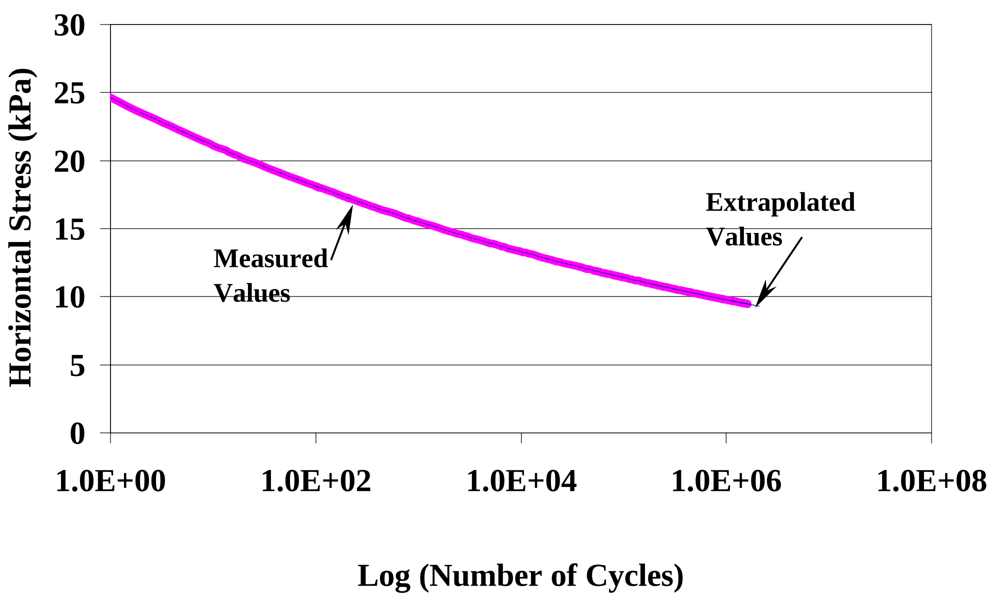

Figure 4.3 Horizontal stress versus number of cycles for silicone sealant used with concrete (with granite aggregate) at a 12.7 mm joint width, 25% static tension, and exposed to distilled water

The synergistic effect of the jet fuel, UV, and moisture on the sealant performance was quite profound. The specimens were first exposed to 1000 hours of UV, followed by 48 hours of jet fuel exposure and 120 hours of moisture exposure. The silicone sealant again became stiffer during UV exposure and swelled tremendously during jet fuel exposure. Following the UV and jet fuel conditioning, over 25% adhesive failure was evident prior to testing; the debonding occurred while the specimen was exposed to jet fuel. One specimen was tested despite the obvious failure that had already occurred. Due to the increased compliance of the sealant, the adhesive debonding did not increase appreciably. The fatigue curve for SG6_25UVJF2 is shown in Figure 4.4. This specimen had 20% adhesion loss after the environmental conditioning. The flaw did not lengthen, however, during ten days of cyclic loading.

In addition, some specimens were used to investigate the simultaneous effect of static horizontal stress and jet fuel. Horizontal deflections at 25% and 50% were applied to specimens of both joint widths. The tensile stress was developed by clamping the sealant specimens around wooden dowels with a larger diameter than the joint width. Each day, 4.93 ml (one teaspoon) of jet fuel was applied to coat the entire surface of the specimen. Despite the simultaneous exposure to the horizontal tension and jet fuel, no cohesive or adhesive failure occurred. The swelling that occurred in the sealant due to the jet fuel relieved the horizontal tension in the specimen.

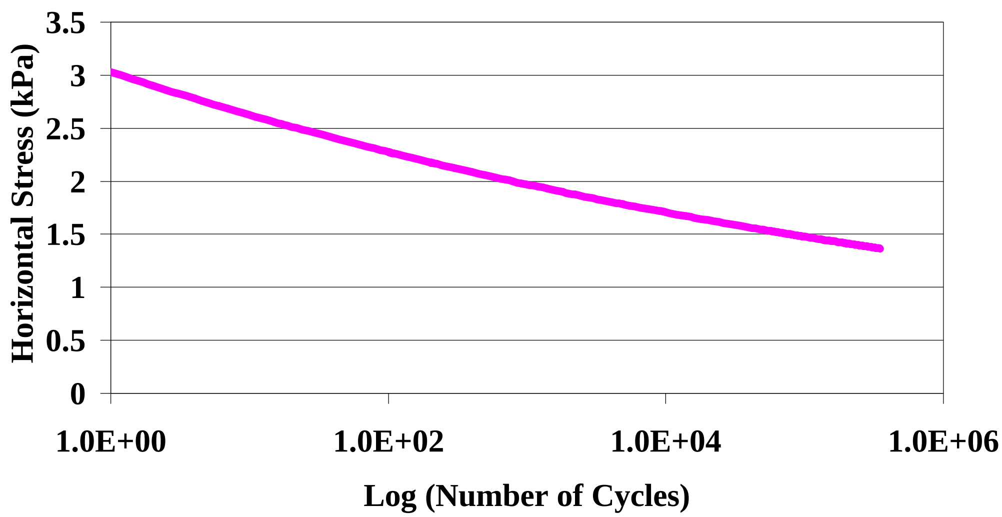

Figure 4.4 Horizontal stress versus number of cycles for silicone sealant used with concrete (with granite aggregate) at a 6.35 mm joint width, 25% static tension, and exposed to jet fuel, UV-A light, and distilled water

4.2.2 Effect of Aggregate Type

The effect of aggregate type on silicone performance was very pronounced in an earlier study at Virginia Tech (Abo-Qudais, 1995). In that study, the silicone sealant failed rather quickly when used with concrete containing limestone aggregate. In this study, the use of a primer has proved effective. The performance of silicone sealant with limestone and granite aggregate concrete seems to be comparable. Similar durability is seen between the two aggregate types despite the environmental conditioning of the specimens. The effect of aggregate type on silicone sealant durability is shown in Figures 4.5, and C.7 and C.8 (Appendix C).

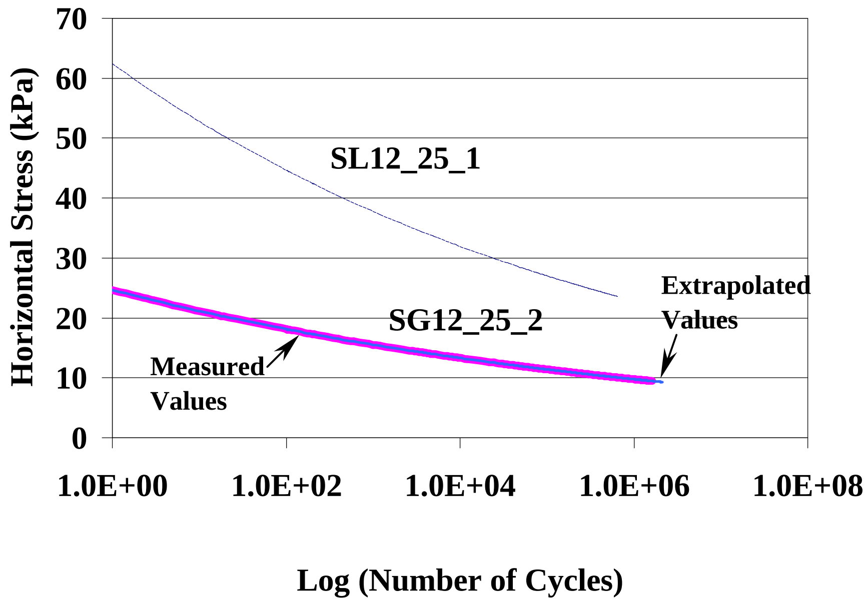

Figure 4.5 Effect of aggregate type on durability of silicone sealant at a 12.7 mm joint width, 25% static tension, and exposed to distilled water

4.2.3 Effect of Joint Width

For the silicone sealants, the large joints (12.7 mm) performed better than the small joints (6.35 mm). The shape factor of the sealant was held constant despite different joint widths; the depth of the sealant is equal to its width. The applied vertical deflection (3.175 mm) is independent of the joint width; therefore, the applied shear strain is different for the two joint widths. The smaller joints (6.35 mm) were subjected to 50% shear strain, while the larger joints (12.7 mm) were subjected to 25% shear strain; the resulting vertical stresses due to the applied cyclic deflection are thus smaller for the larger joints. The larger joints also seem more durable to the environmental conditioning.

Although the swelling is severe in both joint sizes due to jet fuel exposure, the sealant in the larger joint does not seem as fragile once the swelling has subsided. The effect of the UV also seems to depend on the size of the joint. The UV does not seem to penetrate the full depth of the sealant in the larger joints, making them less brittle than the sealants in the smaller joints. The effect of joint width on silicone sealant durability is shown in Figures 4.6, and C.9 and C.10 (Appendix C). Pictures of all failed specimens are included in Appendix D.

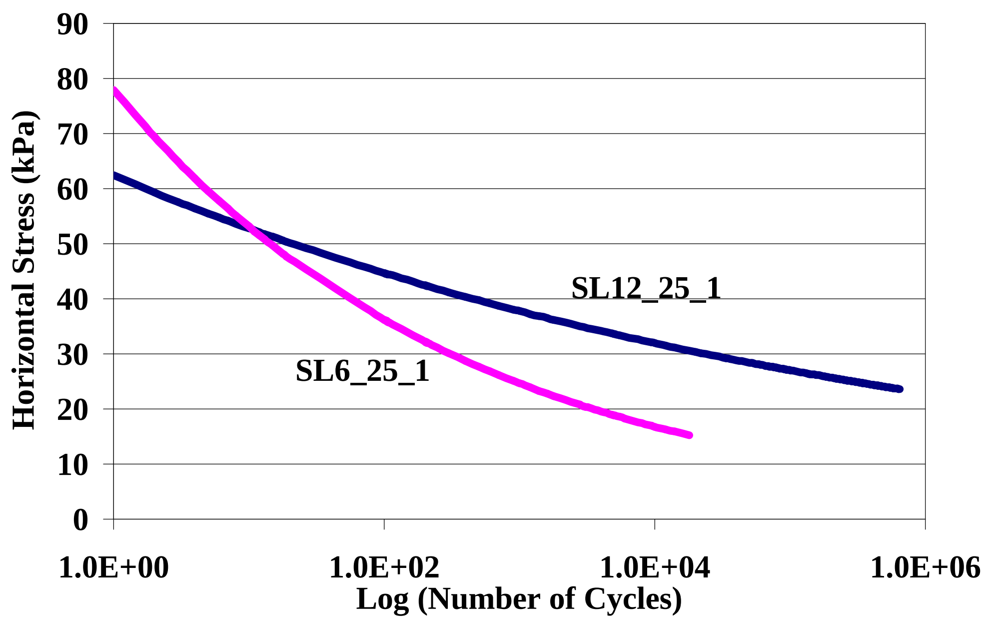

Figure 4.6 Effect of joint width on durability of silicone sealant used with concrete with limestone aggregate, 25% static tension, and exposed to distilled water

4.3 CYCLIC LOADING RESULTS FOR NEOPRENE

The durability of the preformed neoprene sealant was slightly affected by environmental conditioning, the type of aggregate used in the PCC, and joint width (sealant size). Despite the presence of the lubricant/adhesive, the preformed neoprene sealant must be kept in compression to avoid drastic failure. If the sealant is not compressed, or if it is under tension, it fails quickly. Any failure that was observed for this sealant type was purely adhesive.

The same fatigue equation that was applied to fit the silicone sealant data was also used for the neoprene sealant. However, because the neoprene sealant is in compression, the sign convention (Tension +, Compression -) changes the shape of the fatigue curve.

4.3.1 Effect of Environmental Conditioning

The effect of environmental conditioning on neoprene sealant performance was insignificant. Jet fuel exposure was the only type of conditioning that remotely had an effect on the neoprene sealant performance; however, the neoprene specimens were able to endure the entire 1000 hours of partial immersion. The excess lubricant/adhesive on the concrete cubes dissolved in the jet fuel, but only a small amount that actually adhered the sealant to the cubes dissolved. However, these sealant specimens performed similarly to those that were not exposed to jet fuel. The fatigue curve for NGB25JF2 is shown in Figure 4.7. Although, some of the excess adhesive/lubricant had dissolved in the jet fuel, NGB25JF2 withstood two weeks of cyclic loading. The extrapolated number of cycles to failure is also shown in Figure 4.7.

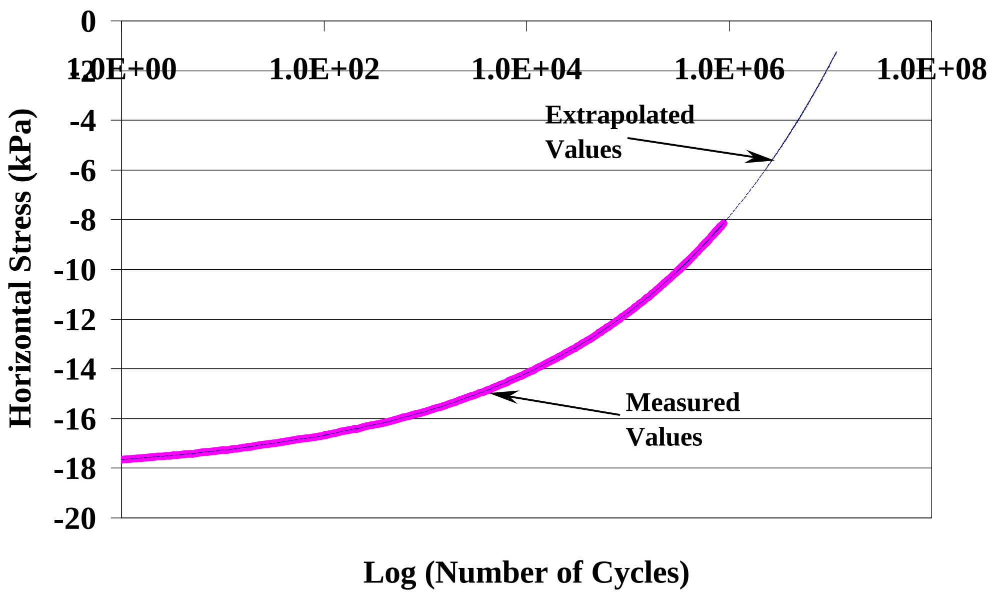

Figure 4.7 Horizontal stress versus number of cycles for large neoprene sealant used with concrete (with granite aggregate), 25% static compression, and exposed to jet fuel and distilled water

The effect of UV exposure was minimal; after 1000 hours of exposure, slight fading of the sealant was evident with no adhesive or cohesive deterioration. No difference in performance was noticeable when the specimens were subjected to cyclic loading, compared to the control. The effect of loading cycles for NGB25UV2 is shown in Figure 4.8. NGB25UV2 also endured the entire two weeks of cyclic loading; the extrapolated number of cycles to failure is shown in Figure 4.8.

The effect of moisture on the neoprene performance was trivial. After 120 hours of partial immersion in deionized water, the neoprene exhibited no swelling, adhesive failure, or cohesive failure. Specimens that were exposed to all three environmental conditions were also quite durable. No deterioration of the sealant or the lubricant/adhesive layer was apparent, as shown in Figure 4.9. The extrapolated number of cycles to failure for NGS25JFUV1 is also illustrated in this figure.

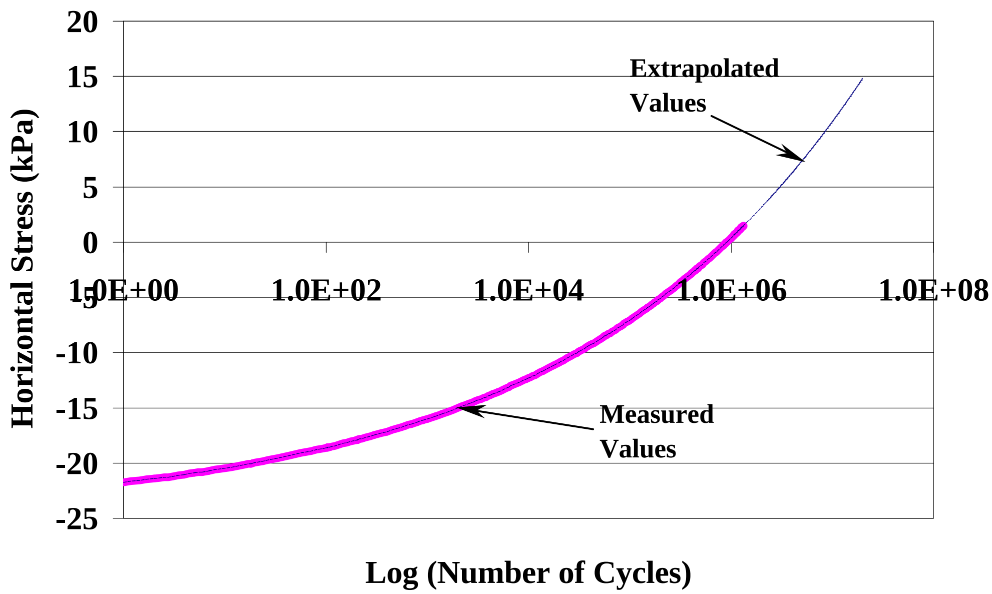

Figure 4.8 Horizontal stress versus number of cycles for large neoprene sealant used with concrete (with granite aggregate), 25% static compression, and exposed to UV-A light and distilled water

4.3.2 Effect of Aggregate Type

The effect of aggregate type on neoprene sealant performance was not expected to be significant since adhesion of the sealant to the concrete surface is not critical for achieving good durability. Specimens with different concrete aggregate types and exposed to identical environmental conditions were expected to perform similarly under cyclic loading. This trend is illustrated in Figure 4.10.

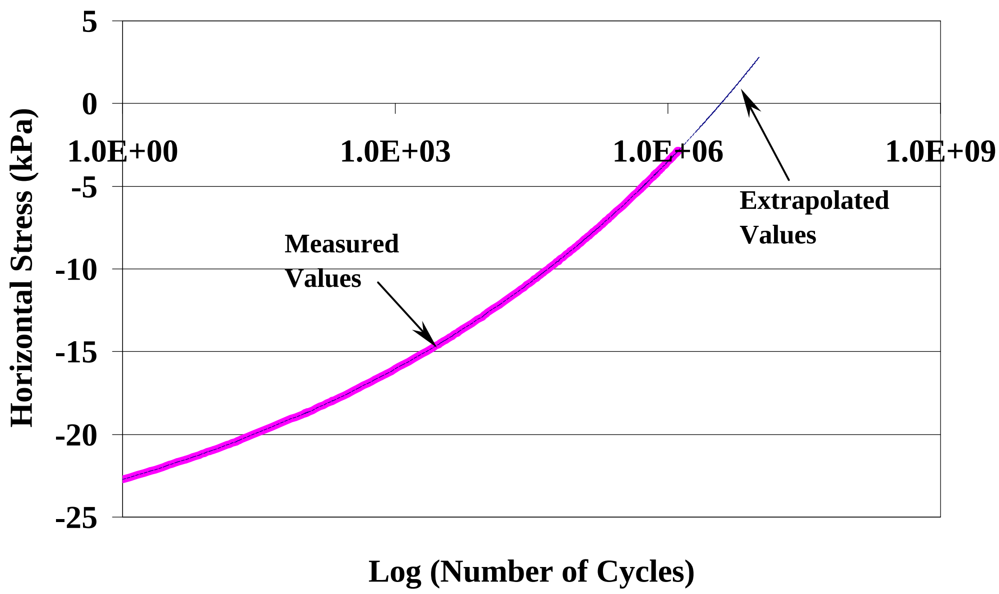

Figure 4.9 Horizontal stress versus number of cycles for small neoprene sealant used with concrete (with granite aggregate), 25% static compression, and exposed to jet fuel, UV-A light, and distilled water

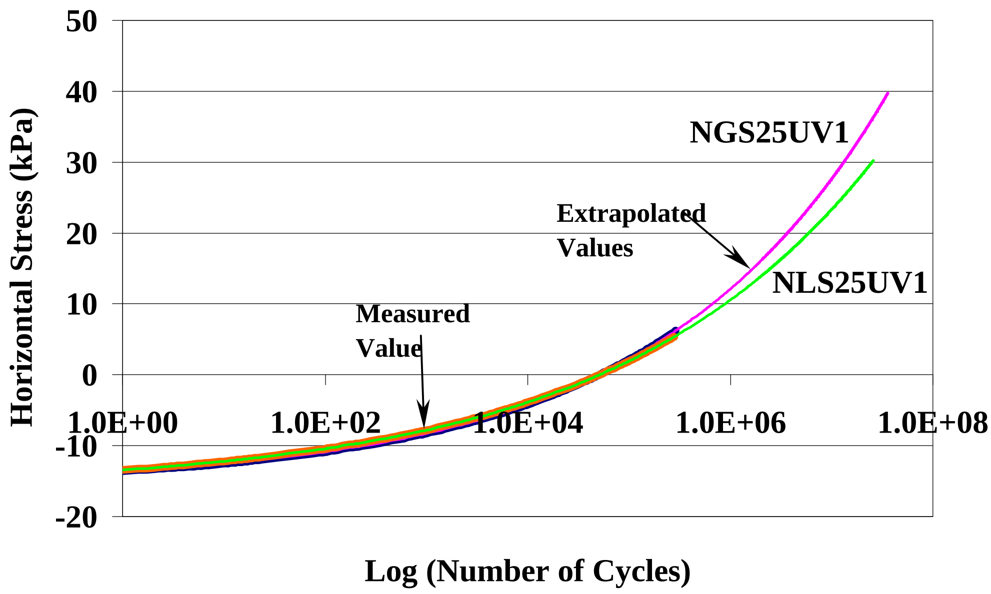

Figure 4.10 Effect of aggregate type on durability of small neoprene sealant at 25% static compression, and exposed to UV-A light and distilled water

4.3.3 Effect of Joint Width

The joint width does not greatly affect the sealant performance as long as the proper size sealant is used for a certain joint width and expected horizontal slab movement, so that the sealant remains in compression. Figure 4.11 illustrates the effect of joint width on neoprene sealant performance. Table 4.1 contains the regression parameters and number of cycles to failure for each specimen.

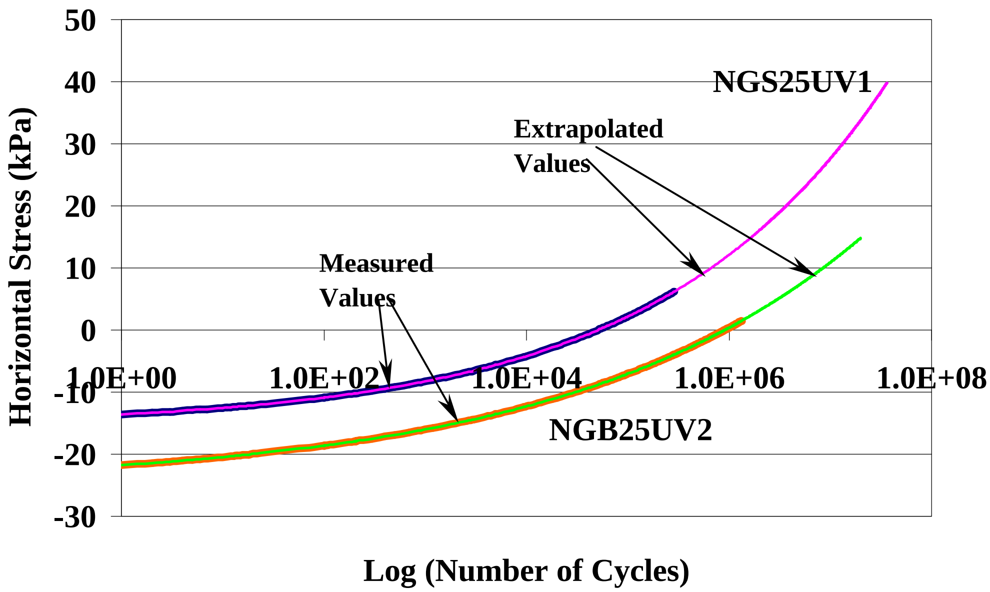

Figure 4.11 Effect of joint width on durability of neoprene sealant used with concrete with granite aggregate, 25% static compression, and exposed to UV-A light and distilled water

Table 4.1 Regression coefficients and number of cycles to failure for each specimen

Specimen	A	B	C	R^2	Number of cycles to failure
NGB25JF2*	0.64	0.202	-18.30	0.938	11,500,000
NGB25UV2*	3.13	0.151	-24.90	0.978	20,000,000
NLS25UV1*	2.49	0.171	-15.92	0.980	26,000,000
NGS25_2*	3.43	0.157	-17.28	0.976	26,000,000
NGS25UV1*	1.91	0.194	-15.53	0.958	36,000,000
NGS25JFUV1*	7.53	0.092	-30.24	0.904	10,000,000
SG12_25_2*	24.65	-0.067	0	0.893	2,100,000
SG6_25JF1	1.05	-0.003	0	0.011	590,000
SG6_25JFUV2**	3.03	-0.062	0	0.117	--
SG6_25UV2	121.02	-0.053	0	0.912	100,000
SL12_25_1	62.40	-0.073	0	0.927	650,000
SL12_25UV1	53.41	-0.056	0	0.947	1,260,000
SL12_25JF1***	12.46	-0.110	0	0.702	660,000
SL6_25_1	77.92	-0.167	0	0.668	18,000
SL6_25UV1	26.42	-0.031	0	0.629	325,000
SL6_25JF2*	41.90	-0.042	0	0.815	3,000,000

*Specimen did not fail during cyclic loading. Regression line was used to project when failure would occur.

**Specimen failed during environmental conditioning.

***Number of cycles to failure for this specimen was at 60% adhesion loss.

CHAPTER FIVE

FINDINGS AND CONCLUSIONS

5.1 FINDINGS

Throughout the course of this research, the following findings were noted:

- The shear at a joint sealant resulting from vehicle axle loading can be accurately simulated by a full sinusoidal wave followed by a relaxation period.
- The installation of preformed neoprene compression sealant is much easier than the field-molded silicone.
- The caulking gun used for mixing and injecting the two-part silicone sealant is unsatisfactory, as to inconsistent mixing of the sealant parts may result.
- Exposure of silicone specimens to simultaneous horizontal tension and jet fuel did not result in any adhesive or cohesive failure. Cyclic shear is necessary to initiate failure.
- Failure of the field-molded silicone usually initiates at the bottom of the sealant (near the approach slab) and then propagates upward.

5.2 CONCLUSIONS

Based on this research, the following conclusions can be made:

- The use of a primer greatly enhances the performance of field-molded silicone sealant used with concrete containing limestone aggregate.
- This silicone sealant should not be used in concrete pavements where frequent fuel spills are expected. In addition, UV exposure tends to stiffen the silicone sealant.
- 12.7-mm-joint width enhances the durability of the silicone sealant compared to a 6.35-mm-joint width, provided that the shape factor remains constant.
- Preformed neoprene sealants must be in compression to maintain good durability. Concrete aggregate type and joint width have no effect on preformed neoprene sealant performance. In addition, environmental conditioning, such as UV, moisture, and jet fuel exposure, has an insignificant effect on the durability of preformed neoprene sealants.

CHAPTER SIX

RECOMMENDATIONS

The following recommendations may be considered for improving the quality of this testing program and to shed further light on joint sealant performance in concrete pavements:

- The effect of environmental conditioning when applied simultaneously to fatigue loading may be examined.
- Life-cycle cost analysis of the evaluated sealants needs to be performed, based on laboratory testing and correlated with field analysis.
- Research needs to be conducted on evaluating the performance of joint sealants in resealed joints.

REFERENCES

Abo-Quadis, S.A. (1995), “Mechanistic Service Life Prediction of Rigid Pavement Joint Sealant: A New Laboratory Testing Technique.” PhD Dissertation, The Via Department of Civil Engineering, Virginia Tech, Blacksburg, VA.

ACI Committee 503 (1992), Guide for the Selection of Polymer Adhesives with Concrete. American Concrete Institute, Detroit, MI.

Aklonis, J. J., and MacKnight, W. J. (1983), Introduction to Polymer Viscoelasticity. John Wiley and Sons, Inc., New York, NY.

Bodocsi, A., Minkarah, I. A., and Arudi, R. S. (1993), “Analysis of Horizontal Movements of Joints and Cracks in Portland Cement Concrete Pavements.” Transportation Research Record, No. 1392, Washington DC, pp. 43 -52.

Bruice, P.Y. (1995), Organic Chemistry, Prentice Hall, Upper Saddle River, NJ.

Bugler, J. W. (1983), "Problems and Solutions in Rigid Pavement Joint Sealing," Journal of Public Work, Vol. 114, No. 9, Ridgewood, NJ, pp. 93-96.

Callister, W.D. (1994), Materials Science and Engineering: An Introduction, 3rd ed., John Wiley and Sons, Inc., New York., NY.

Collins, A. M., Magnum, W. D., Fowler, D. W., and Meyer, A. H. (1986), Improvement Methods for Sealing Joints in Portland Cement Concrete Pavements, Report No. 385-1, Center for Transportation Research, University of Texas at Austin, Austin, TX.

Evans, R. M. (1987), “Waterproofings and Sealants for Concrete.” Polymeric Materials: Science and Engineering, Vol. 56, pp. 486 - 489.

Fedor, G. R. (1992), “Usefulness of Accelerated Test Methods for Sealant Weathering.” ASTM Special Technical Publication, STP 1200, ASTM, Jerome M. Klosowski, Ed., Philadelphia, PA, pp. 10-18.

Gurjar, A., Zollinger, D. G., and Tang, T. (1996), “Laboratory Study of Strain and Age Effects on a Concrete Pavement Joint Sealant.” Presented at the 75th Annual Meeting of the Transportation Research Board, Washington, DC.

Haddad, Y. M. (1995), Viscoelasticity of Engineering Materials. Chapman and Hall, Great Britain.

Huang, Y. H. (1993), Pavement Analysis and Design. Prentice Hall, Inc., Englewood Cliffs, NJ.

Jackson, M. T. (1988), “Silicones & Space-Age Materials for Age Old Problems.” New Pavement Materials, American Society of Civil Engineers, Nashville, TN.

Jones, G. M., Peterson, D. T., and Vayas, R. K. (1973), Evaluation of Preformed Elastomeric Pavement Joint Sealing System and Practices, NCHRP, No. 19, Washington, DC, pp. 32-41.

Kerr, S. R. and Lin, S. B. (1994), “Recent Advances in Silicone PSA Technology,” Adhesives Age, Vol. 37, pp. 36-43.

Kinchen, R. W., Temple, W. H., Brut, W. T., Azar, D. G. (1977), Evaluation of Joint Sealant Materials, Louisiana Highway Research,

Klosowski, J. M. (1989), Sealants in Construction. Marcel Decker, Inc. New York, NY.

Klosowski, J. M. and Gant, G. A. L. (1979), “The Chemistry of Silicone Room Temperature Vulcanizing Sealants,” Plastic Mortars, Sealants, and Caulking Compounds, ACS Symposium Series 113, Washington DC, pp. 113-126.

Kozlov, G. S., and Cosaboom, B. (1977), “Preformed Elastomeric Joint Sealers for Bridges.” Transportation Research Record, No. 651, Washington DC, pp. 53 - 63.

Kuenning, W. H. (1962), "Laboratory Tests of Sealers for Sawed Joints," Highway Research Board, No. 211, Washington DC, pp. 1-12.

Kumar, N.R., Gupta, B.R., and Bhowmick, A.K. (1993), “Rheological Behavior and Processability of Neoprene and Acrylic Rubbers,” Polymer Engineering and Science, Vol. 33, No. 15, pp. 1002-1008.

McGhee, K. H. (1995), "Design, Construction, and Maintenance of PCC Pavement Joints." Synthesis of Highway Practice, Transportation Research Record, Washington DC, No. 211.

McVay, M. C., Smithson, L. D., and Manzione, C. (1993), “Chemical Damage to Airfield Concrete Aprons from Heat and Oils.” ACI Materials Journal, Vol. 90, No. 3, pp. 253 – 258.

Noble, D. F. (1987), Field Evaluation of Three Joint Sealants. Virginia Transportation Research Council, Charlottesville, VA.

Noll, W. (1968), Chemistry and Technology of Silicones, Academic Press, New York, NY.

Oehler, L. T. and Bashore, F. J. (1973), "Michigan's Experience with Neoprone Compression Seals," ACI Journal, No. 70-22, Detroit, MI. pp. 214-220.

Ray, G. K. (1986), “Pavement Joint Sealing – Where Are We and How Did We Get Here?” ACI Special Publication 94-21, pp.371 – 377.

Reagan, F. (1992), “Performance Characteristics of Traffic Deck Membranes.” Concrete International: Design and Construction, Vol. 14, No. 6, pp. 48 - 52.

Rosen, S. L. (1993), Fundamental Principles of Polymeric Materials, 2nd ed., John Wiley and Sons, Inc., New York, NY.

Shisler, III, F. W. and Klosowski, J. M. (1990), "Sealant Stresses in Tension and Shear," Building Sealants: Materials Properties and Performance, STP 1069, ASTM, Thomas F. O’Connor, Ed., Philadelphia, PA, pp. 95-107.

Shober, S. F. (1986), “Portland Cement Concrete Pavement Performance as Influenced by Sealed and Unsealed Contraction Joints.” Transportation Research Record, No. 1083, Washington DC, pp. 7 - 12.

Steffes, R. F. (1993), “Innovative Leak Test for Pavement Joint Seals.” Transportation Research Record, No. 1083, Washington DC, pp. 7-12.

Stevens, M. P. (1990), Polymer Chemistry: An Introduction. 2nd Edition, Oxford University Press, Inc, New York, NY.

Thornton, J. B. (1978), “Investigation into the Performance of Rigid Pavement Joint and Material,” Proceedings of International Conference on Concrete Pavement Design, Purdue University, IN, pp. 435-446.

Tock, R. W. (1990), “Temperature and Moisture Effects on Engineering Properties of Sealants.” Building Sealants: Materials, Properties, and Performance, STP 1069, ASTM, Philadelphia, PA, pp. 167 - 173.

Waddell, J. J. and Dobrowolski, J. A. (1993), Concrete Construction Handbook, 3rd Edition, Joseph J. Waddell, Joseph A. Dobrowolski, Ed., McGraw-Hill, Inc.

Wang, C., and Weisgerber, F. E. (1993), “Effects of Seal Geometry on Adhesive Stresses in Pavement Joint Seals.” Transportation Research Record, No. 1392, Washington DC, pp. 64 - 70.

Weisgerber, F. E., Minkarah, I. A., and Malon, S. R. (1987), “Observations from a Field Study of Expansion Joint Seals in Bridges.” Transportation Research Record, Washington DC, No. 1118, pp. 39 - 42.

Wolters, R. O. (1974), Field Evaluation of Joint Seal Material, Minnesota Department of Highway, Report No. ALA(2), Minneapolis, MN.

Zimmer, T. R., Carpenter, S. H., and Darter, M. I. (1984), "Field Performance of a Low-Modulus Silicone Highway Joint Sealant," Transportation Research Record, No. 990, Washington, DC, pp. 21-37.

APPENDIX A

CONCRETE MIX DESIGN AND SPECIMEN PREPARATION

Table A.1 Concrete coarse aggregate gradation

Sieve Size (mm)	Limestone % Passing	Granite % Passing	AASHTO #57 Specification
25.4	100.0	99.5	95-100
19.1	77.4	74.7	65-82
12.7	26.9	28.6	26-60
9.5	7.0	8.2	17-43
# 4	1.6	2.2	0-10

Table A.2 Concrete fine aggregate gradation

Sieve Size (mm)	Limestone % Passing	Granite % Passing
9.5	100	100
# 4	99.98	98.22
# 8	95.02	89.99
# 16	52.7	69.84
# 30	23.42	30.69
# 50	7.52	11.67
# 100	1.84	7.44
# 200	0.44	5.69

Table A.3 Physical properties of concrete aggregate.

Aggregate Type	Physical Property	Limestone	Granite
Coarse Aggregate	Bulk Dry Specific Gravity	2.80	2.86
	Absorption , %	0.70	0.72
	Unit Weight, kg/m^3	1493.1	1610.0
Fine Aggregate	Bulk Dry Specific Gravity	2.53	2.45
	Absorption , %	3.31	1.39
	Fineness Modulus	3.20	2.92

Table A.4 Chemical properties of concrete aggregate

Component	Concentration in Limestone (%)	Concentration in Granite (%)
SiO_2	3.05	91.20
Al_2O_3	0.54	3.99
Fe_2O_3	0.40	1.06
CaO	-	1.67
$CaCO_3$	53.42	-
MgO	-	1.19
Na_2O	-	0.55
$MgCO_3$	42.53	-
SO_3	0.04	-

Table A.5 Concrete mix design with limestone aggregate

Design Parameters	
Desired Slump	76 mm
Desired Air Content	1.5 %
water/cement ratio	0.42
Portland Cement Type I	
Specific Gravity	3.15
Mix Proportions for 0.04 m^3 concrete	
Water	13.0 kg
Cement	8.9 kg
Coarse Aggregate	29.5 kg
Fine Aggregate	38.6 kg
Mix Properties	
Actual Slump	83 mm
Actual Air Content	2 %
Unit Weight	2451.1 kg/m^3
Compressive Strength	
3 day	30.3 MPa
7 day	34.8 MPa
28 day	41.0 MPa

Table A.6 Concrete mix design with granite aggregate

Design Parameters	
Desired Slump	76 mm
Desired Air Content	1.5 %
Water/cement ratio	0.42
Portland Cement Type I	
Specific Gravity	3.15
Mix Proportions for 0.05 m^3 concrete	
Water	10.1 kg
Cement	22.1 kg
Coarse Aggregate	51.6 kg
Fine Aggregate	34.3 kg
Mix Properties	
Actual Slump	127.0 mm
Actual Air Content	1.4 %
Unit Weight	2495.9 kg/m^3
Compressive Strength	
3 day	33.0 MPa
7 day	39.5 MPa
28 day	47.8 MPa

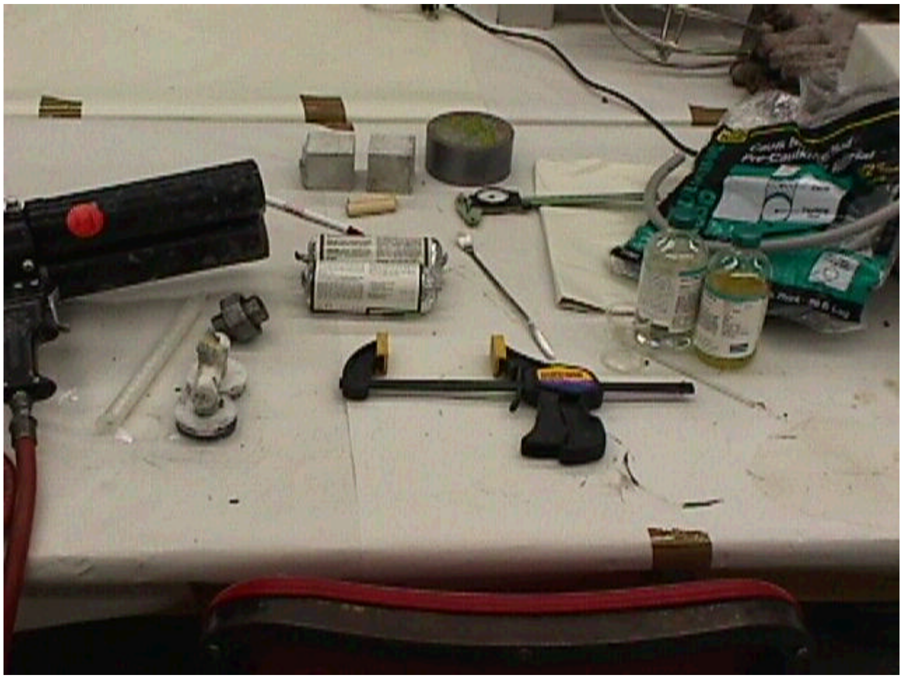

Figure A.1 Tools and components needed to fabricate silicone test specimens

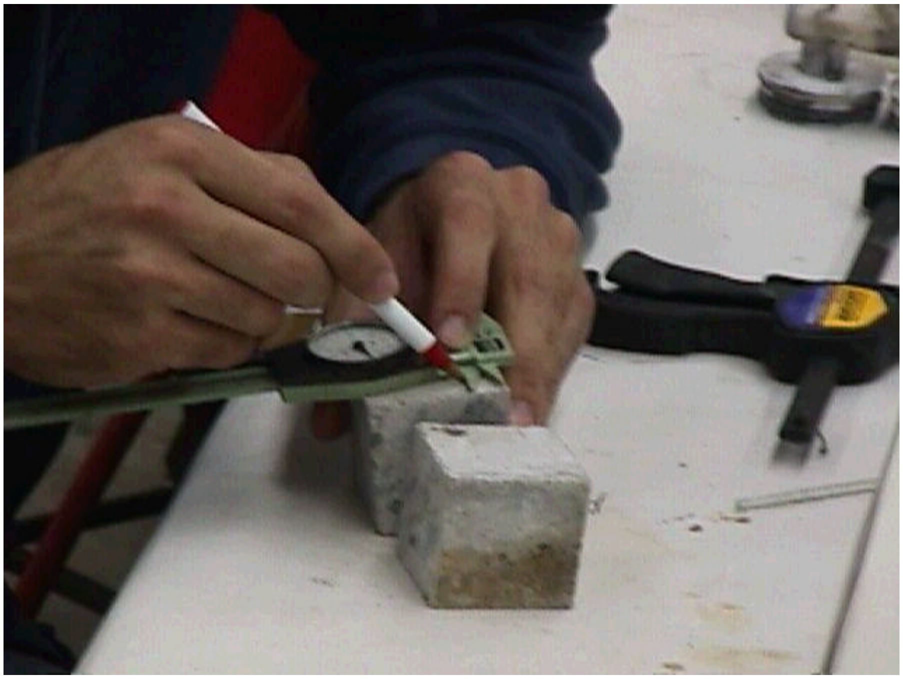

Figure A.2 Marking the sealant depth on the concrete cubes

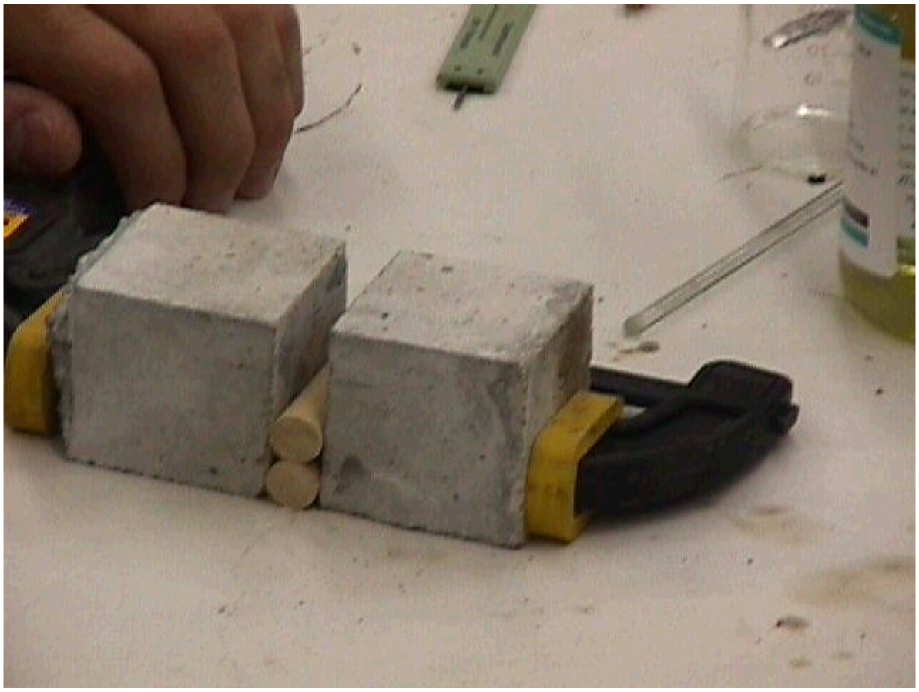

Figure A.3 Clamping the concrete cubes around the wooden dowels maintains a constant joint width

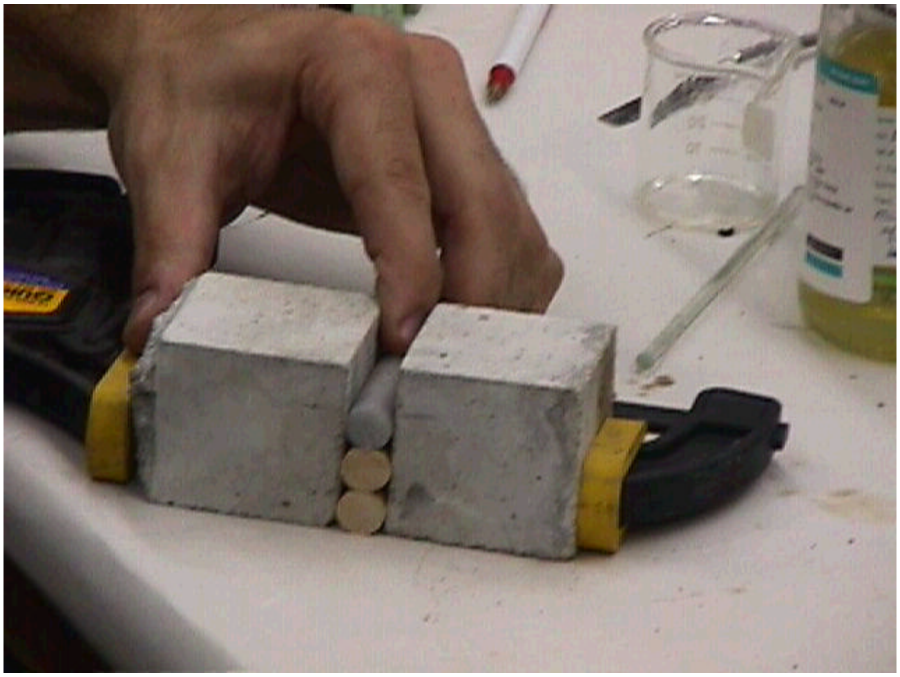

Figure A.4 Inserting the Styrofoam backer rod between the concrete cubes

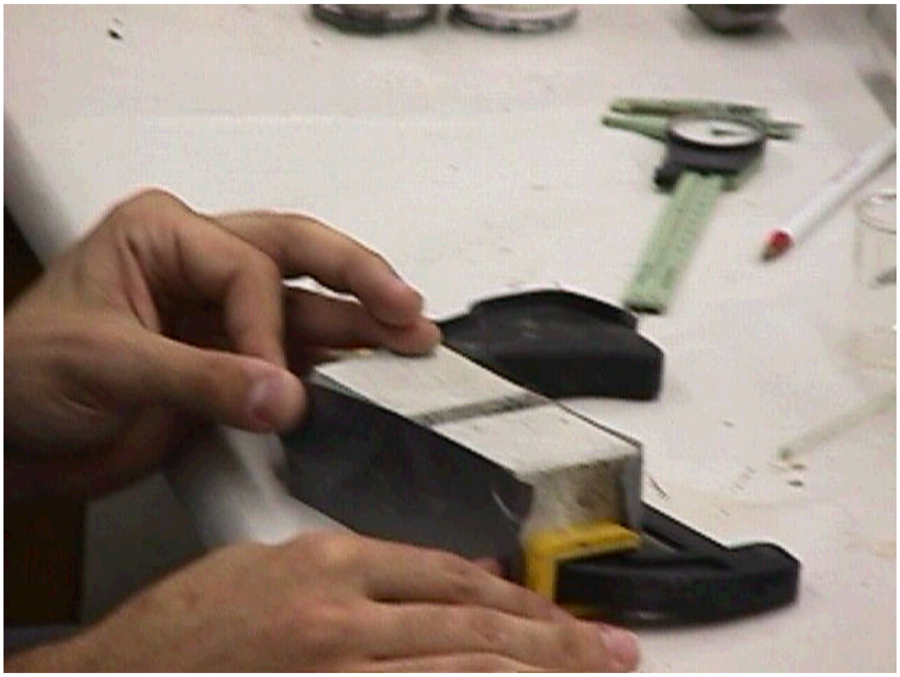

Figure A.5 Taping the sides of the joint provides confinement to the sealant during curing

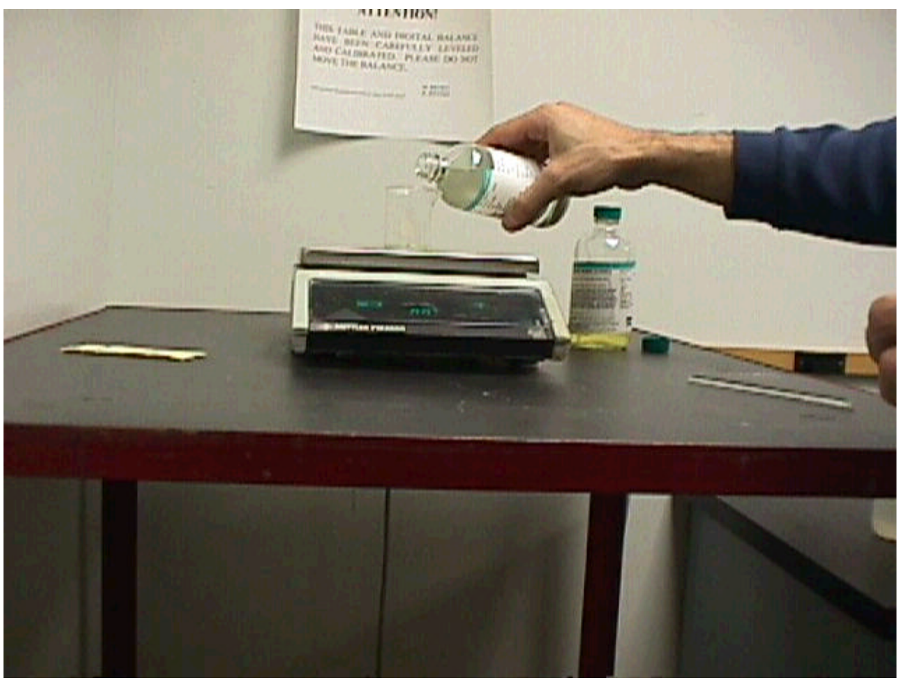

Figure A.6 Weight measurement of the components of the two-part primer

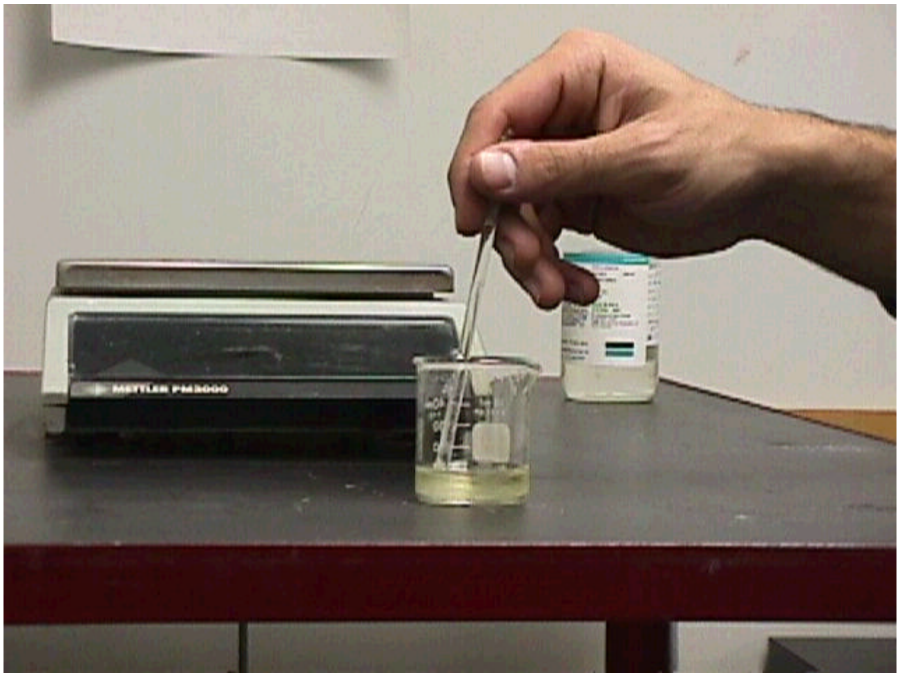

Figure A.7 Mixing the components of the two-part primer

Figure A.8 Applying the primer to the concrete joint wall

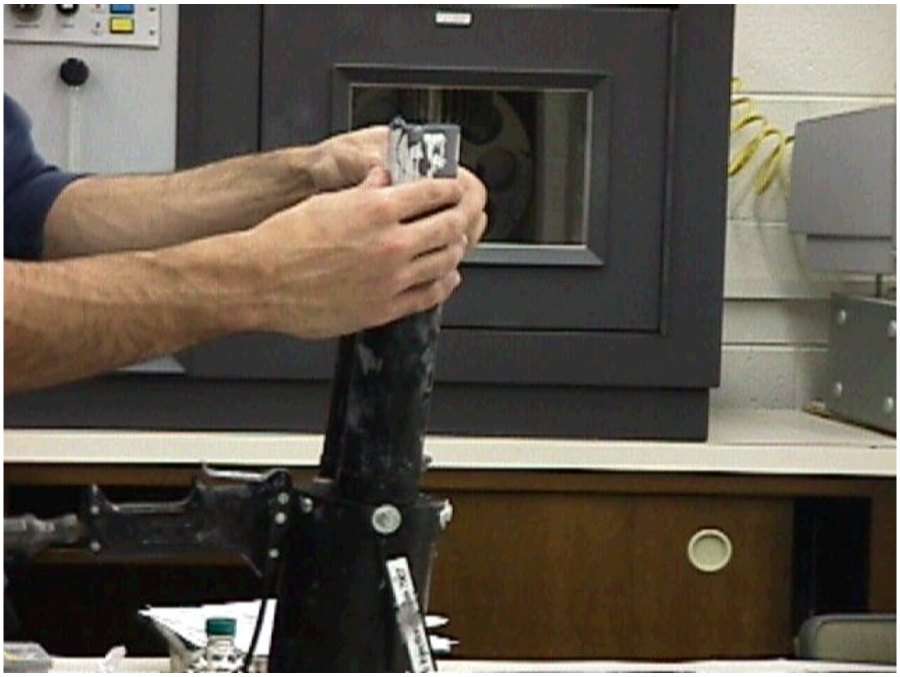

Figure A.9 Assembling the caulking gun used for sealant application

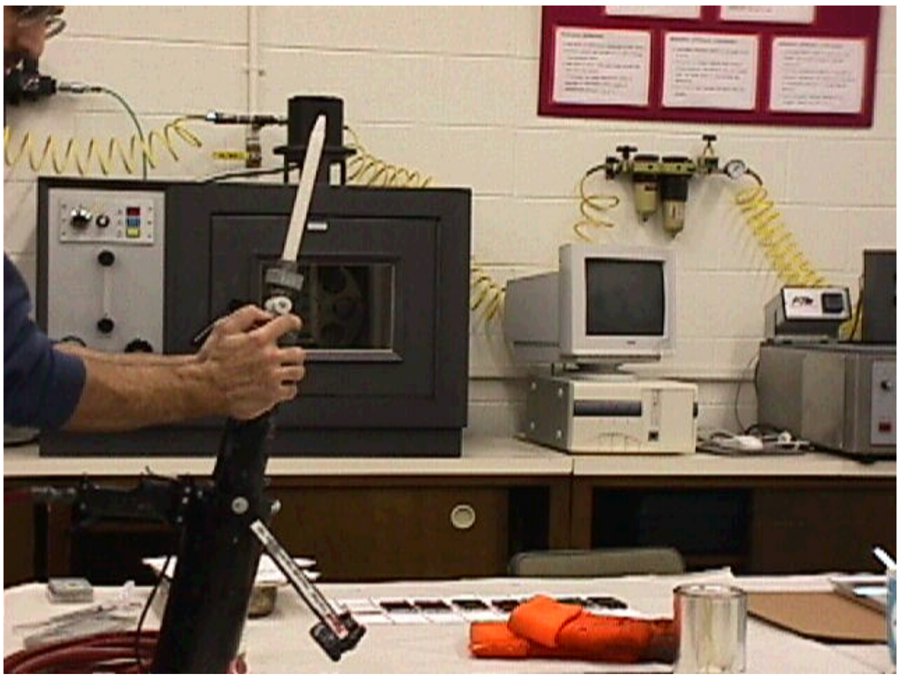

Figure A.10 Attaching the nozzle to the caulking gun

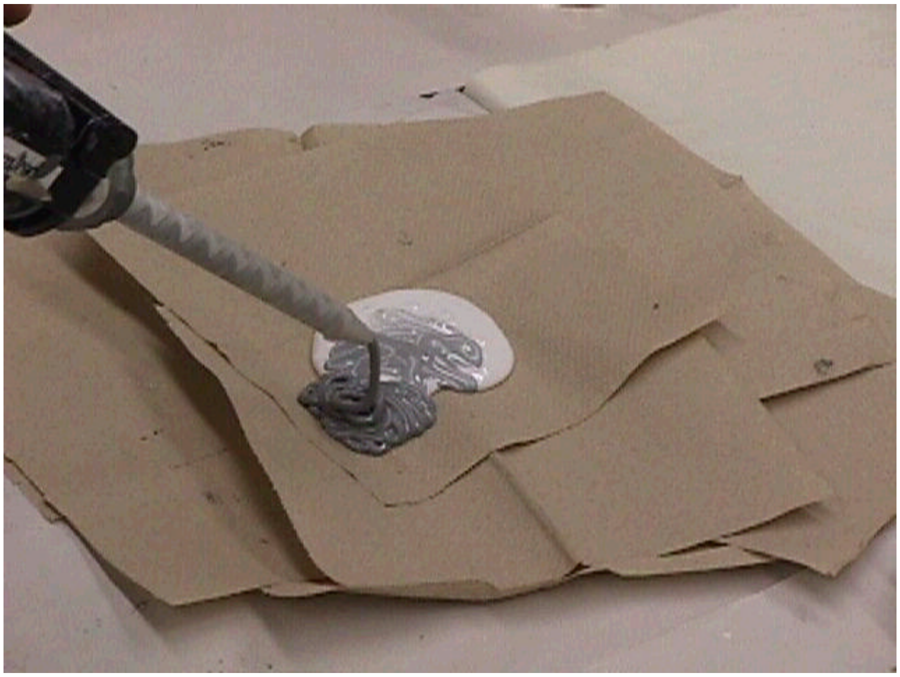

Figure A.11 Insuring that sealant components are mixed adequately before application

Figure A.12 Sealant injection into the joint

Figure A.13 Forming concave shape on top of joint sealant

Figure A.14 The sealant is allowed to cure for 21 days

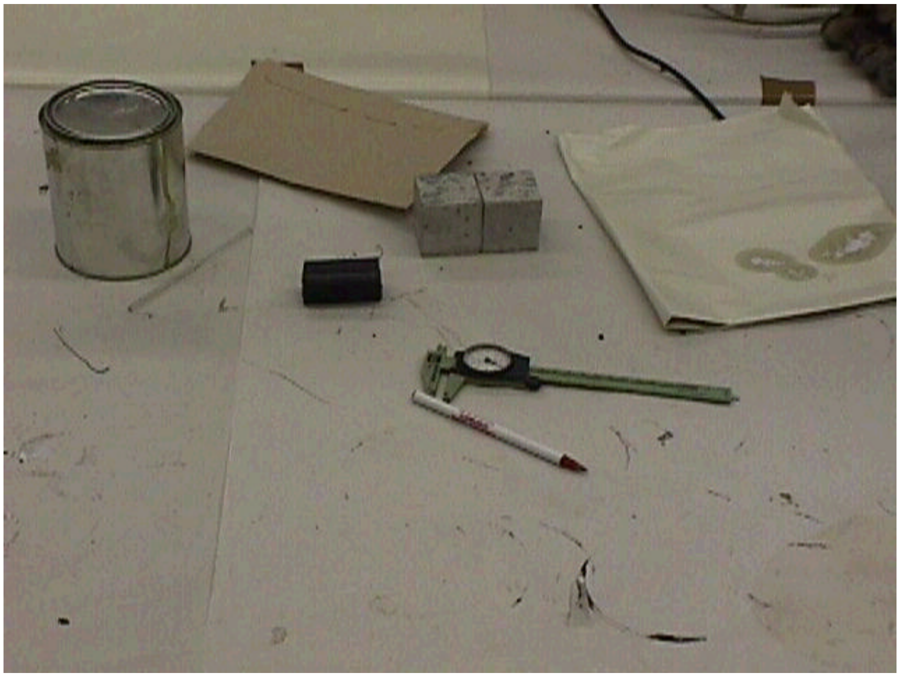

Figure A.15 Tools and components needed to fabricate neoprene test specimens

Figure A.16 Marking the sealant depth on the concrete cubes

Figure A.17 Applying the lubricant/adhesive to the concrete joint wall

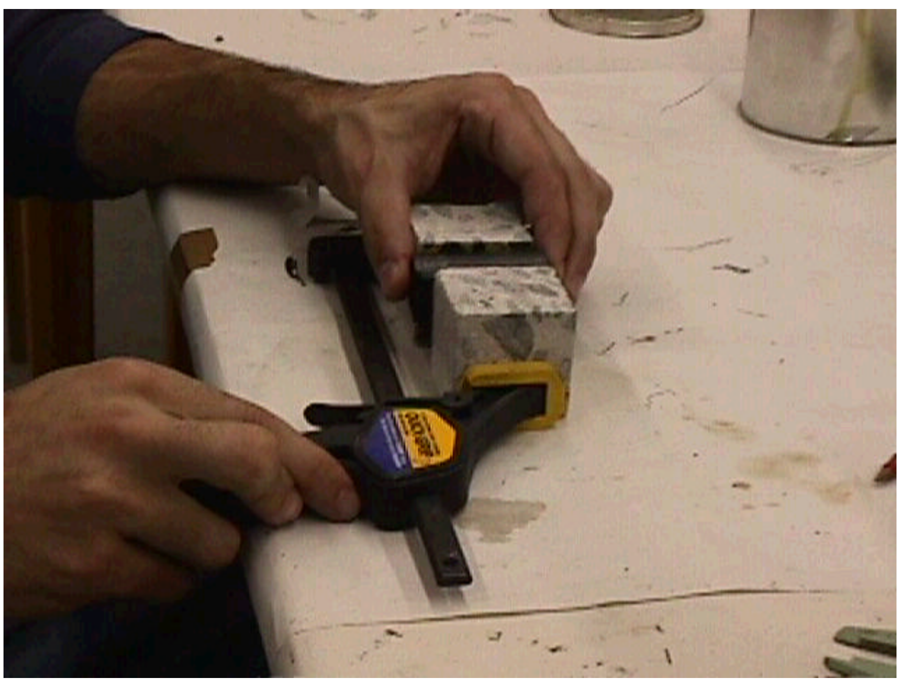

Figure A.18 Compressing the preformed neoprene sealant between the concrete cubes

APPENDIX B

ENVIRONMENTALLY CONDITIONED SPECIMENS

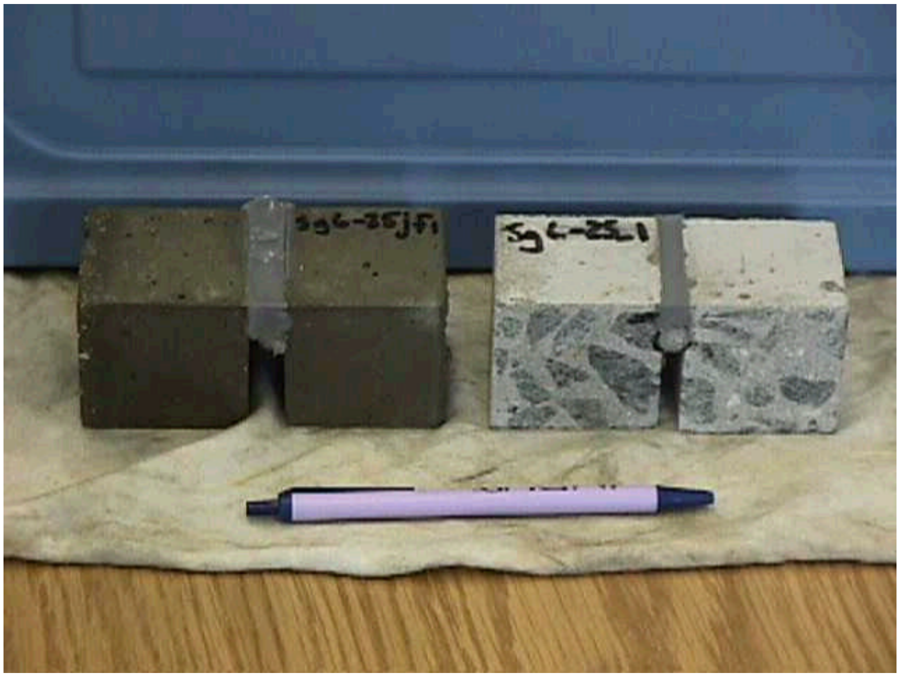

Figure B.1 Silicone specimen with 6.35 mm joint width after two days of exposure to jet fuel

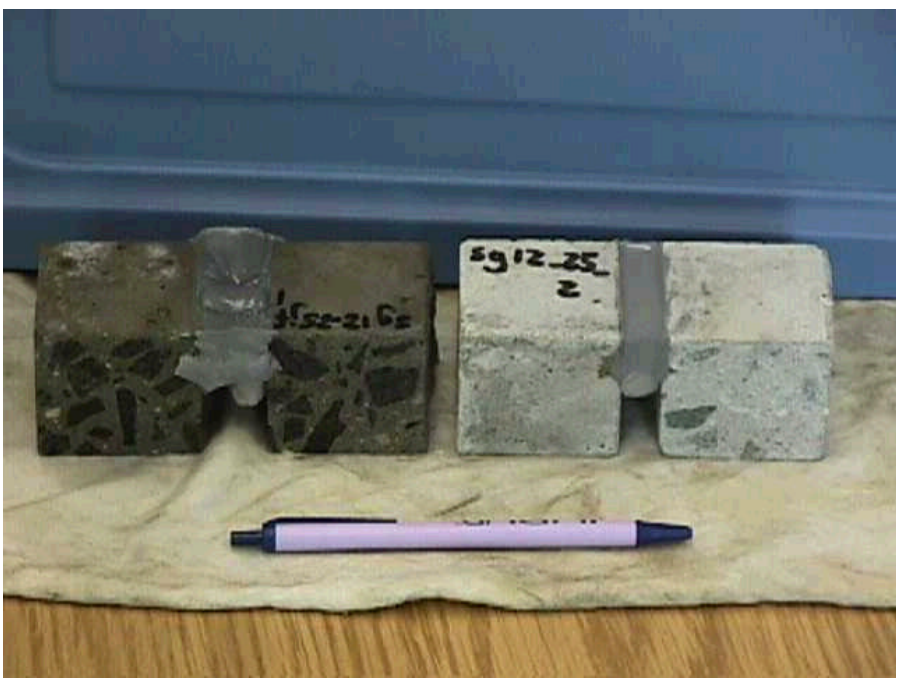

Figure B.2 Silicone specimen with 12.7 mm joint width after two days of exposure to jet fuel

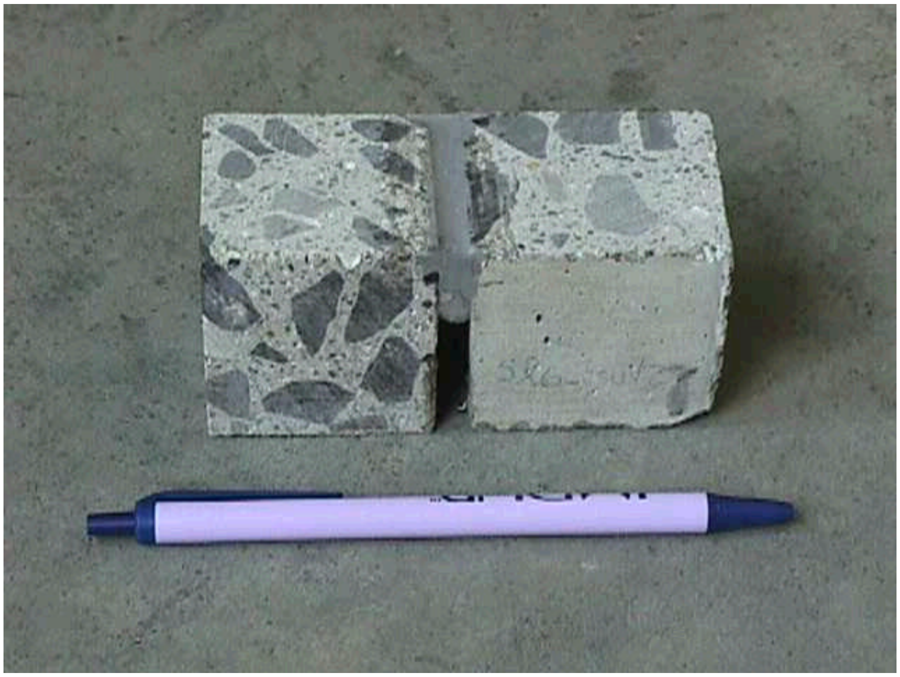

Figure B.3 Silicone specimen with 6.35 mm joint width after 1000 hours of exposure to UV

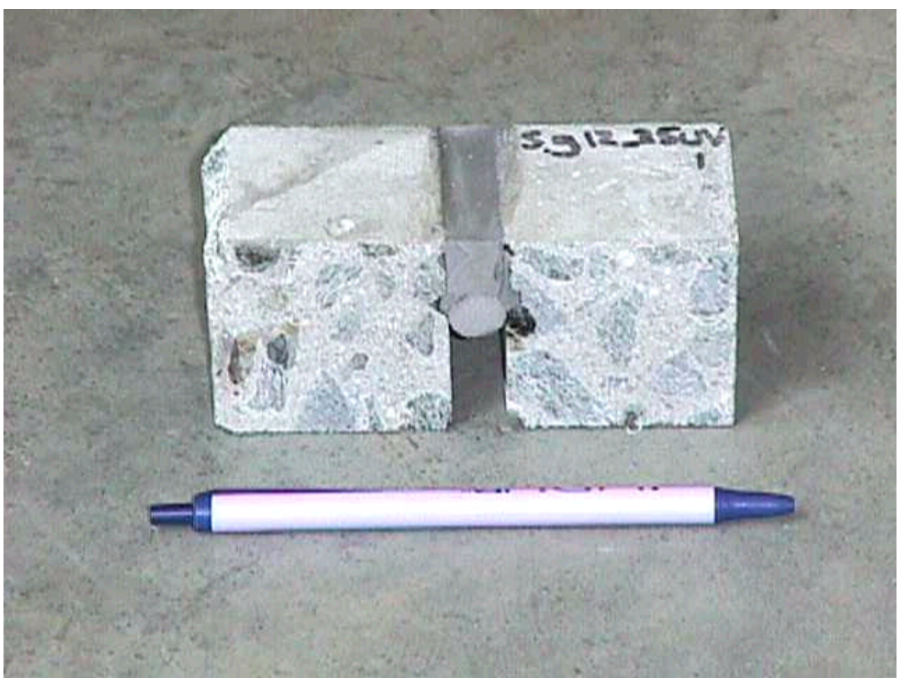

Figure B.4 Silicone specimen with 12.7 mm joint width after 1000 hours of exposure to UV

Figure B.5 Silicone specimen with 6.35 mm joint width after 1000 hours of exposure to UV and two days of exposure to jet fuel

Figure B.6 Small neoprene specimen after two days of exposure to jet fuel

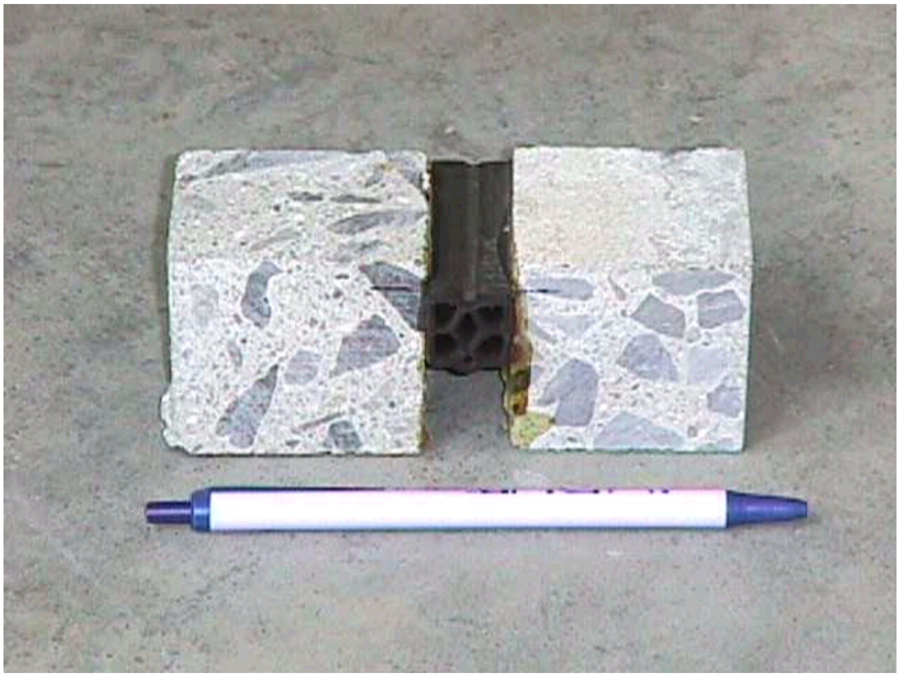

Figure B.7 Small neoprene specimen after 1000 hours of exposure to UV

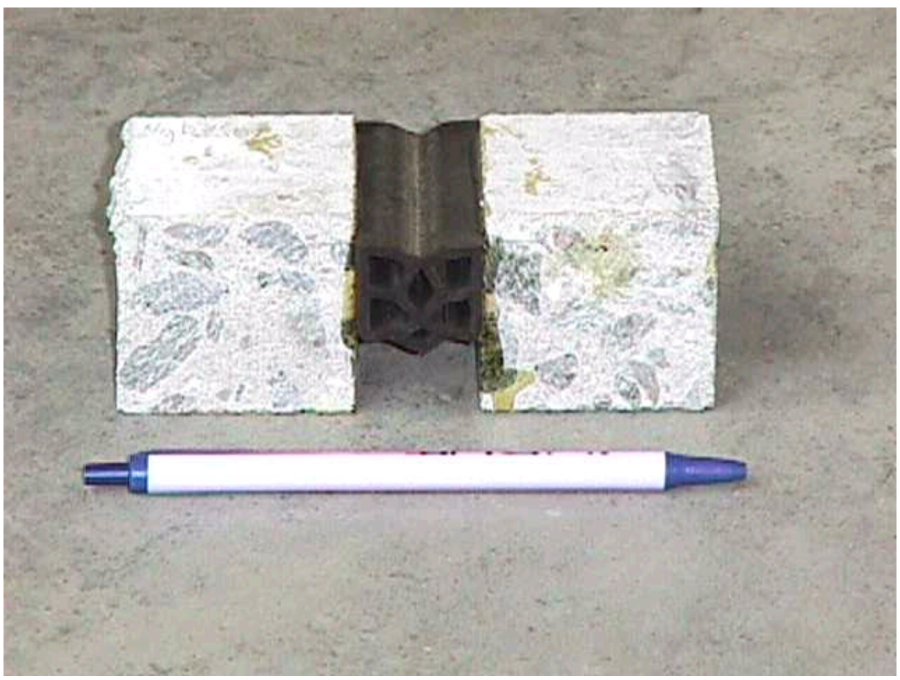

Figure B.8 Large neoprene specimen after 1000 hours of exposure to UV

APPENDIX C

DATA ANALYSIS

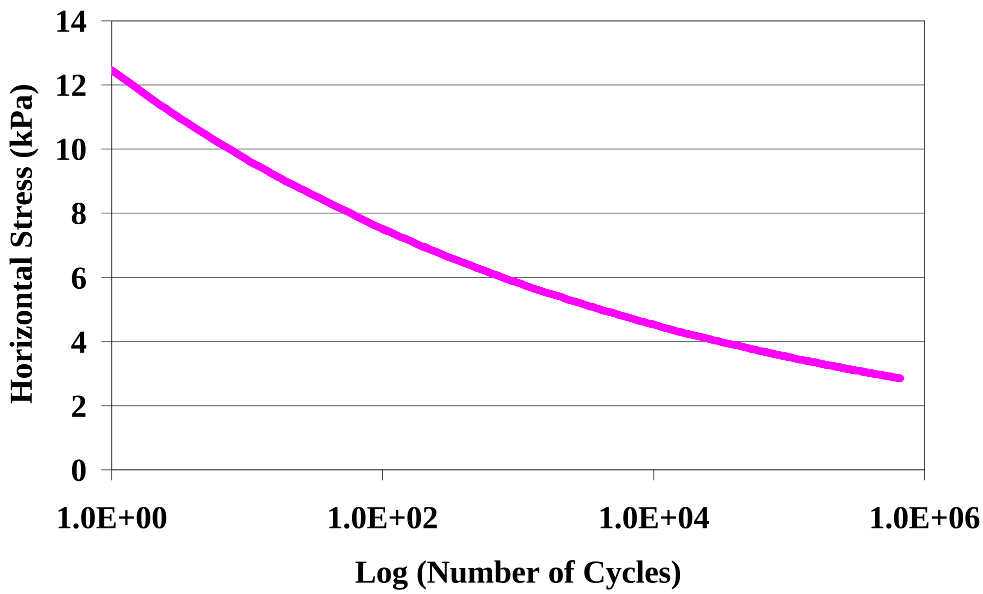

Figure C.1 Horizontal stress versus number of cycles for silicone sealant used with concrete (with limestone aggregate) at a 12.7 mm joint width, 25% static tension, and exposed to jet fuel and distilled water.

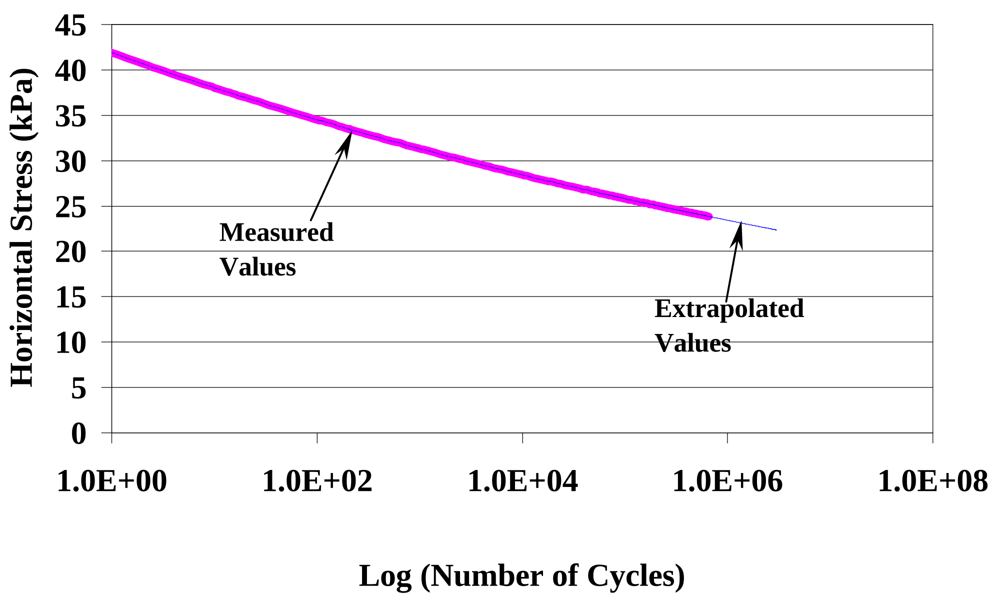

Figure C.2 Horizontal stress versus number of cycles for silicone sealant used with concrete (with limestone aggregate) at a 6.35 mm joint width, 25% static tension, and exposed to jet fuel and distilled water.

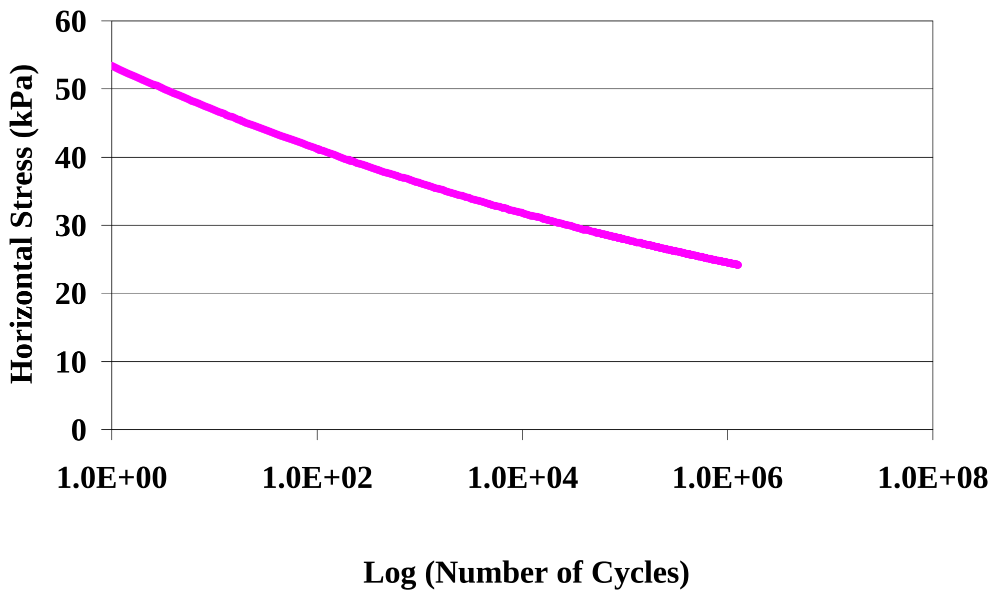

Figure C.3 Horizontal stress versus number of cycles for silicone sealant used with concrete (with limestone aggregate) at a 12.7 mm joint width, 25% static tension, and exposed to UV-A light and distilled water.

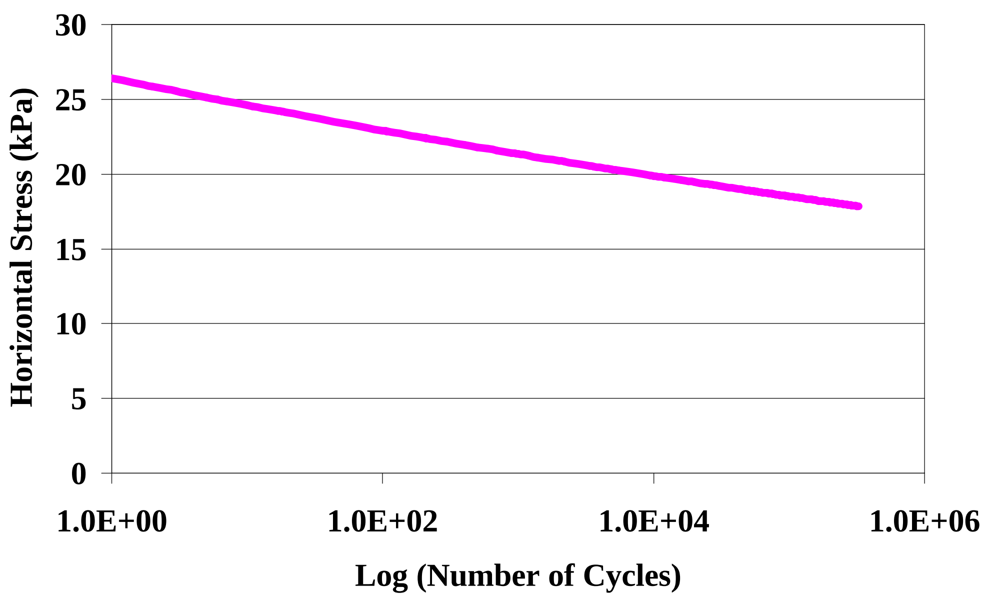

Figure C.4 Horizontal stress versus number of cycles for silicone sealant used with concrete (with limestone aggregate) at a 6.35 mm joint width, 25% static tension, and exposed to UV-A light and distilled water.

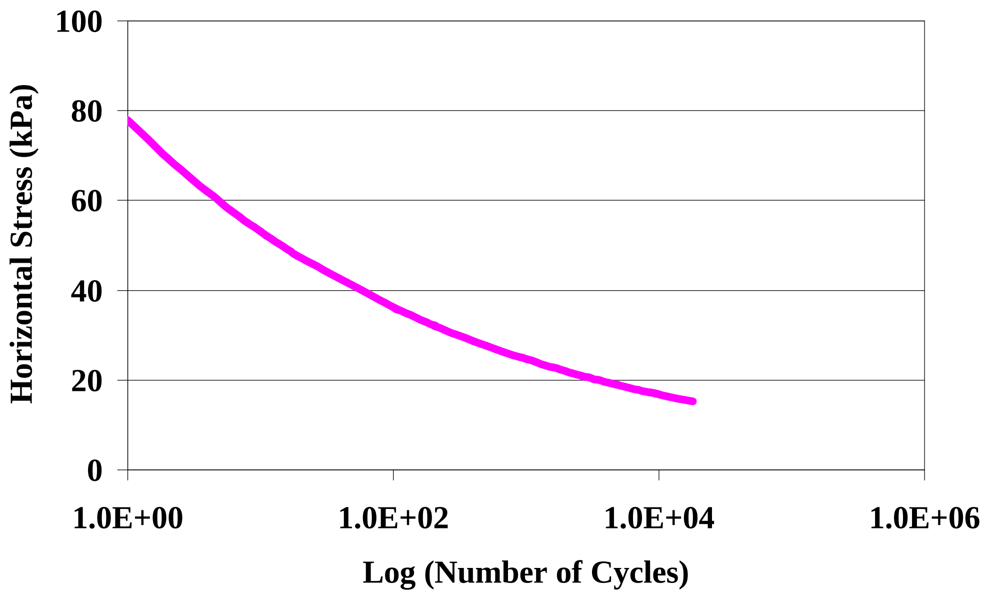

Figure C.5 Horizontal stress versus number of cycles for silicone sealant used with concrete (with limestone aggregate) at a 6.35 mm joint width, 25% static tension, and exposed to distilled water.

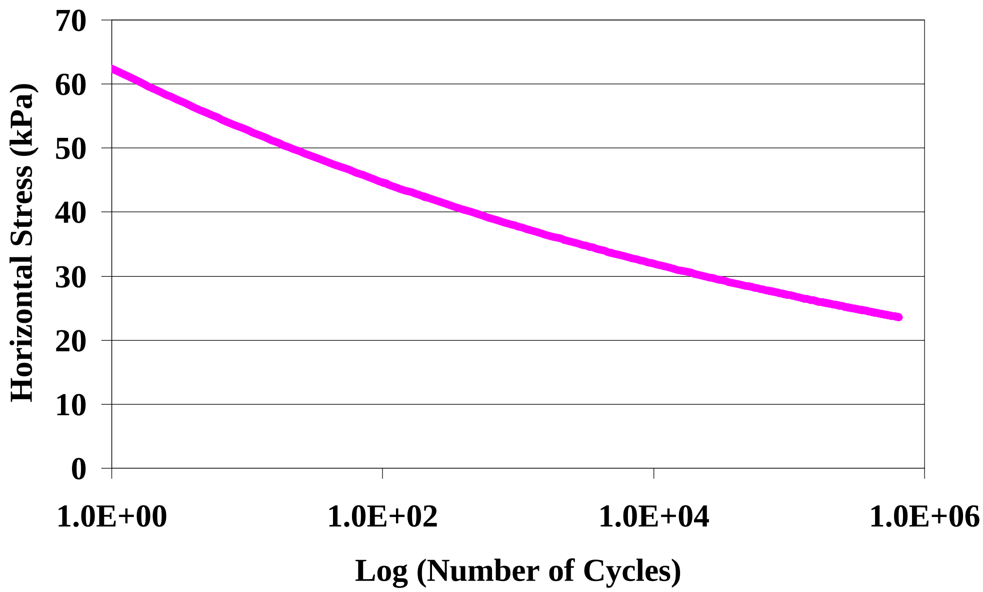

Figure C.6 Horizontal stress versus number of cycles for silicone sealant used with concrete (with limestone aggregate) at a 12.7 mm joint width, 25% static tension, and exposed to distilled water.

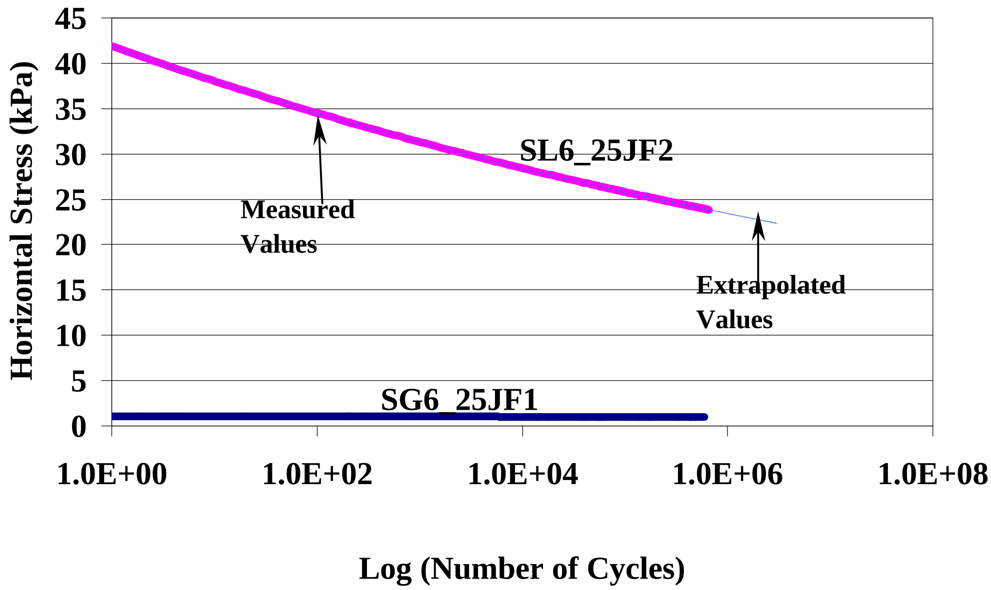

Figure C.7 Effect of aggregate type on durability of silicone sealant at a 6.35 mm joint width, 25% static tension, and exposed to jet fuel and distilled water.

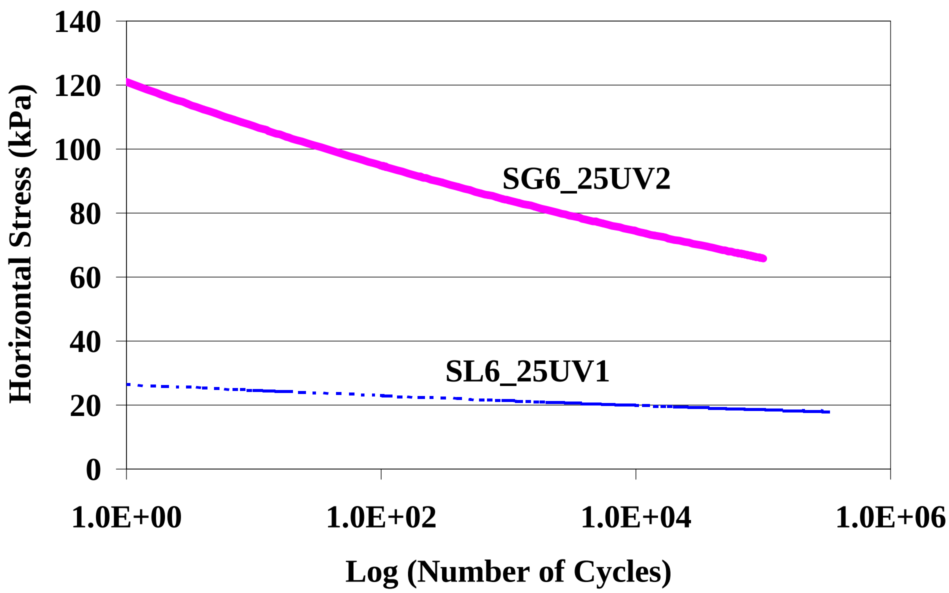

Figure C.8 Effect of aggregate type on durability of silicone sealant at a 6.35 mm joint width, 25% static tension, and exposed to UV-A light and distilled water.

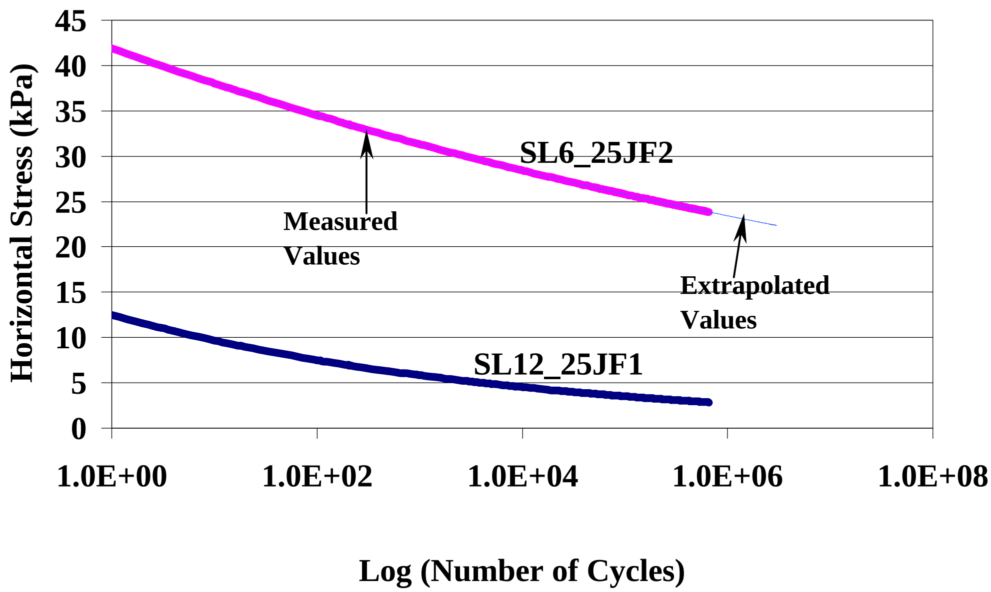

Figure C.9 Effect of joint width on durability of silicone sealant used with concrete (with limestone aggregate), 25% static tension during testing, and exposed to jet fuel and distilled water.

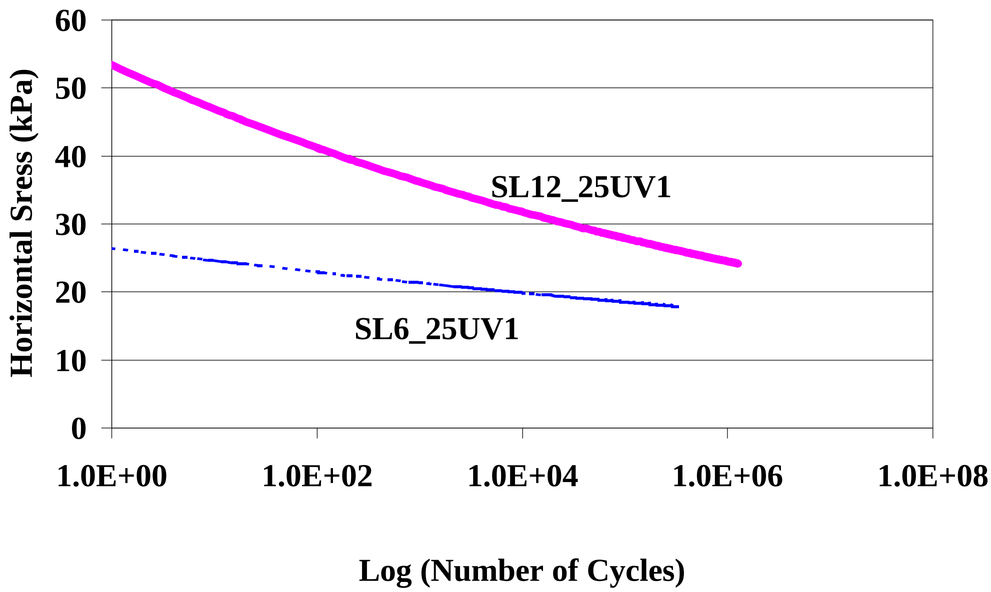

Figure C.10 Effect of joint width on durability of silicone sealant used with concrete (with limestone aggregate), 25% static tension, and exposed to UV-A light and distilled water.

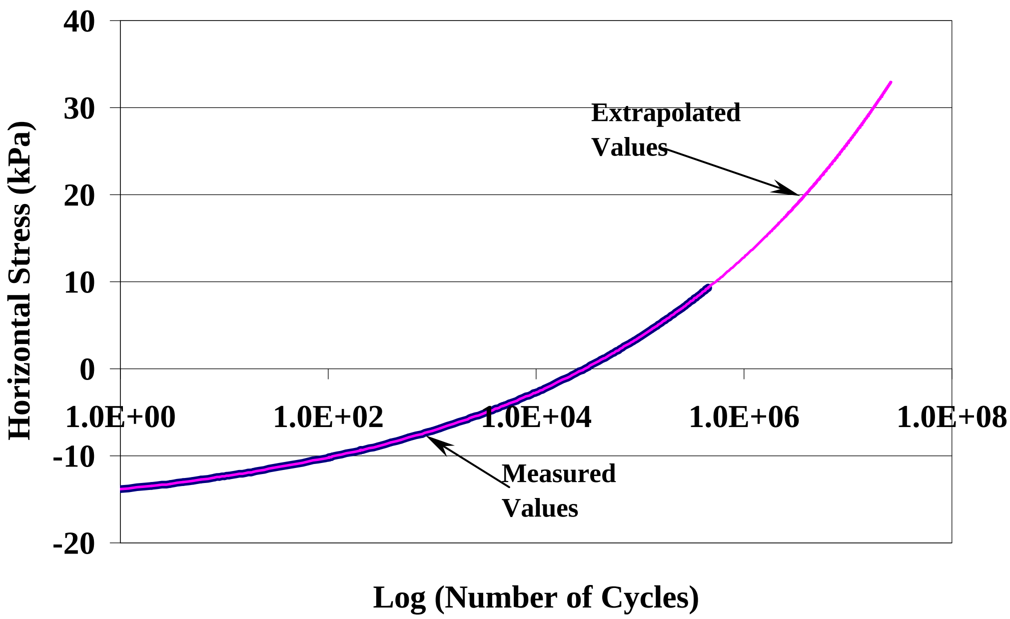

Figure C.11 Horizontal stress versus number of cycles for small neoprene sealant used with concrete (with granite aggregate), 25% static compression, and exposed to distilled water

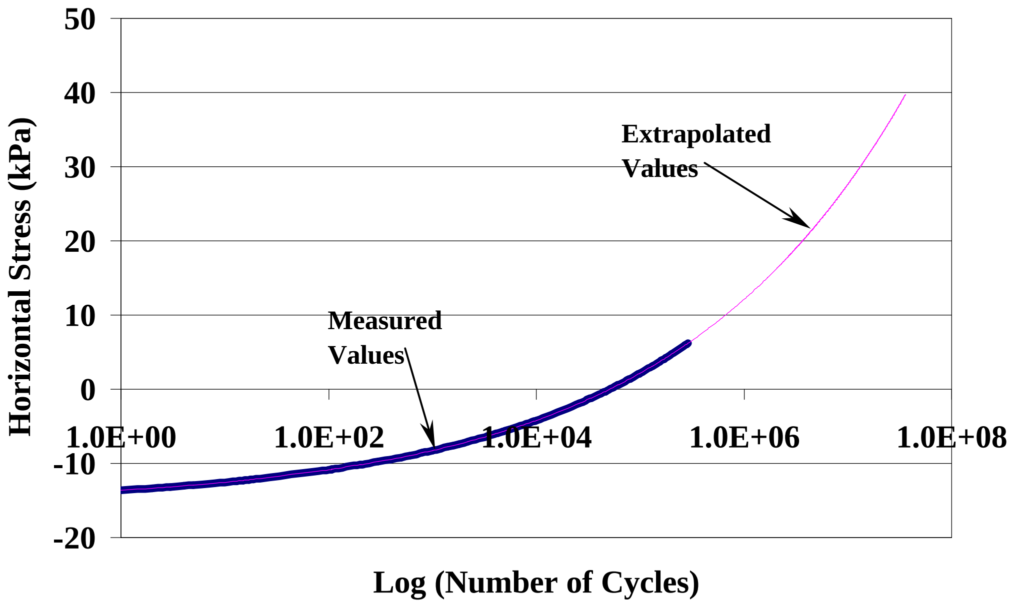

Figure C.12 Horizontal stress versus number of cycles for small neoprene sealant used with concrete (with granite aggregate), 25% static compression, and exposed to UV-A light and distilled water

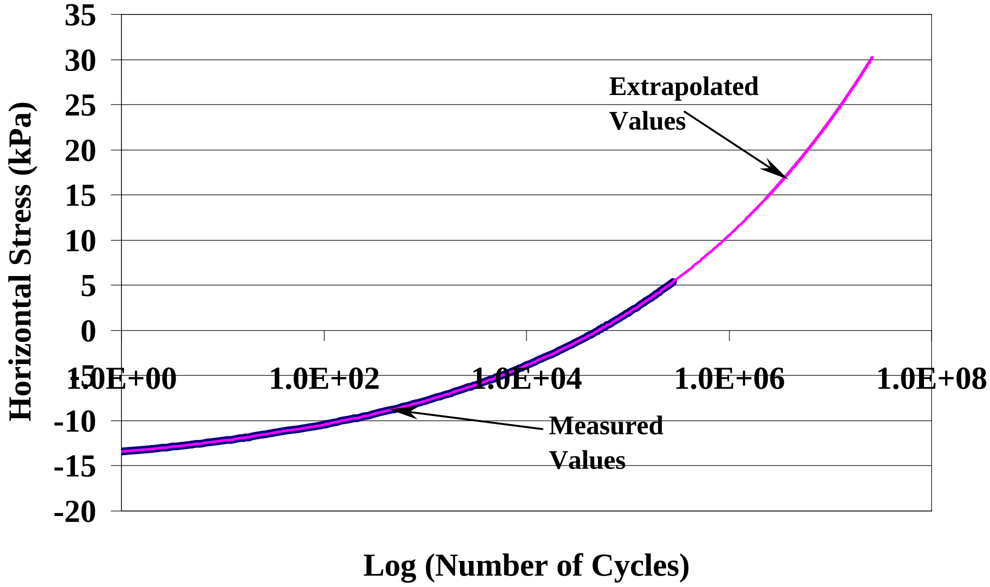

Figure C.13 Horizontal stress versus number of cycles for small neoprene sealant used with concrete (with limestone aggregate), 25% static compression, and exposed to UV-A light and distilled water

APPENDIX D

SPECIMEN FAILURE MODES

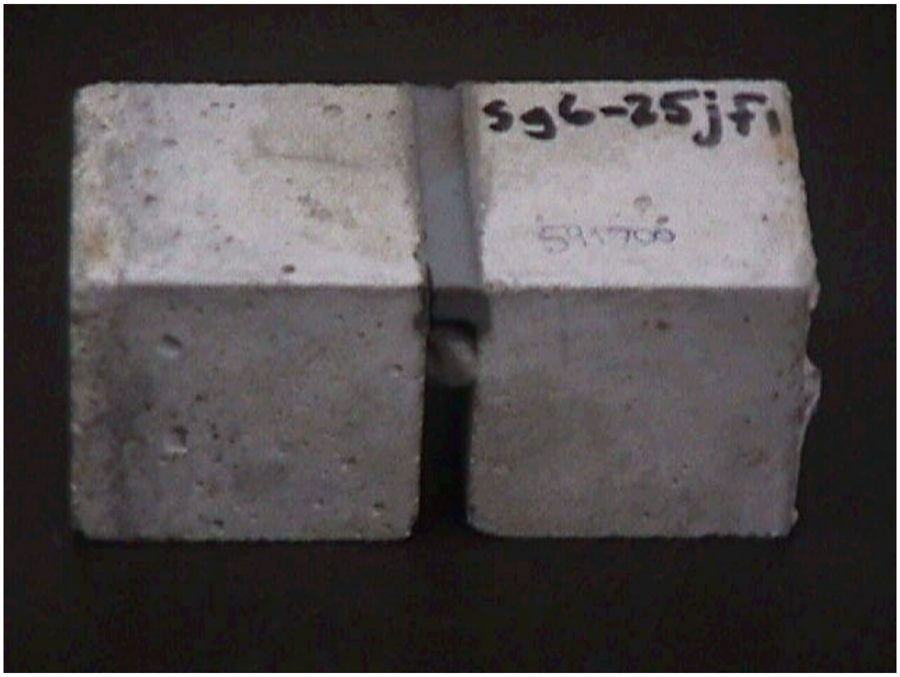

Figure D.1 Top of specimen SG6_25JF1 after environmental conditioning and cyclic loading

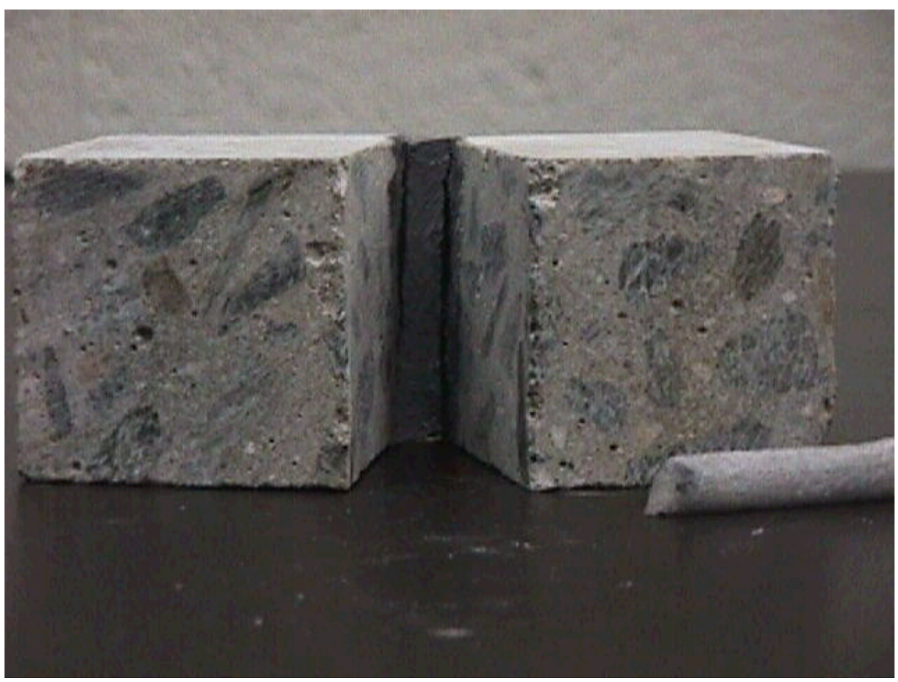

Figure D.2 Bottom of specimen SG6_25JF1 after environmental conditioning and cyclic loading

Figure D.3 Top of specimen SL12_25JF1 after environmental conditioning and cyclic loading

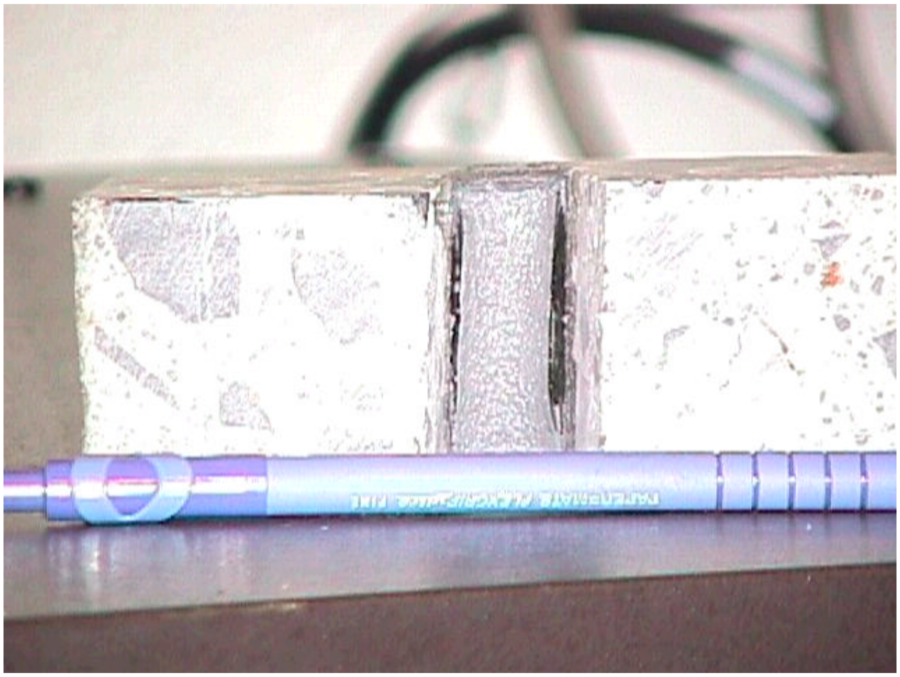

Figure D.4 Bottom of specimen SL12_25JF1 after environmental conditioning and cyclic loading

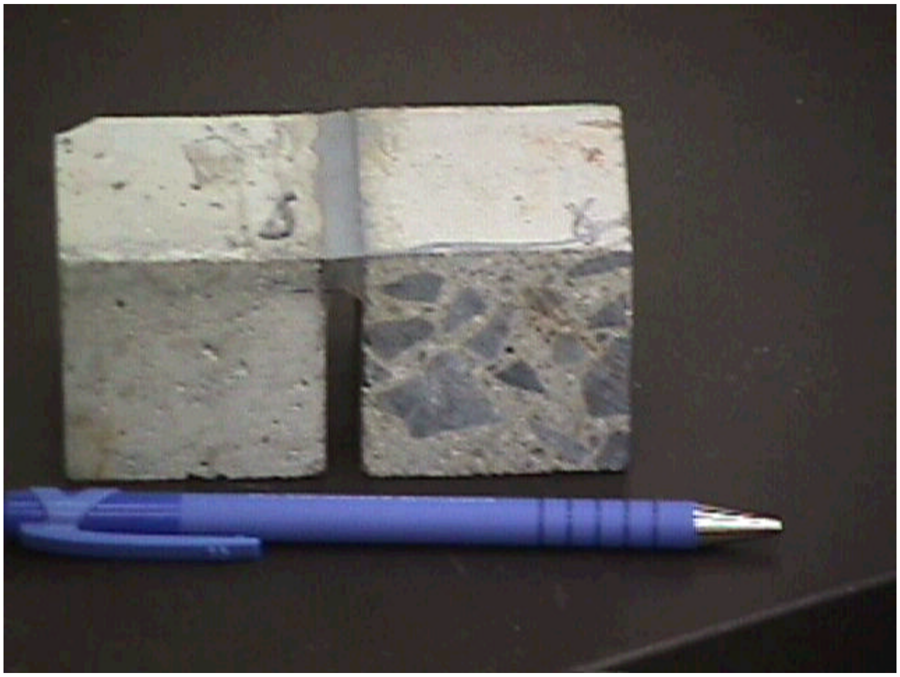

Figure D.5 Top of specimen SL6_25JF2 after environmental conditioning and cyclic loading

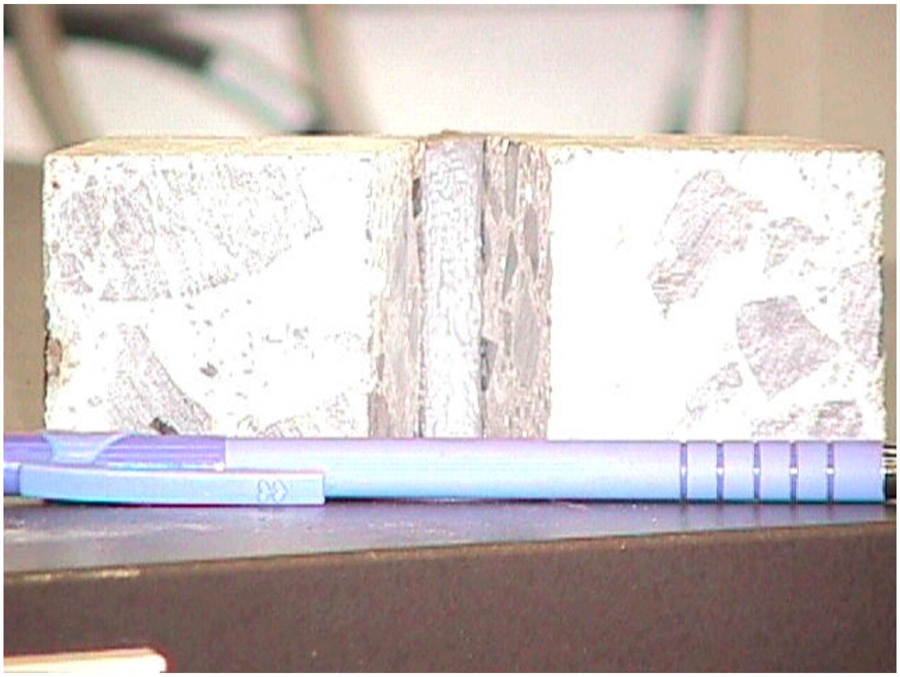

Figure D.6 Bottom of specimen SL6_25JF2 after environmental conditioning and cyclic loading

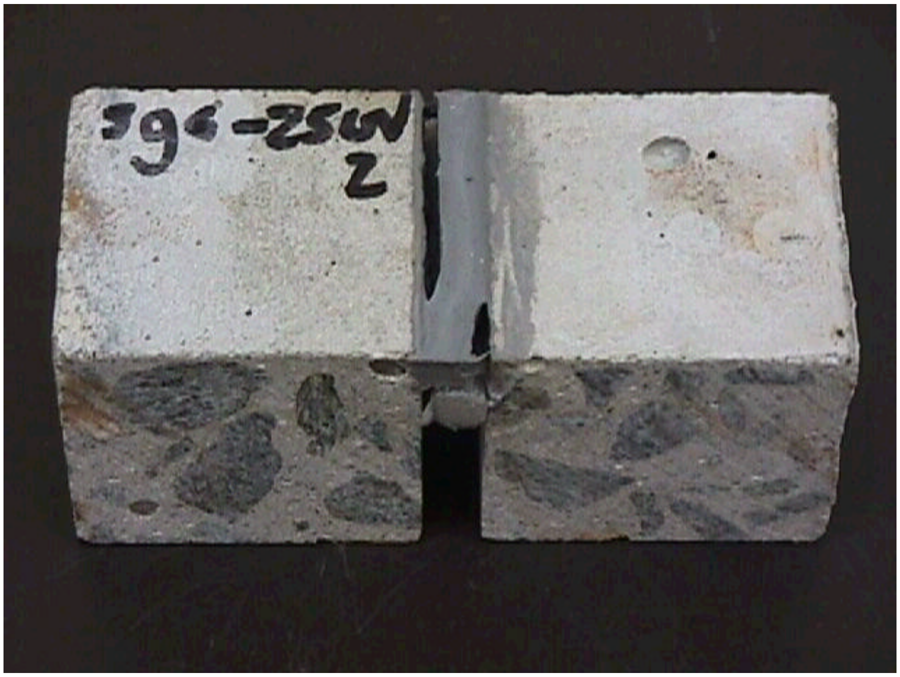

Figure D.7 Top of specimen SG6_25UV2 after environmental conditioning and cyclic loading

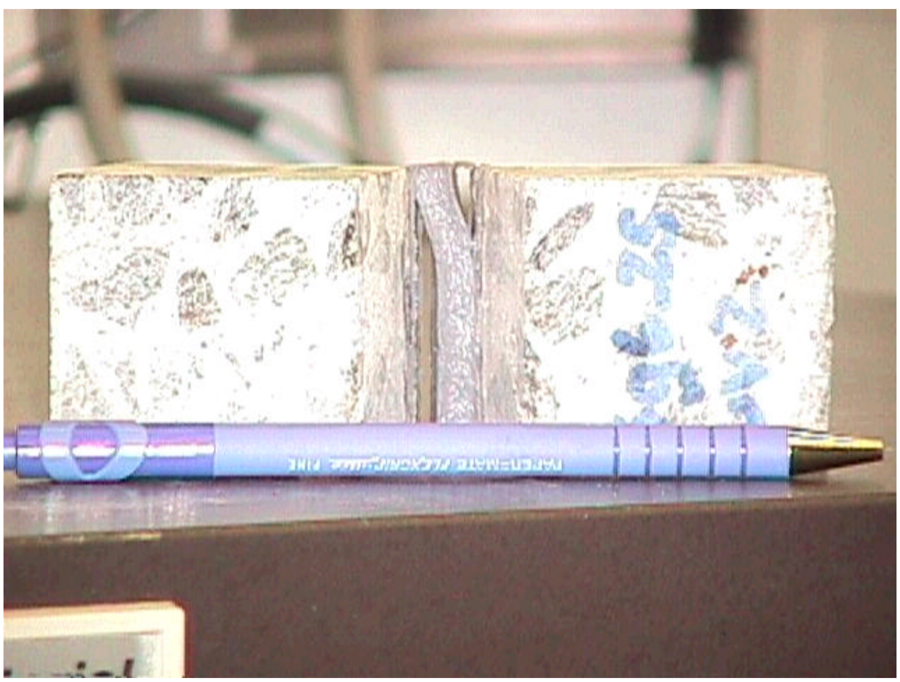

Figure D.8 Bottom of specimen SG6_25UV2 after environmental conditioning and cyclic loading

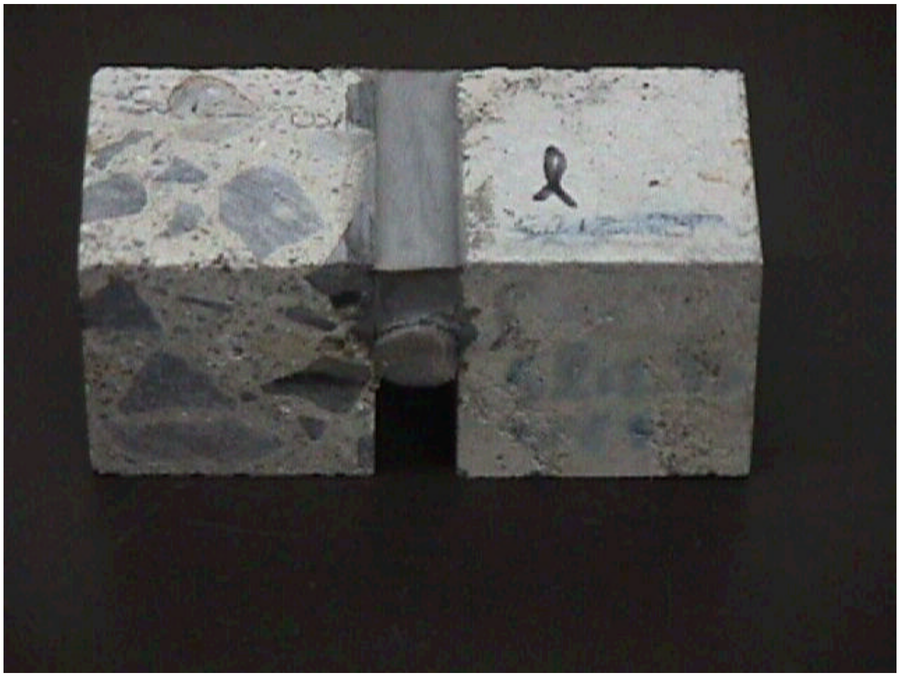

Figure D.9 Top of specimen SL12_25UV1 after environmental conditioning and cyclic loading

Figure D.10 Bottom of specimen SL12_25UV1 after environmental conditioning and cyclic loading

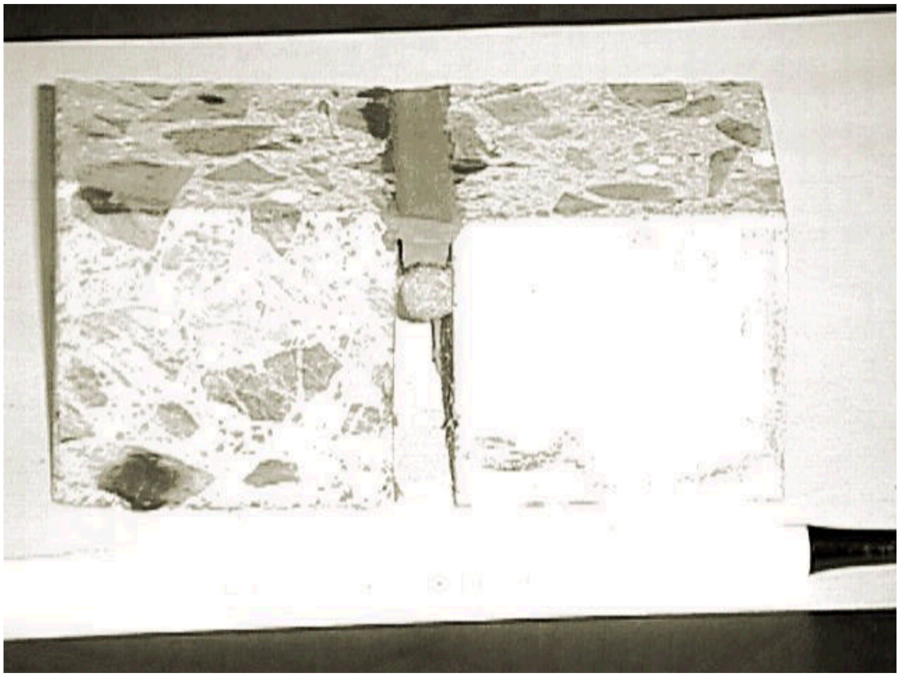

Figure D.11 Top of specimen SL6_25UV1 after environmental conditioning and cyclic loading

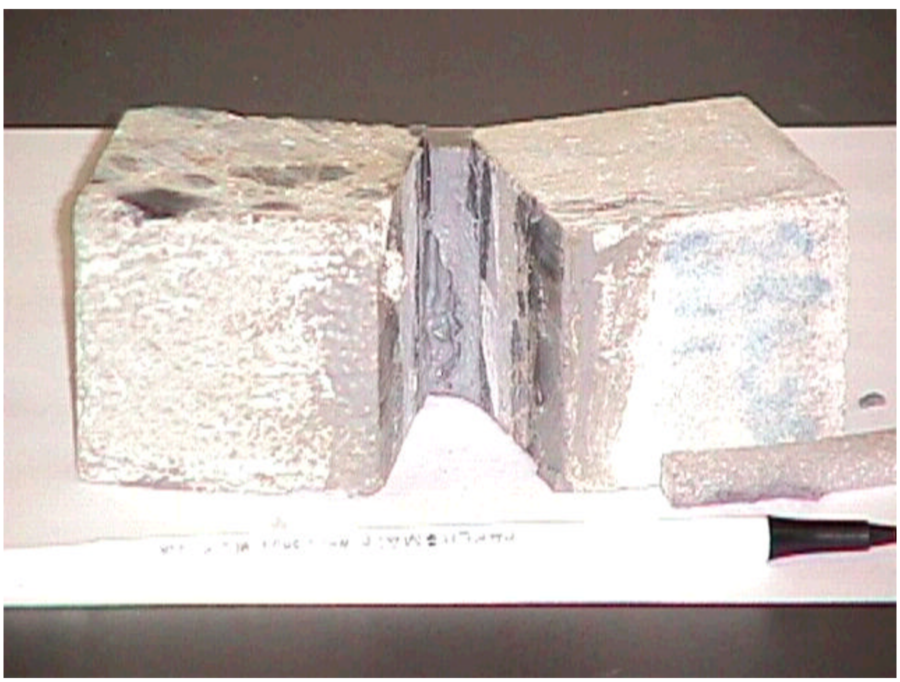

Figure D.12 Bottom of specimen SL6_25UV1 after environmental conditioning and cyclic loading

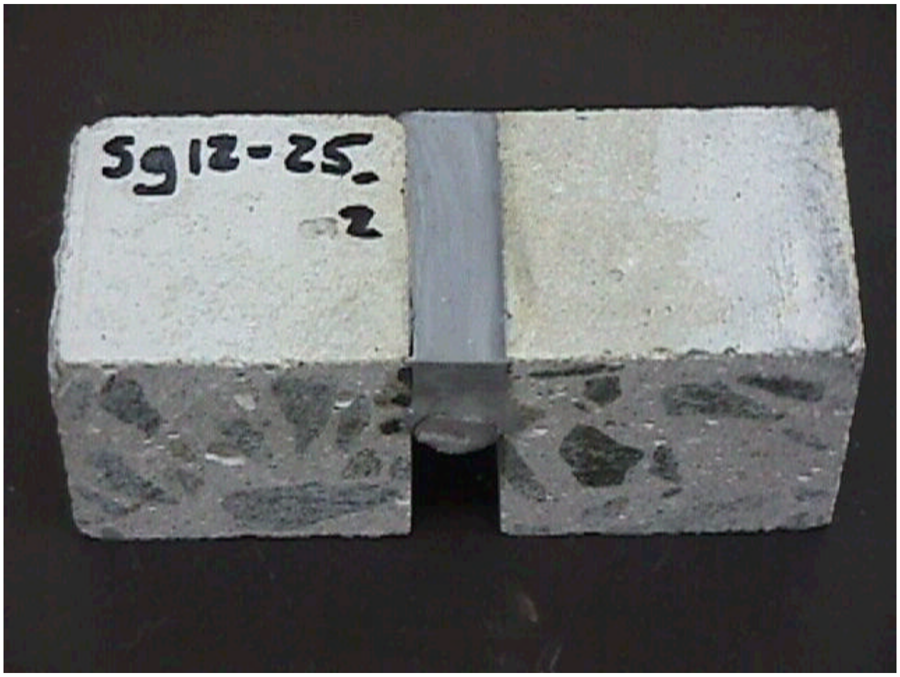

Figure D.13 Top of specimen SG12_25_2 after environmental conditioning and cyclic loading

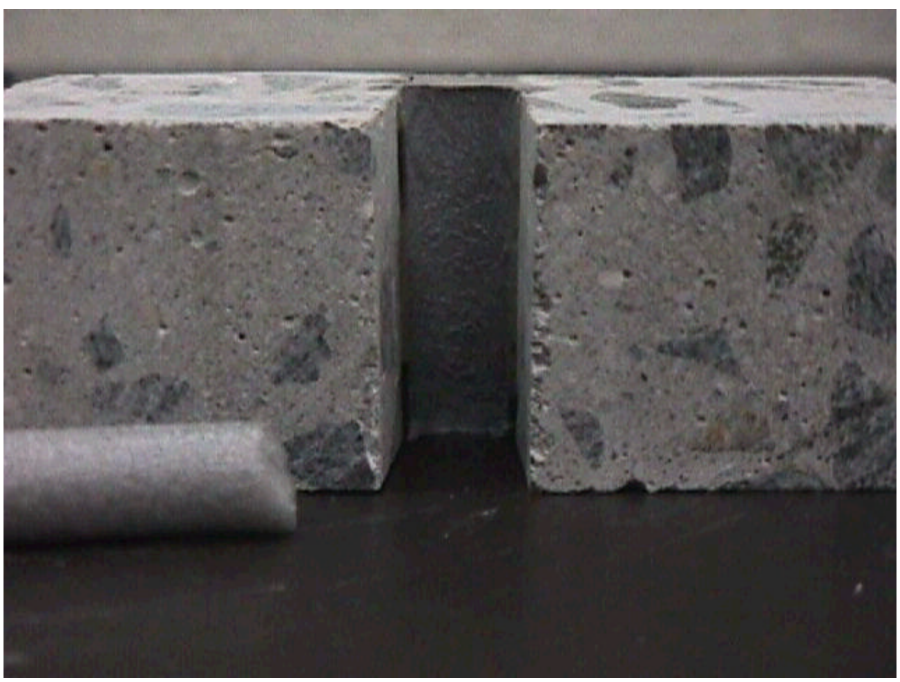

Figure D.14 Bottom of specimen SG12_25_2 after environmental conditioning and cyclic loading

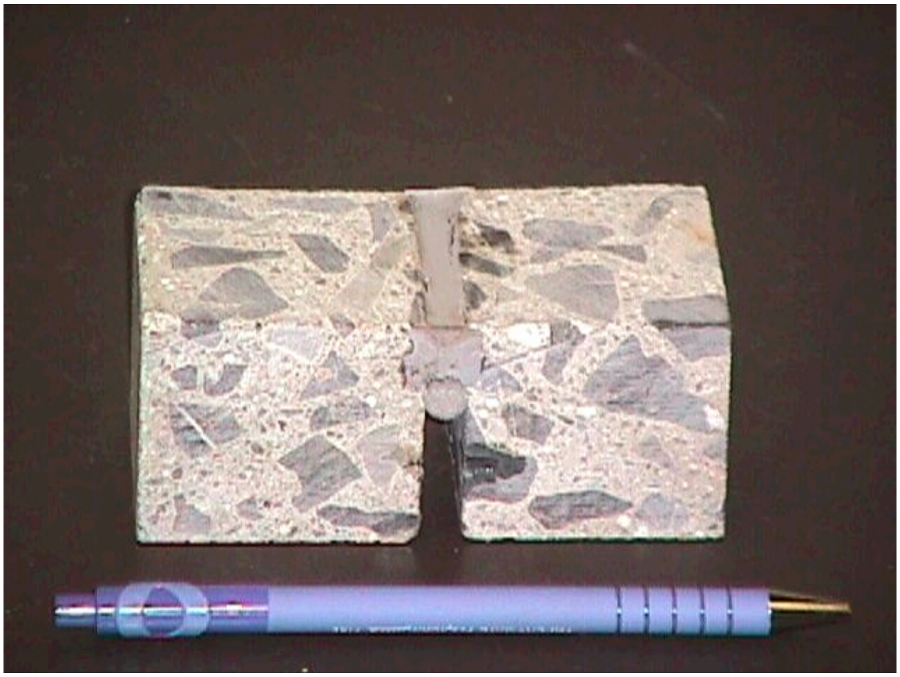

Figure D.15 Top of specimen SL6_25_1 after environmental conditioning and cyclic loading

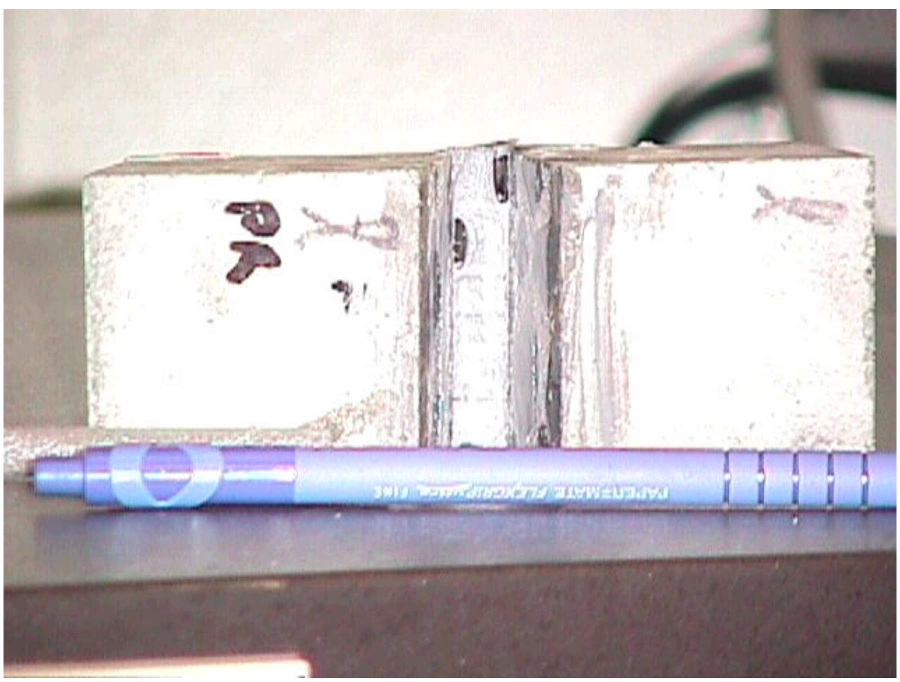

Figure D.16 Bottom of specimen SL6_25_1 after environmental conditioning and cyclic loading

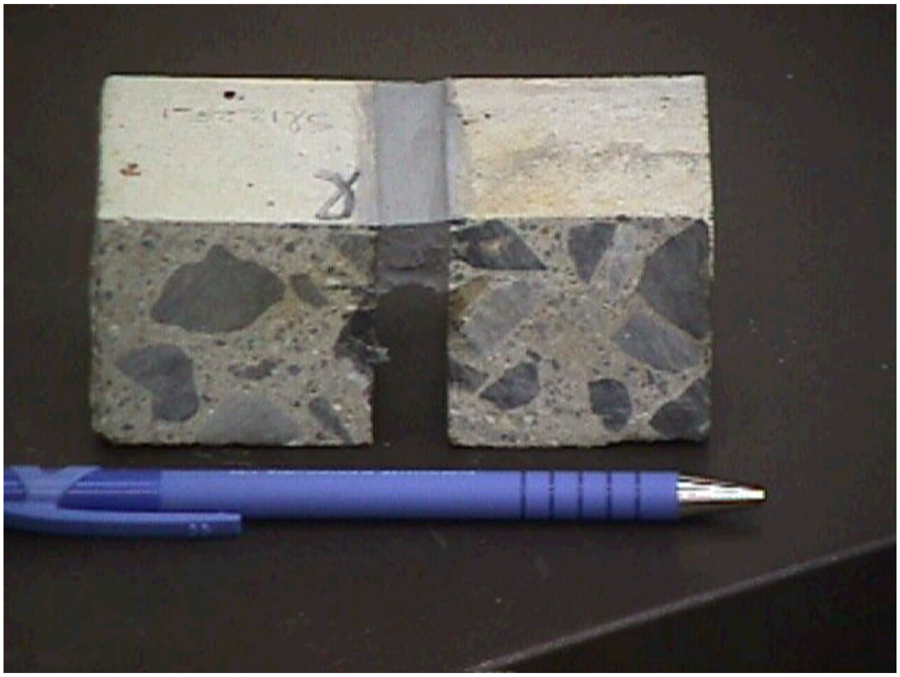

Figure D.17 Top of specimen SL12_25_1 after environmental conditioning and cyclic loading

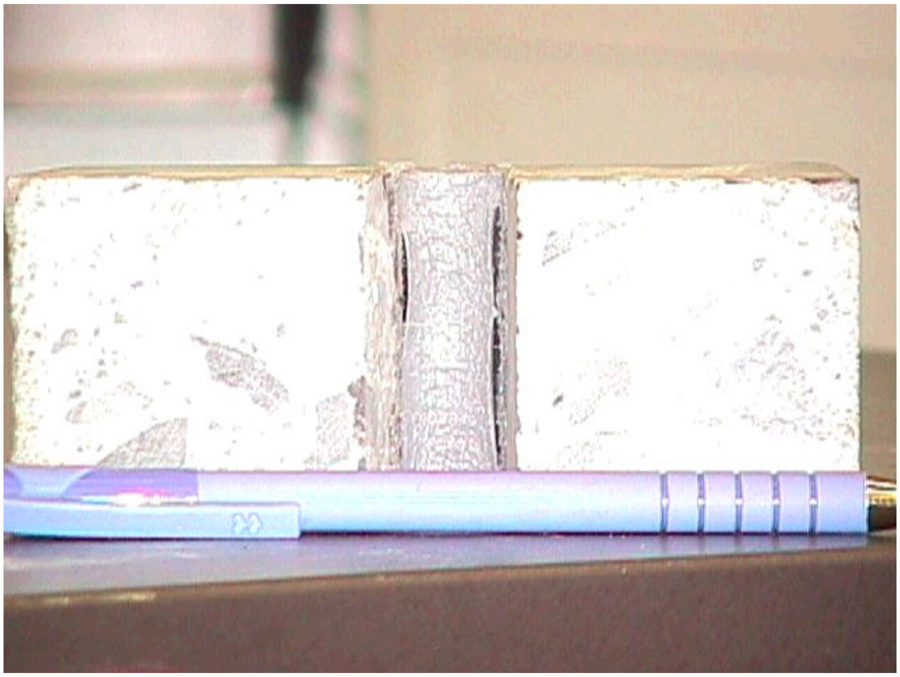

Figure D.18 Bottom of specimen SL12_25_1 after environmental conditioning and cyclic loading

Figure D.19 Top of specimen SG6_25UVJF1 after environmental conditioning and cyclic loading

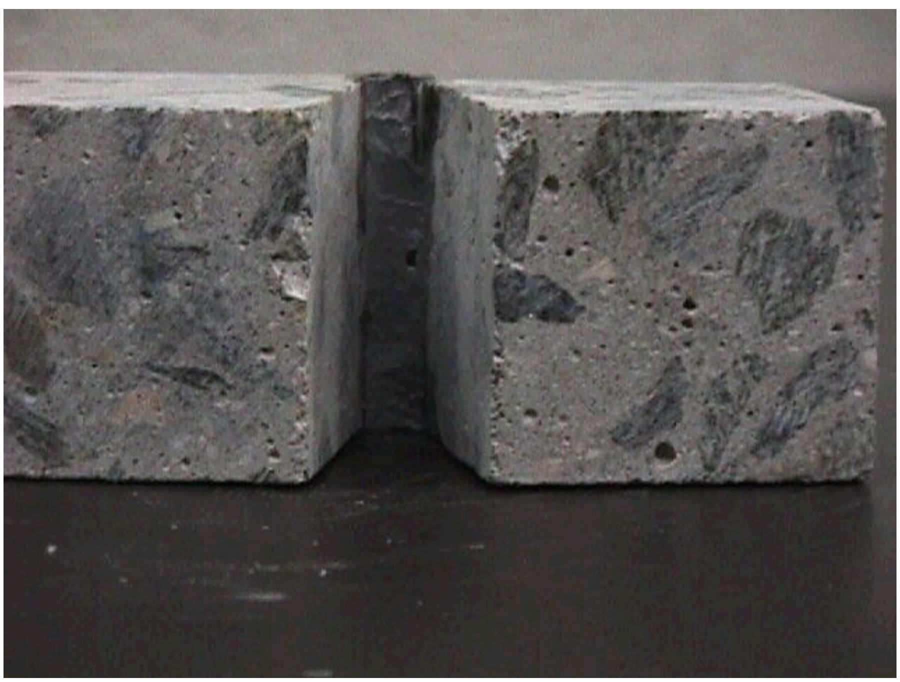

Figure D.20 Bottom of specimen SG6_25UVJF1 after environmental conditioning and cyclic loading

Figure D.21 Top of specimen NGB25JF2 after environmental conditioning and cyclic loading

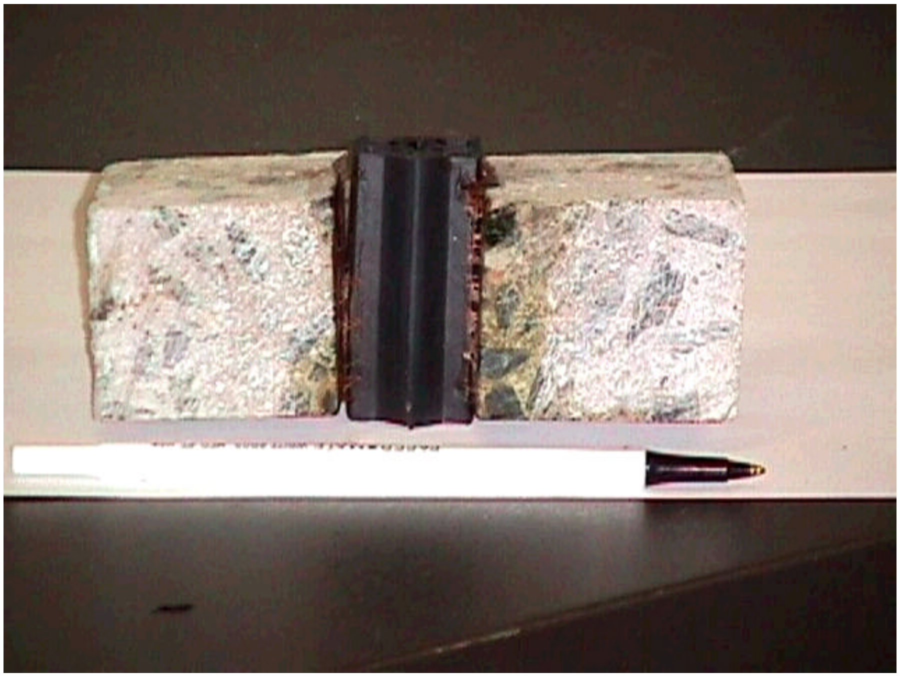

Figure D.22 Bottom of specimen NGB25JF2 after environmental conditioning and cyclic loading

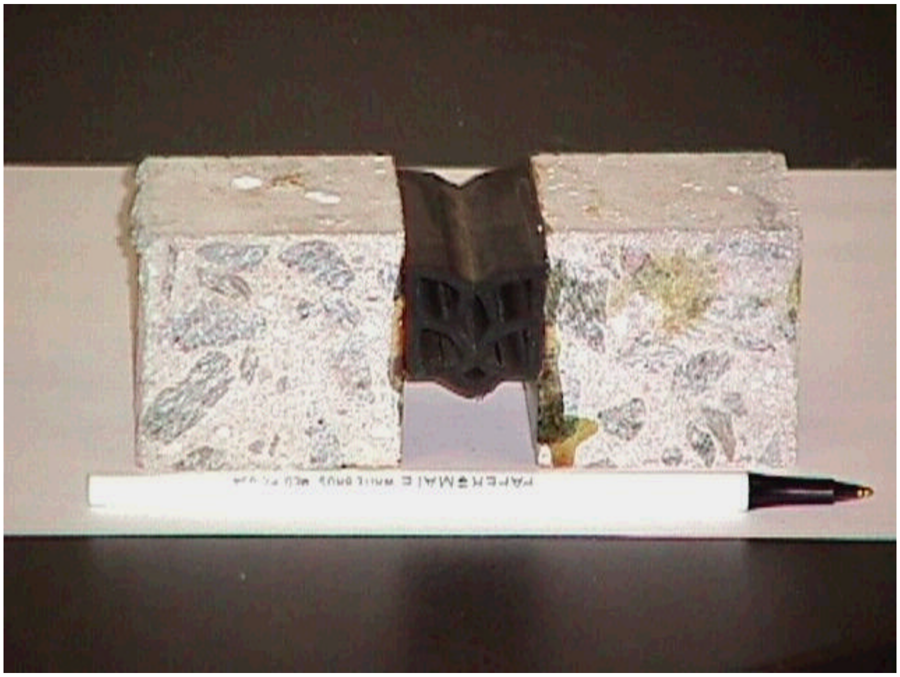

Figure D.23 Top of specimen NGB25UV2 after environmental conditioning and cyclic loading

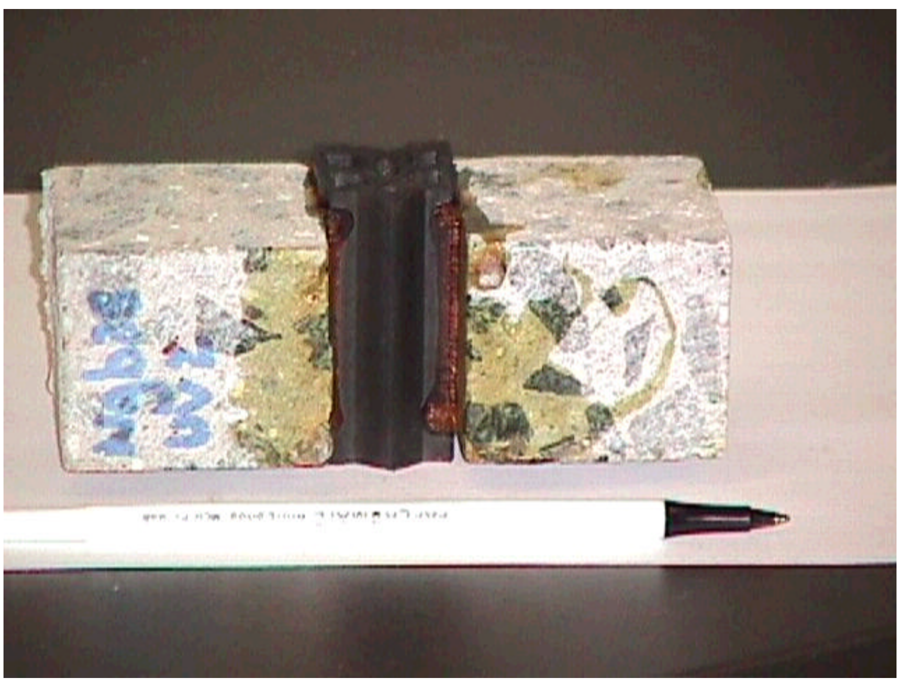

Figure D.24 Bottom of specimen NGB25UV2 after environmental conditioning and cyclic loading

Figure D.25 Top of specimen NGS25UVJF1 after environmental conditioning and cyclic loading

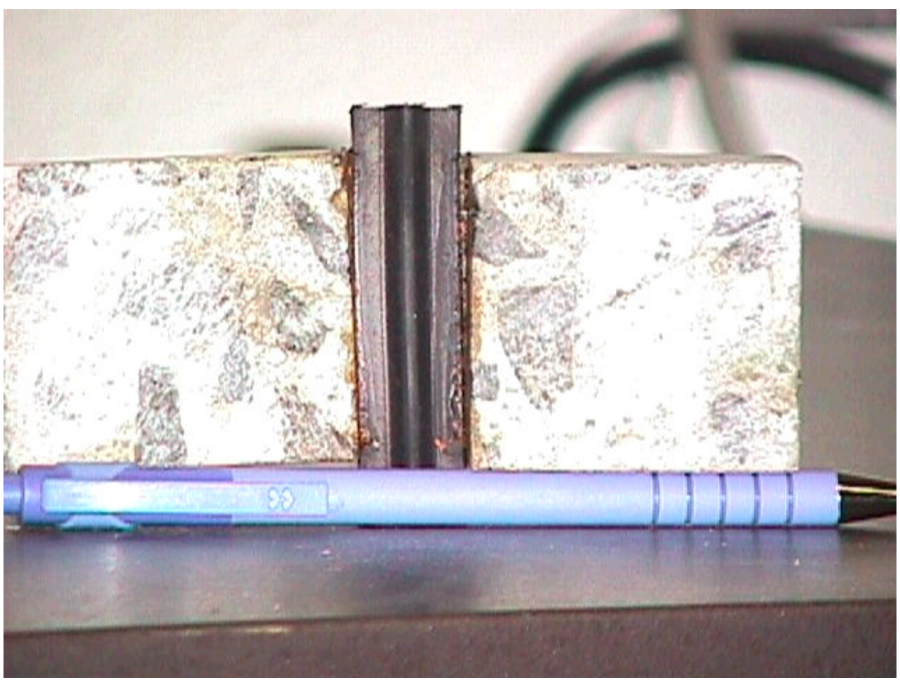

Figure D.26 Bottom of specimen NGS25UVJF1 after environmental conditioning and cyclic loading

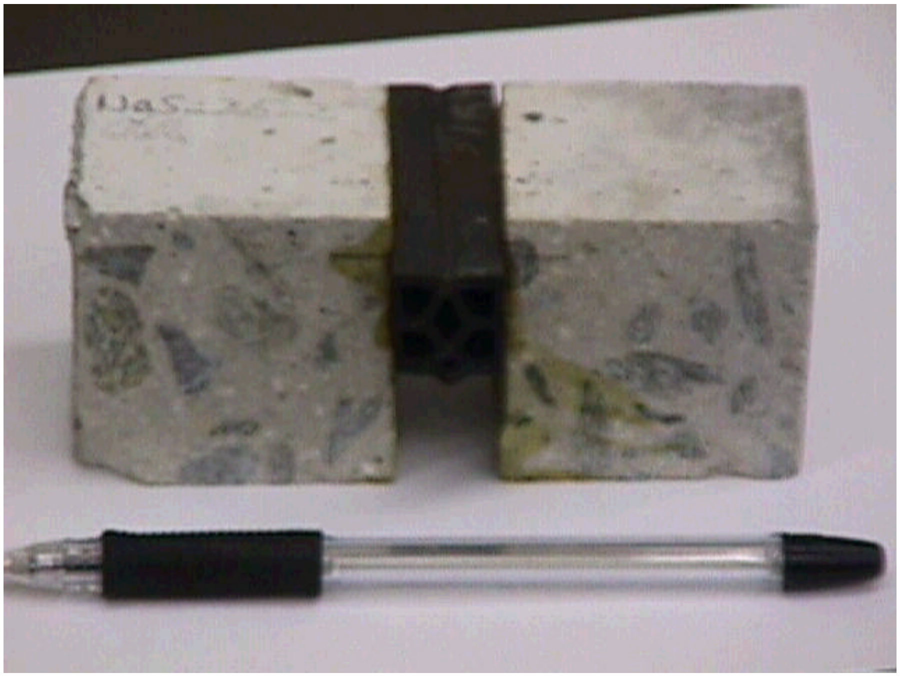

Figure D.27 Top of specimen NGS25_2 after environmental conditioning and cyclic loading

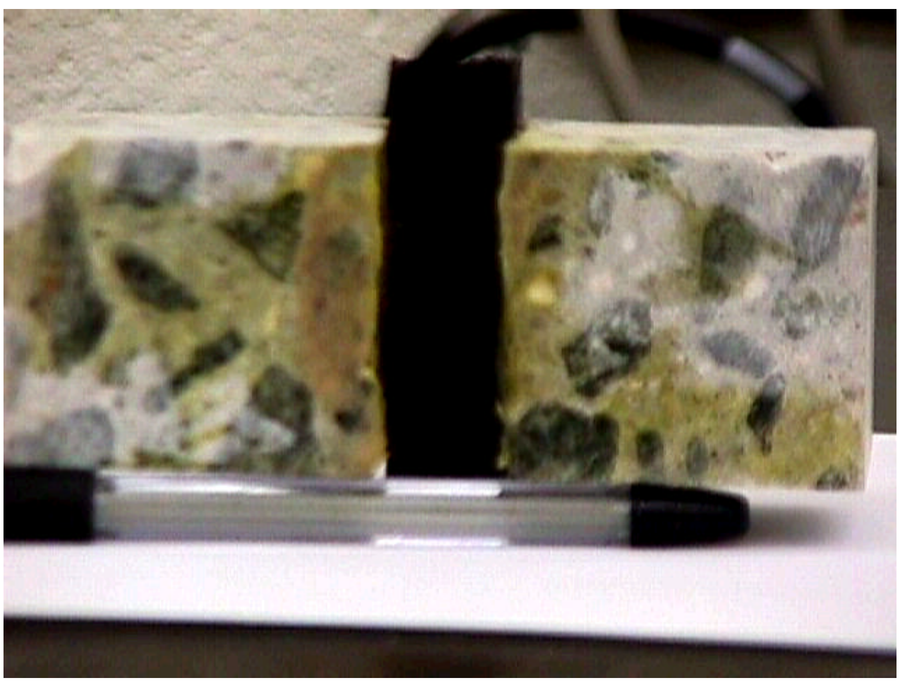

Figure D.28 Bottom of specimen NGS25_2 after environmental conditioning and cyclic loading

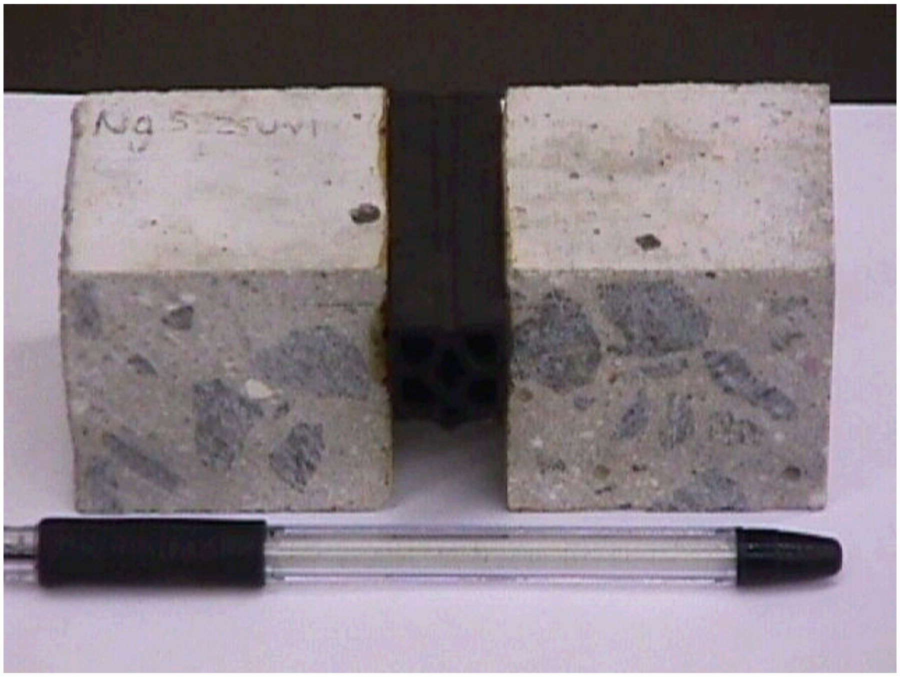

Figure D.29 Top of specimen NGS25UV1 after environmental conditioning and cyclic loading

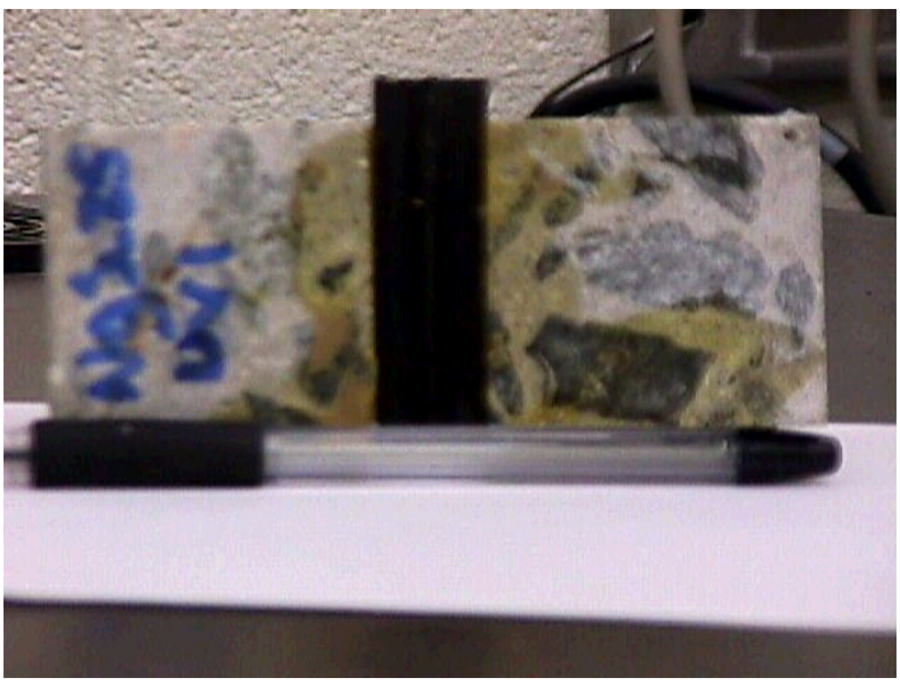

Figure D.30 Bottom of specimen NGS25UV1 after environmental conditioning and cyclic loading

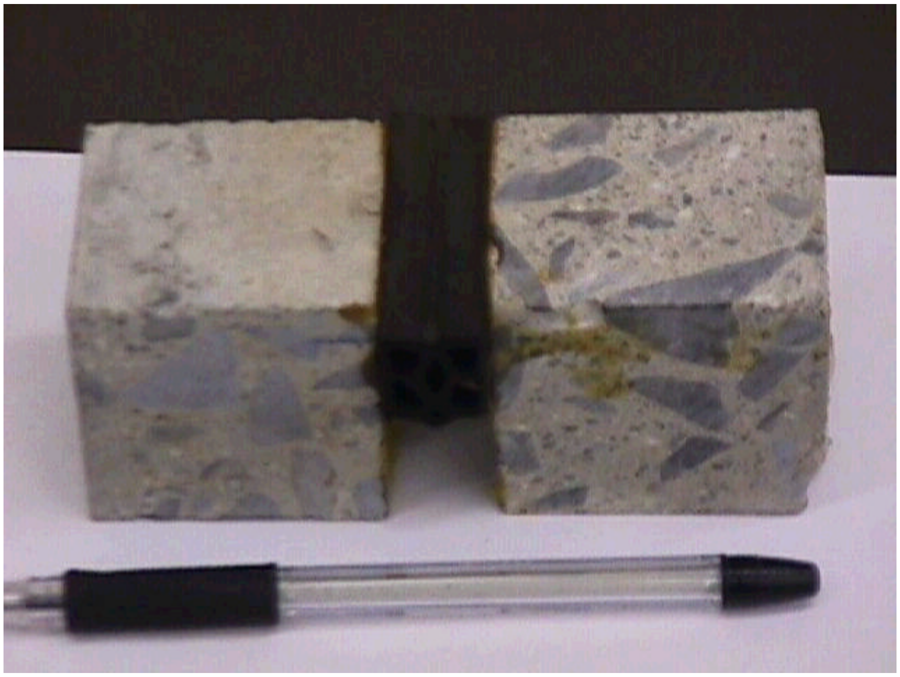

Figure D.31 Top of specimen NLS25UV1 after environmental conditioning and cyclic loading

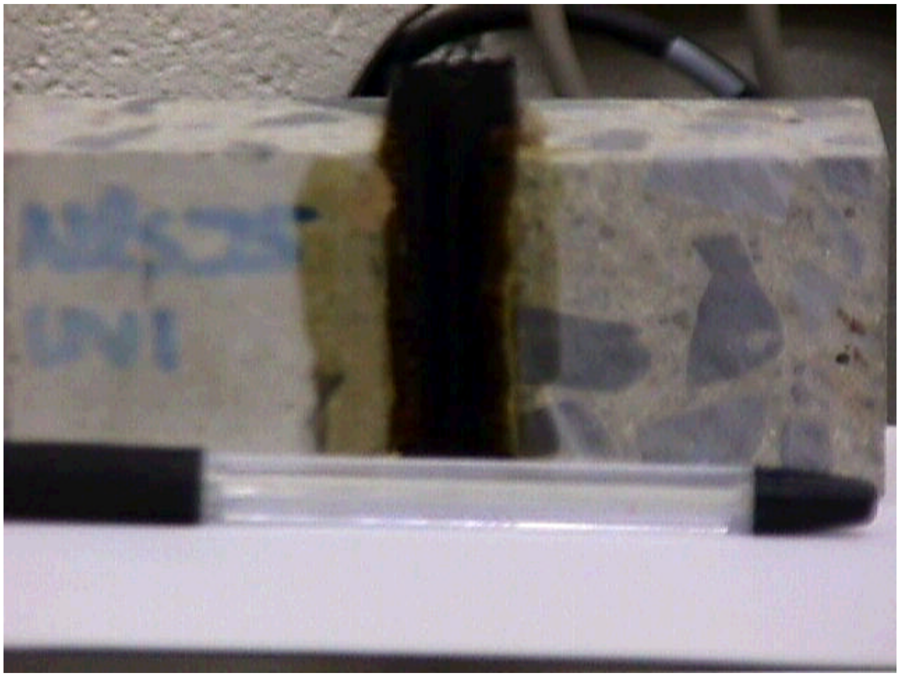

Figure D.32 Bottom of specimen NLS25UV1 after environmental conditioning and cyclic loading

VITA

Ramzi Emile Khuri was born in Richlands, Virginia on November 2, 1974. He attended Richlands High School and graduated in June, 1992. Ramzi joined a long line of family members to attend the Virginia Polytechnic Institute and State University. He received his Bachelor of Science Degree in Civil Engineering in May 1996.

Ramzi entered VPI & SU again in September 1996 to pursue a Masters Degree in Civil Engineering. He entered the Materials of the Civil Engineering Department and worked as a graduate research assistant in the Structures and Materials Lab. He expects his Masters of Science Degree in Civil Engineering in May 1999.

Ramzi Emile Khuri